ABSTRACT

Title of thesis: ANALYSIS OF RHEOLOGICAL PROPERTIES AND MOLECULAR WEIGHT DISTRIBUTIONS IN CONTINUOUS POLYMERIZATION REACTORS

Kedar Himanshu Dave, Master of Science, 2004

Thesis directed by: Professor Kyu Yong Choi
Department of Chemical Engineering

This work explores the possibility of exploiting structure-property relationships to manufacture tailor-made polymers with target end-use properties. A novel framework which aims to improve upon current industrial practices in polymerization process and product quality control is proposed. The strong inter-relationship between the molecular architecture and rheological properties of polymers is the basis of this framework.

The melt index is one of the most commonly used industrial measures of a polymer's processibilty. However, this single-point non-Newtonian viscosity is inadequate to accurately reflect the polymer melt's flow behavior. This justifies monitoring the entire viscosity-shear rate behavior during the polymerization stage. In addition, the crucial role played by the polymer melt's elastic characteristics is not reflected in it's shear viscosity and so elasticity meaurements are also warranted. In this study, rheological models available in the open literature are utillized to demonstrate these critical issues at industrially relevant operating conditions. The observations made are also compared with published experimental results and found to be qualitatively similar.

Two case studies are presented. The first one is the free-radical solution polymerization of styrene with binary initiators in a cascade of two CSTRs. In the second case, the solution polymerization of ethylene in a single CSTR with a mixture of two single-site transition metal catalysts is considered. The feasibility of the proposed framework to tailor the product's MWD, irrespective of the underlying reactor configuration or kinetic mechanism, is demonstrated via steady state simulations. Relative gain analysis reveals the non-linearity and interactions in the

control loops.

Although the main contributions of this study primarily deal with the viscoelastic behavior of linear homopolymers, potential extensions to systems involving polymers with small amounts of long chain branching or the control of other end-use properties are also discussed.

ANALYSIS OF RHEOLOGICAL PROPERTIES AND MOLECULAR WEIGHT DISTRIBUTIONS IN CONTINUOUS POLYMERIZATION REACTORS

by

Kedar Himanshu Dave

Thesis submitted to the Faculty of the Graduate School of the
University of Maryland, College Park in partial fulfillment
of the requirements for the degree of
Master of Science
2004

Advisory Commmittee:

Professor Kyu Yong Choi, Chair/Advisor
Professor Richard V. Calabrese
Associate Professor Nam Sun Wang

ACKNOWLEDGMENTS

I would like to take this opportunity to thank my advisor Prof. Kyu Yong Choi. He sets the same high academic standards for himself that he does for his group. I consider myself fortunate that he asked me to work on this topic: a research problem very dear to him. He always has new ideas and I think I have learned a lot from him. I am also grateful to my thesis committee members Profs. Calabrese and Wang for their helpful suggestions. My lab mates Ju-Yong Kim, Richard Wu and Brook Kebede were positive collaborators.

Outside the academic world the companionship of Rajiv and Tejas Gandhi, Len Jones, Dzul Scherber, Ved Mishra and Ramesh Gopalan kept me going. Last, but not the least, I want to thank my parents and my brothers, Parag and Malhar.

TABLE OF CONTENTS

LIST OF TABLES

LIST OF FIGURES

Chapter 1

Introduction

In the past few years, the polymer industry has been undergoing a major shift in paradigm. The emphasis is now more on product quality and performance rather than on productivity or throughput. This study deals with product quality control issues in continuous polymerization processes.

1.1 Motivation

Research work to improve upon the techniques for process and quality control in continuous polymerization reactors can be justified based on the following needs unique to polymer manufacturing:

1. Recent trends in the polymer industry are towards high-mix, low-volume manufacturing, supply-chain logistics and Six Sigma benchmarking. Schemes to manufacture differentiated products from the same plant have led to frequent (grade) transitions, startups, amd shutdowns. This has made the demands on product quality control and process flexibility increasingly stringent (see Harold and Ogunnaike [42]).

2. Most improvements in existing processes and designs for new ones are aimed towards providing the product with a certain level of properties (e.g., mechanical, optical, electrical or barrier). In order to achieve this, scientists face the challenging task of "tailoring" the polymer microstructure with greater accuracy.

3. Earlier it was believed that if a given polymer system did not meet the desirable requiremnents, a new polymer had to be used. However nowadays the product's properties are routinely altered by processing or by adding (blending) other materials such as polymers, fillers, glass fibers, or plasticizers (Table (1.1)). This being the last stage of manufacturing,

the degree to which one can alter the product's molecular architecture and hence it's properties is rather limited. These operations also increase the overall cost and time involved (see Fried [36]).

4. Adopting a "the earlier, the better" approach to get the right design in the intial stages itself (Table (1.1)), i.e. when there is maximum scope for change has shown limited success. Polymer product design at a molecular level using group contribution methods cannot distinguish between different grades of the same material (Vaidyanathan and El-Halwagi [77], Maranas [56]) and so pilot-scale testing and verification is essential. Owing to the complexity of the physicochemical interactions and the kinetics of polymerization reactions, there is often a lack of fundamnetal understanding of the underlying phenomena. As a result scale-up from laboratory or pilot-plant experiments is unreliable. Usually, the recipes devised at the design stage have to be altered ("fine tuned") significantly at the commercial scale. The usual approach to these activities is one of trial and error. Instead of such an empirical approach, a physically meaningful framework is necessary.

5. Unlike other, low molecular weight products from the chemical industries, polymer molecules cannot easily be separated from each other. So, in order to minimize the adjusting of the product's properties in the final stages of manufacturing, it would be more appropriate to obtain the desirable specifications during the polymerization stage itself. Thereby, if the product conforms to the specifications the first time, rework, blending, waste, or selling at reduced prices are avoided (see Congalidis and Richards [25]).

It can be concluded from the above discussion that there is strong motivation in reviewing current practices in polymerization process control, identifying opportunities for improvement and conducting further research to overcome these shortcomings.

1.2 Polymer properties

Polymer properties may be classified as:

Table 1.1: Various methods of manipulating polymer properties

Manufacturing stage	Tools
Initial design	Group contribution methods and iterative experimentation
Polymerization	Process control using on-line and off-line measurements
Final processing	Blending

1. Structural properties: These include the Molecular Weight Distribution (MWD), Copolymer Composition Distribution (CCD), Long Chain Branching Distribution (LCBD), stereospecificity, etc. They do not provide a direct measure of the performance of the polymer product during processing or during it's end use. However the end-use properties are strongly dependent on the polymer's structure.

2. Thermophysical properties: These include properties such as solubility and interaction parameters. They reflect the thermodynamic behavior of polymers.

3. Thermochemical properties: These include properties such as heat capacity, melting temperature, glass transition temperature, etc. They also provide an indication on thermal stability.

4. Transport properties: These include properties such as gas permeability, thermal conductivity, diffusivity, etc.

5. End-use properties: These properies are the polymer product's specifications from the customer's (end-user) perspective. They provide the most important information because vital engineering decisions are usually made based solely upon these properties without paying attention to the polymer's structure. In certain situations, these properties are abstract to the operating personnel. Additionally, no standards for quantifying them in numerical form might be available. In such a case, manufacturers rely on adhoc definitions based on

experience which might be grossly inconsistent. These may be further classified into:

(a) Processibilty: In order to use polymers, the material has to be converted into useful shapes such as fibres, films, or molded articles. This is done using polymer procesing (unit operations such as fibre spinning and injection molding). Rheological properties such as the melt index, die swell ratio, moldability, etc. play a crucial role in these activities. The end-user would typically use these properties to:

- estimate the pumping efficiency of an extruder, or
- estimate the pressure drop through a die, or
- design balanced flow runner systems in multiple cavity injection molding, or
- compute the temperature rise due to viscous heat generation during processing, etc.

(b) Performance: Deformation, toughness/hardness, blockiness, softness, color, flammability, etc. reflect the product's performance. Usually properties associated with performance are difficult to quantify.

There is no clear-cut demarcation when categorizing the type of polymer property. However, the bottom line is that commercially, the end-use properties are of primary interest.

1.3 Current practices in polymerization process and product quality control

During polymerization reactor operation, the ultimate goal is the accurate control of the final product quality. This is a very complex problem since the variables used to quantify polymer quality are quite large in number. Ideally it is desirable to control the strucure and composition of each and every polymer molecule. This is practically impossible. A simpler approach would be to control the entire MWD, CCD and LCBD. This too is unrealistic because of measurement and control relevant infeasibilities. Instead, in industrial practice, the entire space of quality variables is indirectly controlled by controlling a select few.

Congalidis and Richards [25] have provided an industrial perspective to polymerization process control. A hierarchical, Figure (1.1) Bulk polymers are usually manufactured by maintaining

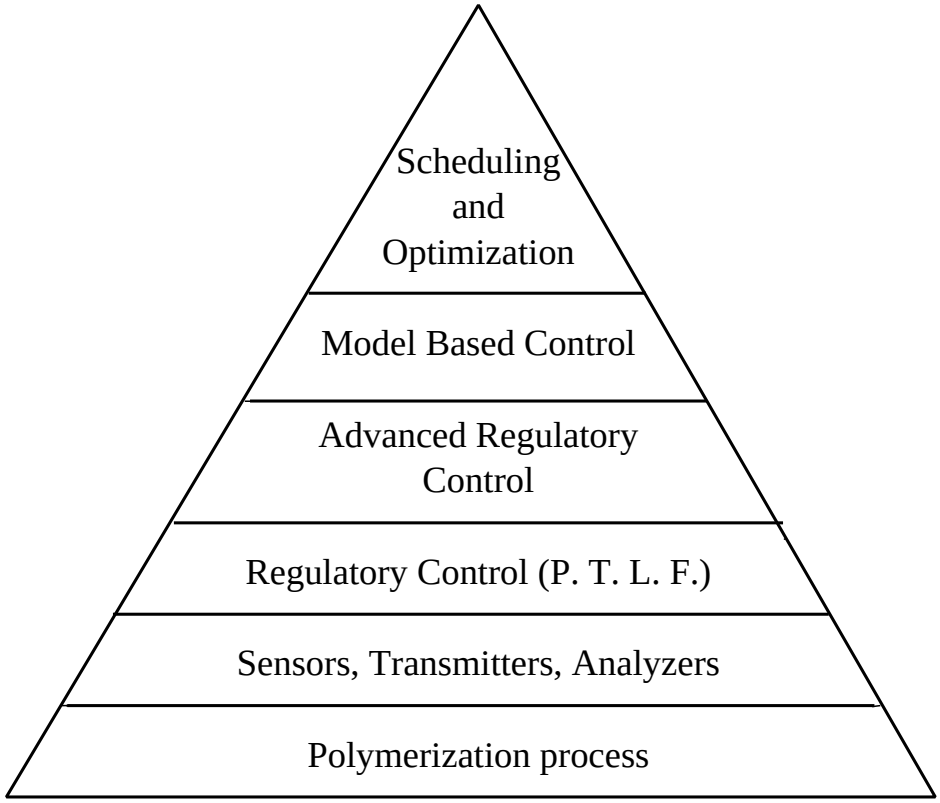

Figure 1.1: The hierarchy for polymerization process control [25].

the process at it's Standard Operating Conditions (SOC) i.e. regulatory control of the pressure, temperature, level and flow (PTLF) loops. This is the lowest level in the hierarchy. Usually, the reduction of off-spec material produced during process upsets and grade transitions is handled solely by controlling the PTLF loops because these are easy to measure. Periodic adjustments in the operating conditions may be made by the feedback of off-line or on-line density and/or Melt Index (MI) measurements which have predetermined specifications. This is the second level.

Quite often detailed models are used to estimate and control unmeasurable state variables like molecular weight averages or polydispersity. However, none of these traditional approaches take into account the polymer product's end-use properties in a direct way.

1.3.1 Limitations imposed by control in reduced dimensions spaces

In commercial practice, it is rare that structural properties like the molecular weight averages or composition (in the case of copolymers) are used as specifications for on-line monitoring and control. Some insigth into such an approach was provided by Clarke-Pringle and MacGregor [24]. They have demonstrated the limitations imposed by controlling only the weight-average chain length to indirectly control the entire MWD. It was observed that when a disturbance affects the system, the controller attempts to eliminate this but in this process

In order to conduct further research for overcoming the present deficiencies in the field, the above discussion has revealed three areas of opportunity:

1. Development of appropriate on-line sensors for characterizing polymer properties.
2. Setting up of performance goals for the process control system which are consistent and commercially relevant, i.e. consumer oriented.
3. Development of feasible control strategies capable of achieving these performance goals.

It is hoped that ideas derived from polymer rheology will help bridge this gap to some extent.

1.4 Direct control of end-use properties

During some process disturbances, although small in size, the upsets might get amplified and lead to large fluctuations in the final product properties. On the other hand, situations might arise where a disturbance might not affect the process enough to cause a significant variation. This would lead to an unnecessary wastage of control action. It is very important that one is able to judge when tight control is warranted and when it isn't justified. Polymerization reactor dynamics and structure-property relationships often involve extremely complex, non-linear interdependancies. As a result, intiutive engineering judgement is not effective. Even highly advanced control systems based entirely upon PTLF measurements alone might not perform satisfactorily. Hence there is a strong incentive to measure and directly control the polymer product properties around their specification targets in order to minimize the variability of the product quality. However we are

still faced with an important question - Out of the numerous polymer properties, which should be chosen as a variable to define product quality?

An alternative approach to the problem of choosing the controlled variables for a polymerization process is the direct control of the product's end-use properties. This choice makes intuitive sense because of all the properties, the end-use properties provide the most important information to the product's end-user. Critical decisions like regarding the final stage of manufacturing are made based upon this information. Also, upon carefully selecting the end-use property to be controlled, the dimensionality of the control problem would be kept small without affecting the control performance. Now, the question at hand is - Among the several end-use properties which one is the most appropriate for on-line monitoring and control purposes?

1.5 Rheology as a tool for polymer characterization

The polymer's MWD is it's single most important structural characteristic. Some of the traditional methods used for determining the MWD of polymers are Light scattering, Osmometry. Gel Permeation Chromatography (GPC) and Viscometry. Methods such as can only be used off-line in the analytical laboratory.

Among these, GPC, also called Size Exclusion Chromatography (SEC), is the most commonly used method for on-line applications. The salient features of various methods are compared in order to investigate the possibility of using rheological measurements instead of traditional methods for polymer charecterization (see Table).

1.5.1 Theoretical viability

Paraphrasing from Mead [60] - "Whenever a measurable physical property depends on molecular weight in a known manner, it is in principle possible to invert that relationship and determine the molecular weight distribution by measuring that property.....The stronger the dependance on molecular weight, the greater the sensitivity of the molecular weight determination, at least to the highest component of the distribution". As seen in Table, rheological methods are most sensitive to

Table 1.2: Molecular weight scaling of various methods of discriminating linear flexible polymers (Adapted from Mead [60])

Method	Discrimination scaling	Sensitivity scaling	Comments
Gel Permeation Chromatography	$M^{1/2}$	$M^{-1/2}$	Size exclusion, insensitive to high MW
Intrinsic viscosity	$M^{0.6}$	$M^{-0.4}$	Hydrodynamic size method
Light scattering	M^{1}	M^{0}	Good sensitivity to high MW
Osmotic pressure	M^{-1}	M^{-2}	Good indicator of $\overline{M}_n$ for low MW polymer
Zero shear viscosity	$M^{3.4}$	$M^{2.4}$	Principally a function of $\overline{M}_w$ for systems with similarly MWDs
Recoverable compliance	$(M_z/M_w)^{\sim 3.5}$	-	Indicative of the dispersion in the MWD. Insensitive to the absolute value of M.

the high end of the MWD because of the strong dependency of rheological properties on molecular weight. On the other hand, traditional methods like the GPC often lack resolution for the high molecular weight tails of MWDs due either to a column resolution problem or to degradation of the long chains.

Several researchers have questioned the solution of this "inverse problem" owing to the ill-posedness of the calculation.

1.5.2 Practical reasons

In traditional methods like the GPC, it is required that the polymer sample be soluble in a suitable solvent. However, many important polymers such as fluoropolymers (PTFE), melt anisotropic (rigid-rod) polymers, and polyamides are often insoluble in any suitable solvent. So the traditional methods cannot be applied in such situations. No solvent is involved and no solids have to be filtered.

1.5.3 Time-related issues

Sampling and measurement related time delays are key issues in process control. Delays are often the culprits at rendering some traditional measurements, although extremely accurate, useless for on-line control. Modern rheological methods allow four decades of frequency to be gathered in about 20 minutes by using the melt sampled from a process stream. Solution methods take more time,not so much for the SEC run itself but often for dissolving the polymer. An additional advantage is that of piece-wise data collection. Two or more rheometers used in parallel could be used to gather data for different frequency ranges. This data can then be combined to obtain the dynamic viscosity data for a larger range of shear rate or for a shorter sample processing time.

Besides, other characteristics such as the degree of reaction, the concentration of an additive, etc. can also be tracked which is ideal for process control. This has lead to the widespread use of rheometers for quality control in the plastics industry (Dealy [30]). In order to minimize the time involved in monitoring the quality, on-line rheometers which measure well-defined properties such as the viscosity-shear rate behavior are preferable. When used in conjunction with an advanced model predictive control scheme, such measurements could provide very effective product quality control.

1.5.4 Economic considerations

For materials like polypropylene, a typical GPC costs nearly triple that of the corresponding characterization via rheological methods, primarily due to the high operating temperatures involved in GPCs (Mead [60]). On-line and off-line rheometers cost upto US$ 100,000 (Dealy [30]) but their uasge is quite simple and routine. As a result, the capital and human energy savings associated with rheological measurements is substantial over the long run.

Besides these, on-line melt-indexers are also commonly employed. It is difficult to relate melt index to polymerization conditions.

As discussed earlier, the rheological properties of polymer melts are sensitive to several

Table 1.3: Typical $\dot{\gamma}$ range for polymer processing operations

Operation	$\dot{\gamma}$ range (s^{-1})
Compression molding	1 to 10
Calendering	10 to 10^2
Extrusion	10^2 to 10^3
Injection molding	10^3 to 10^4

important structural characteristics of the polymer-particularly it's MWD and LCBD. This makes rheological measurements a very important indicator of fluctuations in the polymer product's end-use properties during manufacture. Almost all the reports of on-line rheological measurements for quality control that have been made so far are limited to polymer processing applications.

1.6 Preliminaries

In this section some fundamentals of polymer rheology are summarized. The terminolgy used is described in Appendix. The aim of obtaining a better understanding of polymer rheology is vital since it is the basis for this new approach to polymer product quality control. It's utility is two fold. Not only is rheology being used as a measurement tool (i.e. measured variable) but it is also a target for control (i.e. controlled variable). Even when it isn't a target, it's measurement could be useful in back-calculating the molecular architecture. And if a suitable structure-property relationship is available, an unmeasurable property can be estimated and controlled.

1.6.1 General observations

Most traditional engineering materials may be well approximated as either one of the two extremes: viscous fluids or elastic solids. Polymer systems however cannot be classified accurately as either one of these two. They fall somewhere in between and so are called viscoelastic.

The measurable quantity commonly used to represent the viscous behavior of polymer melts and solutions is it's viscosity, i.e. it's resistance to flow. Polymer melts and solutions are always pseudoplastic, i.e. their viscosity decreases with the intensity of shearing.

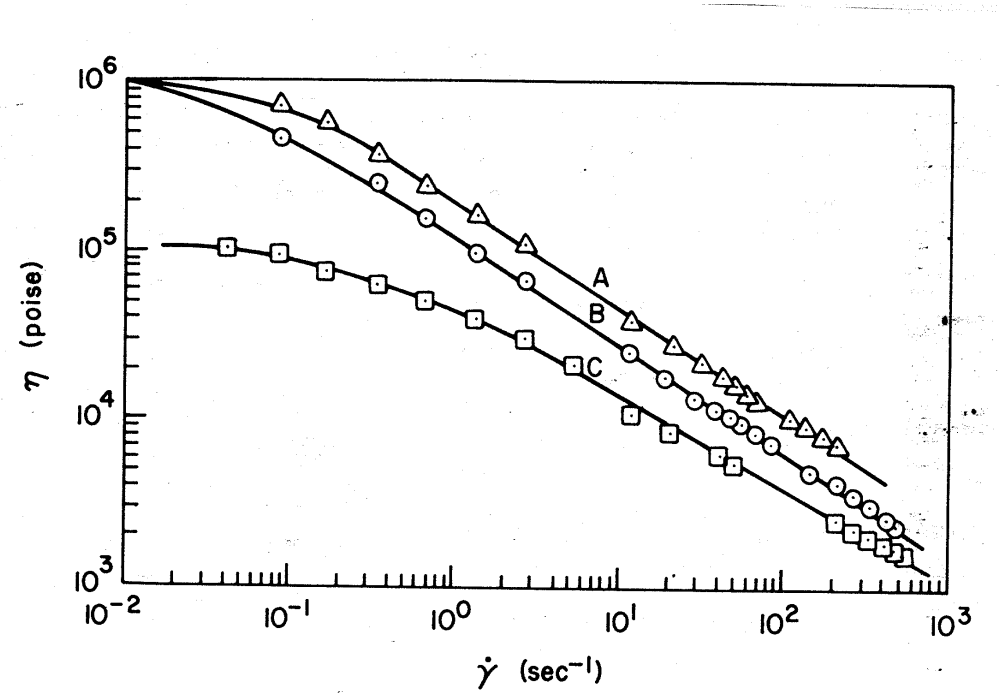

Figure 1.2: Melt viscosity versus shear rate: (A) HDPE, $\overline{M}_w/\overline{M}_n = 16$, (B) HDPE, $\overline{M}_w/\overline{M}_n = 84$ and (C) LDPE, $\overline{M}_w/\overline{M}_n = 20$ (from Han [40]).

The following general observations can be made regarding the influence of the rate of shear on polymer viscosity:

1. At low shear-rates (or stresses), a "lower Newtonian" region is reached with a so-called zero-shear viscosity η_0.

2. Over several decades of intermediate shear rates, the material is pseudoplastic.

3. At very high shear rates, an "upper Newtonian" region, with viscosity η_∞ is attained.

Unlike it's viscous counterpart, there is no clear-cut choice for the measurable quantity to use for representing the elastic behavior of polymer melts and solutions. Elastic recovery, characterized by the steady state elastic compliance (J_e), is often referred to as a measure of the stored elastic energy and is a useful parameter for determining the fluid elasticity. However, J_e cannot be measured directly and has to be obtained via first normal stress $N_1 = \tau_{11} - \tau_{22}$ measuremnts. Unfortunately, there is no consistent way to obtain J_e from N_1 over large ranges of shear rate (or streses). Hence it is preferable to use N_1 itself to represent the fluid elasticity. Han [40] has concluded that a plot of $\tau_{11} - \tau_{22}$ versus τ_w (and not versus $\dot{\gamma}$) yields a correlation consistent with a J_e versus $\dot{\gamma}$ plot. In this study, the $\tau_{11} - \tau_{22}$ versus τ_w behavior is used as a measure of polymer elasticity.

The following general observations can be made regarding the influence of shear stress on polymer elasticity:

1. At low shear stresses (τ_w), the first normal stress difference is proportional to the square of τ_w. This is a direct consequence of the definition of the steady state compliance, i.e.

$$N_1 = 2J_e\tau_w^2 \tag{1.1}$$

2. At high shear stresses, N_1 is proportional to τ_w rather than the square of τ_w. As a result, Equation (1.1) is no longer valid.

As far as industrial measures of polymer elasticity are concerned, the analogue to MFI is the die swell ratio (S_R). The phenomena of die -swell is extremely complicated and theories relating die-

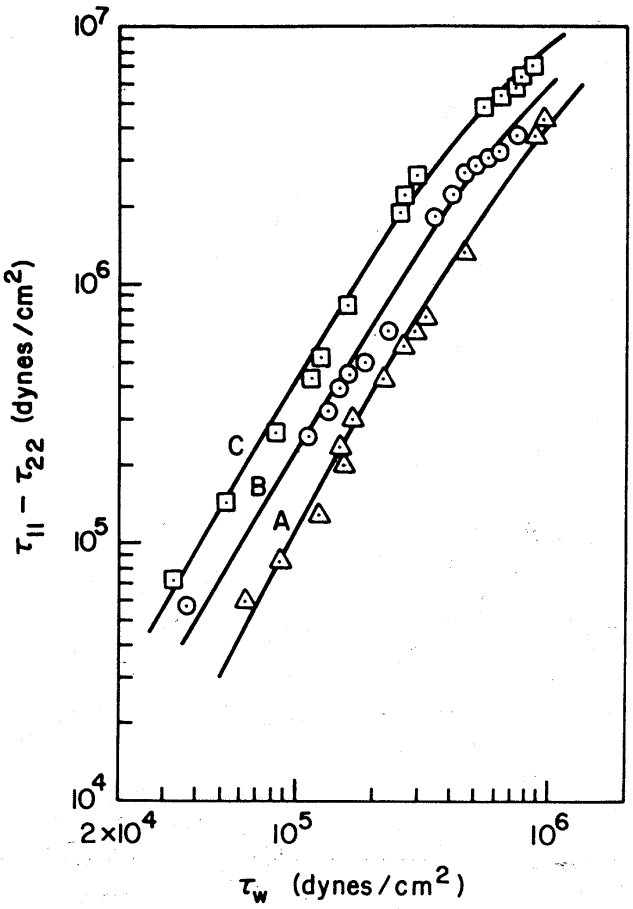

Figure 1.3: First normal stress difference versus shear stress: (A) HDPE, $\overline{M}_w/\overline{M}_n = 16$, (B) HDPE, $\overline{M}_w/\overline{M}_n = 84$ and (C) LDPE, $\overline{M}_w/\overline{M}_n = 20$ (from Han [40]).

Table 1.4: Molecular characteristics of PE samples (from Han [40]).

Sample code	Polymer	$\overline{M}_n$	$\overline{M}_w$	$\overline{M}_w/\overline{M}_n$	η_0 (poise) at 200^{o}C
A	HDPE	1.40×10^4	2.20×10^5	16	9.40×10^5
B	HDPE	2.00×10^3	1.68×10^5	84	1.9×10^6
C	LDPE	2.00×10^4	4.00×10^5	20	1.1×10^5

swell and first normal stress difference are only qualitatively successful [38]. The Tanner equation captures the essential features for polymer melts:

$$S_R = 0.13 + \left\{1 + \frac{1}{8}\left(\frac{N_1}{\tau_w}\right)^2\right\}^{1/6} \tag{1.2}$$

1.6.2 Influence of MW, MWD and temperature

It has long been known that a polymer's molecular weight exerts a strong influence on its melt or solution viscosity. The cause of this dependance can be explained as follows. Polymer chains are in the form of entanglements (often compared to a bowl of live worms) which give rise to molecular interactions. The primary effect of shear is the breakdown of such interactions. Chain entanglement is a function of both size and the number of molecules and so MW and MWD are the controlling factors in determining the viscosity of polymeric materials. Experiments show that

$$\eta_0 \propto \begin{cases} \overline{M}_w^1 & \text{for } \overline{M}_w < \overline{M}_{wc} \\ \overline{M}_w^{3.4} & \text{for } \overline{M}_w > \overline{M}_{wc} \end{cases} \tag{1.3}$$

Where $\overline{M}_{wc}$ is a critical average molecular weight, thought to be the point at which molecular entanglements begin to dominate the rate of slippage of molecules. It depends on the temperature and polymer type, but most commercial polymers are well above $\overline{M}_{wc}$. Empirical correlations of the following form are also used:

$$\eta_0 = K\overline{M}_w^{3.4} \tag{1.4}$$

where K is a constant. The temperature dependance of vicosity is often represented in the Arrhenius equation form:

$$\eta(T) = \eta(T_0) \exp\left[\frac{E_0}{R}\left(\frac{1}{T} - \frac{1}{T_0}\right)\right] \tag{1.5}$$

or

$$E_0 = 2.3R\Big(\log\eta(T) - \log\eta(T_0)\Big)\Big[\frac{1}{T} - \frac{1}{T_0}\Big]^{-1} \tag{1.6}$$

where, E_0 is an apparent activation energy of flow. A frequently encountered plot in the literature is the rheological "master curve". These are usually $\eta(\dot{\gamma})/\eta_0$ versus $\dot{\gamma}\tau_0$ and N_1 versus τ_w plots. They are useful for extrapolation purposes because of the insensitivity to temperature i.e. the data at all temperatures superimpose.

1.6.3 Constitutive equations

The traditional engineering model for purely viscous non-Newtonian flow is the so-called "Power Law Model":

$$\tau = K(\dot{\gamma})^n \tag{1.7}$$

This is a two - parameter model, the adjustable parameters being the consistency K and the flow index n. Also,

$$\eta = \frac{\tau}{\dot{\gamma}} = K(\dot{\gamma})^{n-1} \tag{1.8}$$

Other models for purely viscous flow are enlisted in Table (1.5). Among these, the Cross model is the most widely used. Material parameters can be obtained only after experimentally determining the flow behavior of each sample.

1.6.4 Linear Viscoelasticity

Models consisting of springs and dashpots are often used to represent the viscoelastic response of polymeric fluids. The response is linear because the ratio of overall stress to overall strain is a function of time only, not of the magnitudes of stress or strain. Material properties are time-invariant and so the history of usage is not considered important.

Table 1.5: Models for purely viscous flow (Adapted from Gordon and Shaw [37])

Parameters	Name	n	$\eta_r = \eta/\eta_0$
2	Bueche - Harding	1/4	$[1 + (\tau\dot{\gamma})^{0.75}]^{-1}$
	Ferry	1/2	$[1 + \eta_r\tau\dot{\gamma}]^{-1}$
	DeHaven	1/3	$[1 + (\eta_r\tau\dot{\gamma})^2]^{-1}$
	Spencer-Dillon	0	$[\exp(\eta_r\tau\dot{\gamma})]^{-1}$
	Eyring	0	$\sinh^{-1}(\tau\dot{\gamma})/\tau\dot{\gamma}$
3	Carreau	n	$[1 + (\tau\dot{\gamma})^2]^{(n-1)/2}$
	Cross	n	$[1 + (\tau\dot{\gamma})^{1-n}]^{-1}$
	Ellis	n	$[1 + (\eta_r\tau\dot{\gamma})^{(1-n)/n}]^{-1}$
	Mieras	n	$[1 + (\eta_r\tau\dot{\gamma})^2]^{(1-n)/2n}$
	Sutterby	n	$[\sinh^{-1}(\tau\dot{\gamma})/\tau\dot{\gamma}]^{1-n}$
	Quadratic	-	$\exp[-a(ln\tau\dot{\gamma})^2]$
4	Sabia	n	$[1 + (\tau\dot{\gamma})^{(1-n)/a}]^{\eta_r - a}$
	Vinogradov	n	$[1 + a(\tau\dot{\gamma})^{(1-n)/2} + (\tau\dot{\gamma})^{1-n}]^{-1}$
	Generalized rate	1-ab	$[1 + (\tau\dot{\gamma})^a]^{-b}$
	Generalized stress	$1/(1+ab)$	$[1 + (\eta_r\tau\dot{\gamma})^a]^{-b}$

The Maxwell Element

This is the simplest mathematical model. Although it is inadequate for quantitative correlation of polymer properties, it illustrates the qualitative nature of real behavior. It combines one viscous parameter and one elastic parameter. Mechanically. it can be visualized as the Hookean spring and a Newtonian dashpot in series. So they support the same stress. Therefore,

$$\tau = \tau_{spring} = \tau_{dashpot} \tag{1.9}$$

Differentiating equation

$$\dot{\gamma} = \dot{\gamma}_{spring} + \dot{\gamma}_{dashpot} = \frac{\dot{\tau}}{G} + \frac{\tau}{\eta} \tag{1.10}$$

Rearranging,

$$\tau = \eta\dot{\gamma} - \frac{\eta}{G}\dot{\tau} = \eta\dot{\gamma} - \lambda\dot{\tau} \tag{1.11}$$

The quantity $\lambda = \eta/G$ is known as the relaxation time.

The creep response of a Maxwell element is given by

$$\gamma(t) = \frac{\tau_0}{G} + \frac{\tau_0}{\eta}t \tag{1.12}$$

the stress relaxation response

The Generalized Models

The Generalized Maxwell model is used to describe stress-relaxation experiments while a generalized Voigt - Kelvin model is used to describe creep tests. The Maxwell element described in section can be generalized by the concept of a distribution of relaxation times so that it becomes adequate for quantitative evaluation. The stress relaxation of an individual Maxwell element is given by

$$\tau_i(t) = \gamma_0 G_i e^{t/\lambda_i} \tag{1.13}$$

where $\lambda_i = \eta_i/g_i$. The relaxation of the generalized model, in which the individual elements are all subjected to the same constant strain γ_0 is then

The creep response of an individual Voigt-Kelvin element is given by

$$\gamma_i(t) = \tau_0 J_i(1 - e^{-t/\lambda_i}) \tag{1.14}$$

where $J_i = 1/G_i$ is the individual spring compliance. The response of the array, in which each element is subjected to the same constant applied stress τ_0 is then

$$\gamma(t) = \tau_0 \sum_{i=1}^{n} J_i(1 - e^{-t/\lambda_i}) \tag{1.15}$$

or in terms of the overall creep compliance $J_c(t)$,

$$J_c(t) \equiv \frac{\gamma(t)}{\tau_0} = \sum_{i=1}^{n} J_i(1 - e^{-t/\lambda_i}) \tag{1.16}$$

Again, for large n, the discrete summation above may be approximated by

$$J_c(t) = \int_0^{\infty} J(\lambda)(1 - e^{-t/\lambda}) d\lambda \tag{1.17}$$

where $J(\lambda)$ is the continuous distribution of retardation times.

1.7 Overview of the research

This study combines the fields of reaction kinetics, polymer rheology and process control. The main objective is to examine the use of rheological models as an on-line measurement tool in the predictive control of product properties in polymer reactors. Although simulations have been used to illustrate this new methodology, the actual implementation does not necessiate any first-principles or empirical models.

The organization of this thesis is as follows. Chapter 2 provides a survey of important models available in the polymer rheology literature relevant to this study. Rather than presenting the new framework, it's application is first demonstrated via two example case studies given in Chapters 3 and 4. These chapters have been written in an identical fashion in order to facilitate comparison. Summarizing the results obtained in the two case studies, a generalized framework is presented in Chapter 5. Possible extensions to the applicability of the proposed framework are also given here. The concluding chapter, i.e. Chapter 6, contains a summary of the thesis and

recommendation for future work. There are two appendices. Appendix A describes the terminlogy used. Appendix B provides a concise discussion on polymer molecular weight distributions and their moments.

Chapter 2

Literature Review

This chapter provides various semi - empirical schemes available in the literature to predict the rheological properties of polydisperse polymer samples when the MWD is available. Estimating the relaxation spectrum has the advantage that all other linear viscoelastic properties can be evaluated from it. For example, the Loss and Storage moduli can be evaluated using equation (A.10) and (A.15) respectively. Methods for the inverse tranform of rheological data into the MWD are also reviewed.

2.1 Molecular models for polymer viscoelasticity

The constitutive equation listed in Chapter1 suffer from the handicap that model parameters cannot be related to polymer structural variables; to accomplish this, a molecular approach has to be employed.. Three types of molecular models are popular amongst polymer rheologists:

1. Bead-spring models for dilute solutions.

2. Network models for melts.

3. Reptation models for concentrated solutions and melts.

2.1.1 Bead-spring models

This model is based on the "Random coil theory" (see Gupta [39]). According to this theory, each polymer molecule is modeled as a dumbbell that consists of tow equal masses connected by an infintely extensible, linear, elastic sporing. Rouse utilized a "spring and bead" model to propose the following relation for the relaxation time λ_p of the pth segment

$$\lambda_p = \frac{6(\eta_0 - \eta_s)M}{\pi^2 p^2 cRT} \tag{2.1}$$

Also according to the Rouse theory, the steady-state compliance is given by:

$$J_e = \frac{2M}{5\rho RT} \tag{2.2}$$

The Maxwell equation predicts that the first normal stres difference is given by:

$$N_1 = \frac{2\theta\tau^2}{\eta} \tag{2.3}$$

2.1.2 Network models

These models owe their origin to the theory of ribber elasticity. Unlike vulcanized rubber, the network joints are temporary rather than permanent links. It is noteworthy that the simplest constitutive equation that emerges from this theory is the Maxwell equation (also known as the Lodge rubberlike liquid in the case of polymer melts).

2.1.3 Reptation models

Reptation (or entanglement) model was developed by Doi and Edwards [34]. The theory is fairly involved but the important aspect of an explicit expression for the zero shear viscosity. Its dependance on the weight average molecular weight is calculated to be to the third power rather than the expected 3.4 power. Nevertheless, the reptation model provides a consistent interrelationship between various viscoelastic functions.

2.2 Mixing Rules

The molecular theories presented in the previous section are primarily for monodisperse samples. In order to use them for polydisperse samples, the usual approach is to use some sort of a mixing rule. The general parametric mixing rule (see Thimm et al [74]) is:

$$\frac{G(t)}{G_N^0} = \left(\int_{ln(M_e)}^{\infty} F^{1/\beta}(t, M) w(M) d(lnM) \right)^{\beta} \tag{2.4}$$

where F((t,M) is an integral kernel function. It describes the relaxation behavior of a fraction with a normalized molecular weight M. β is a parameter which characterizes the mixing behavior. Althoough it is generally believed that $1 \leq \beta \leq 2$, it has been experimentally found that

quite often β is about 3.84. The Linear mixing rule predicts $\beta = 1$. des Cloizeaux [33] derived the Quadratic mixing rule which can be obtained by setting $\beta = 2$:

$$\frac{G(t)}{G_N^0} = [\sum_{i=1}^{c} w_i F^{1/2}(t)]^2 \tag{2.5}$$

2.3 Rheological models for polydisperse polymer melts

Although simulations based on first-principles and empirical models have been used to illustrate this new methodology, the actual implementation does not require any of these models. The models presented in this section are useful in simulating the behavior of an on-line rheometer installed in any polymer carrying pipe section, when the MWD of the polymer is known. For example one can predict the rheological behavior of the polymer of known MWD downstream of a polymerization reactor. The general approach employed in these models is to extend the molecular theories (Section2.1) to polydisperse systms using some sort of mixing rule (Section2.2).

2.3.1 Middleman's equation

Improving upon the theory put forward by Bueche [17], Middleman [61] proposed the following equation to calculate viscosity of polymer melts

$$\frac{\eta - \eta_s}{\eta_0 - \eta_s} = \int_0^\infty \frac{M^2 \varphi(M) F(\lambda_1 \dot{\gamma})}{\overline{M}_n \overline{M}_w} dM \tag{2.6}$$

where

$$F(\lambda_1 \dot{\gamma}) = 1 - \frac{6}{\pi^2} \sum_{n=1}^{N} \frac{\lambda_1^2 \dot{\gamma}^2}{n^2(n^4 + \lambda_1^2 \dot{\gamma}^2)} \left(2 - \frac{\lambda_1^2 \dot{\gamma}^2}{n^2(\lambda_1^2 \dot{\gamma}^2)}\right) \tag{2.7}$$

2.3.2 Bersted model

In a series of papers, Bersted and his coworkers [5, 6, 7, 8, 9, 10, 11, 12] developed the following model to predict the steady shear viscosity, first normal stress difference, dynamic small strain, stress overshoot and extensional behavior of polyethylene and polystyrene. Here, first the model capable of describing the rheological behavior of linear HDPE melts is presented. Then the model applicable to HDPE with low levels of LCB is described. Finally for the case of a blend of

linear and branched components, it is shown how these two completely different relationships are incoporated into an appropriate mixing law.

For linear polymers

Although applicable in modeling several different rheological characteristics, only the one involving viscosity-shear rate relationships is described here. It is assumed that the viscosity η_L at any shear rate $\dot{\gamma}$ can be obtained using

$$\log\ \eta_L(\dot{\gamma}) = A \log\,(\overline{M}_w*) + b \log\,(\overline{M}_z * /\overline{M}_w*) + \log \mathrm{K} \tag{2.8}$$

where, for the case of HDPE at 190^o, it is found experimentally that the constant A is 3.36, K is 3.16×10^{-13} and b is 0.51. Hence,

$$\log \eta_L(\dot{\gamma}) = -12.296 + 3.36 \log\,(\overline{M}_w*) + 0.51 \log\,(\overline{M}_z * /\overline{M}_w*) \tag{2.9}$$

where

$$\overline{M}w* = \sum_{i=1}^{c-1} h_i M_i + M_c \sum_{i=c}^{\infty} h_i \tag{2.10}$$

and

$$\overline{M}z* = \frac{\sum_{i=1}^{c-1} h_i M_i^2 + M_c^2 \sum_{i=c}^{\infty} h_i}{\overline{M}w*} \tag{2.11}$$

and w_i is the weight fraction of the ith component. In terms of GPC data, the MWD is split into a histogram with rectangles of width ΔV_i, of $\frac{1}{10}$ count, i.e.

$$w_i = \frac{h_i \Delta V_i}{\sum_{i=1}^{\infty} h_i \Delta V_i} \tag{2.12}$$

where h_i is the peak height of of the ith rectangle and ΔV_i is the elution volume increment; M_i is determined from the universal calibration curve at the elution volume V_i. $M_c(\dot{\gamma})$ is a shear

rate parameter defined to be the largest molecular species contributing as though it were Newtonian at $\dot{\gamma}$. In other words, it partitions molecular weights into two sections:

(1) Molecular weights below M_c contribute to the viscosity as at zero shear rate, and

(2) Molecular weights greater than M_c contribute to the viscosity as though they were of molecular weight M_c.

For the case of HDPE, the relation between M_c and $\dot{\gamma}$ was found experimentally to be

$$\log(M_c) = 5.929 - 0.290 \log \dot{\gamma} \tag{2.13}$$

or

$$M_c = 540,000(\dot{\gamma}^{-0.300}) \tag{2.14}$$

For branched polymers

The model for linear polymers is extended to branched polymers by the use of the distribution of the mean square radius of gyration instead instead of the molecular weight. The mean square radius of gyration is proportional to gM, where g is defined as the ratio of the mean square radius of gyration for a branched to linear molecule of identical molecular weight.

$$\log\eta(\dot{\gamma}) = -30.18 + 7.9\log(g\overline{M})_w* \tag{2.15}$$

where $(g\overline{M})_w*$, the weight average of gM is found using

$$\log\eta(\dot{\gamma}) = -30.18 + 7.9\log(g\overline{M})_w* \tag{2.16}$$

where $(g\overline{M})_w*$, the weight average of gM is found using

$$(g\overline{M})_w* = \sum_{i=1}^{c-1} h_i(g\overline{M})_i + (gM)_c \sum_{i=c}^{\infty} h_i \tag{2.17}$$

Moreover, $(gM)_c$, the critical value of gM, depends upon the shear rate according to the relation

$$\log (gM)_c = 4.67 - 0.112 \log \dot{\gamma} \tag{2.18}$$

For a blend of linear and branched components

Since this model assumes that the shear rate effects on the Newtonian - Non-Newtonian behavior of the various molecular species is independent, when the polydisperse polymer sample is a blend of linear and branched components, the following mixing rule maybe used.

$$\eta(\dot{\gamma}, blend) = [\eta_L(\dot{\gamma})]^{w_L} [\eta_B(\dot{\gamma})]^{w_B} \tag{2.19}$$

where $\eta_L(\dot{\gamma})$ is the viscosity of the linear distribution obtained using whereas $\eta_B(\dot{\gamma})$ is the viscosity of the branched distribution obtained from w_L and w_B are the weight fractions of the linear and branched components respectively.

2.3.3 Nichetti and Manas-Zloczowers' method

Nichetti and Manas-Zloczower [63] proposed a simple superposition model for calculating the viscosity of linear polydisperse polymer melts. At a given shear rate $\dot{\gamma}$,

$$\eta(\dot{\gamma}) = k\left[\int_0^{(\tau_c/k\dot{\gamma})^{1/\alpha}} M\omega(M)dM + \left(\frac{\tau_c}{k\dot{\gamma}}\right)^{(1-n)/\alpha} \int_{M(\dot{\gamma})}^{\infty} M^n \omega(M)dM + 2^{(\alpha-1)/\alpha} M_e \int_0^{M_\infty(\dot{\gamma})} \omega(M)dM\right]^{\alpha} \tag{2.20}$$

In this model the value of α is chosen to be 3.4. Here $M(\dot{\gamma})$ is the molecular weight of a monodisperse fraction for which $\dot{\gamma}$ is the shear rate for the onset of shear thinning behavior. It is determined using:

$$M(\dot{\gamma}) = \begin{cases} \left(\dfrac{\tau_c}{k\dot{\gamma}}\right)^{1/\alpha} & \dot{\gamma} \leq \dot{\gamma_L} \\ M_\infty(\dot{\gamma}) & \dot{\gamma} > \dot{\gamma_L} \end{cases} \tag{2.21}$$

where

$$M_\infty(\dot{\gamma}) = \left[\frac{M_c}{2^{1/\alpha}} \left(\frac{k\dot{\gamma}}{\tau_c} \right)^{(1-n)/\alpha} \right]^{1/n} \tag{2.22}$$

M_c is the critical entanglement molecular weight whereas M_e is the average molecular weight between entanglements and can be calculated using:

$$M_e = \left(\frac{\eta_\infty}{2^{\alpha-1}k} \right)^{1/\alpha} \tag{2.23}$$

The minimum value for the shear rate at the onset of the second Newtonian regime is given by:

$$\dot{\gamma_L} = \frac{\tau_c 2^{1/(1-n)}}{k M_c^\alpha} \tag{2.24}$$

Below a certain critical value of the shear rate, the viscosity does not depend on the shear rate and is called the zero-shear viscosity. It is obtained using:

$$\eta_0 = k\overline{M}_w^\alpha \tag{2.25}$$

2.3.4 Ferry's equations

Ferry [35] proposed the following correlation to predict the relaxation spectrum for polydisperse systems

$$H(\lambda) = (\rho RT/\overline{M}_n) \int_0^\infty \sum_{p=1}^{N} \lambda_{p,M} \delta(\lambda - \lambda_{p,M}) \varphi(M) dM \tag{2.26}$$

where $\lambda_{p,M} = 6\eta_0 M^2/\pi^2 p^2 \rho \overline{M}_w RT$

For the steady state compliance:

$$J_e = \left(\frac{2}{5\rho RT} \right) \frac{\overline{M}_z \overline{M}_{z+1}}{\overline{M}_w} \tag{2.27}$$

2.4 Methods to estimate the MWD from the rheological data of polymer melts

2.4.1 Inverse Bersted Method

The Bersted [5] Partition Model may be applied in the reverse to obtain the Molecular weight distribution from rhological data. However, Mavridis and Shroff [58] point out that this

method is practically infeasible for broad MWD polymers. The method may be summarized as follows. The inputs are the Relaxation Spectrum, $H(\lambda)$ over the full range of relaxation times and Material parameters k_1, k_2, α_1 and α_2,. The sequence of calculations at each relaxation time step $[\lambda_i = i * \Delta\lambda]$:

1. Calculate corresponding Molecular weight using

$$M_i = \left(\frac{\lambda_i}{k_2}\right)^{1/\alpha_2} \tag{2.28}$$

2. Calculate the viscosity using

$$\eta_0(\lambda_i) = \int_0^{\lambda_i} H(\lambda) d\lambda \tag{2.29}$$

3. Calculate M_w^* using

$$M_w^*(\eta_0) = \left(\frac{\eta_0}{k_1}\right)^{1/\alpha_1} \tag{2.30}$$

4. Substitute in

$$\phi(\ln\, M_c) = 1 - \frac{M_w^*}{M_c}\frac{\alpha_2}{\alpha_1}\frac{\partial \ln\, \eta_0}{\partial \ln\, \tau_c} \tag{2.31}$$

to calculate the cumulative MWD and finally the differential MWD.

2.4.2 Wu's and Wasserman's methods

Wu's method is based on the reptation concept of Doi-Edwards. The basic assumptions are:

(1) The cumulative MWD curve has the same shape as the $G(t)$ or the $G'(\omega)$ curves

(2) $G(t)$, or $G'(\omega)$ of a polydisperse polymer is determined by the linear mixing rule.

$$G'(\lambda) = \int_{-\infty}^{\infty} D(\lambda)\frac{8}{\pi^2}G_N^o \sum_{oddp}\frac{(1/p^2)(\omega\lambda/p^2)^2}{1+(\omega\lambda/p^2)^2} dlog\lambda \tag{2.32}$$

$$G_N^o = \left(\frac{4}{\pi}\right)\int_{-\infty}^{\omega_{max}} G'' dln\omega \tag{2.33}$$

Wasserman method uses the method of Tokhonov regularization, the dynamic moduli master curve data is fit to the relaxation spectrum.

An extension of this is the Tuminello storage modulus transform. In this technique, the storage modulus in the treminal zone is transformed into the cumulative Molecular Weight Distribution using the mixing rule described by Wassermann and Graessley with the storage modulus replacing the relaxation modulus.

2.4.3 Liu et al. [51, 52, 53, 54] method

In order to obtain the MWD of linear polymers quantitatively from rheological data, several methods have been reported in the literature. Among these, the method proposed by Liu et al. is the most appropriate for on-line use owing to the short computation times involved. They have developed a new algorithm to increase the accuracy and the reliability of Gordon and Shaw's method. This extension also provided means to optimize the rheological data collectionby defining quantitative relations between resolution and test time.

Two approaches are suggested:

Differential approach

This approach is capable of expressing the MWD very accurately since it can detect small inflections in the viscosity data and convert them into MWD information. But this also makes it overly sensitive. The explicit differential form of the working equation is:

$$f(m) = -\frac{1}{\nu^2 m}\left(\frac{\eta}{\eta_0}\right)^{1/\alpha}\left(\frac{\dot{\gamma}}{\dot{\gamma}_c}\right)^{1/\alpha}\left[\alpha\frac{d^2\ln\eta}{d\ln\dot{\gamma}^2} + \nu\frac{d\ln\eta}{d\ln\dot{\gamma}} + \left(\frac{d\ln\eta}{d\ln\dot{\gamma}}\right)^2\right. \tag{2.34}$$

where f(m) is the differential MWD, i.e. the weight fraction of material with relative molecular weight between m and m + δm. α is the mixing rule exponent and is assumed to be a constant value of 3.4. m is given by:

$$m = \frac{M}{\overline{M}_w} = \left(\frac{\dot{\gamma}}{\dot{\gamma}_c}\right)^{-\nu/\alpha} \tag{2.35}$$

and $-\nu$ is the final slope of the power-law region.

When compared to the Integral approach, this methodhas several advantages. It makes no assumptions concerning the slope of the MWD prior to analysis.

Integral approach

The Integral approach is capable of handling moderately incomplete data and is often more robust, i.e. less sensitive to noisy data. It essentially first assumes a shape for the MWD to avoid ill-posedness. This assumption isn't a limitation when a general idea of the expected shape of the MWD is available.

The model parameters are obtained by iteratively solving the Bersted model to minimize the difference between the predicted and measured values.

$$f(m) = \sum_{i=1}^{n} \frac{a_i}{m} \exp\left[-\frac{(\ln m - b_i)^2}{c_i^2}\right] \tag{2.36}$$

$$\int_0^\infty f(m)\, dm = 1 \tag{2.37}$$

where R^* is an adjustable parameter. A large value of R^* gives a smoother but less accurate solution.

To obtain the absolute molecular weight, the weight average molecular weight ($\overline{M}_w$) is needed which has to be provided by other sources. Liu et al. suggest using an empirical rule such as those in Section 5.3.3.

Amongst the several methods available, this one is the most suitable for process monitoring and control. Berker and Driscoll have pointed out the sensitivity of the predicted polydispersity to varaitions in the final slope of the viscosity curve and Tuminello argues that this is a weakness of the approach.

Data collection

During the collection of rheological data, the objective is to get good resolution in the shortest period of time in order to minimze the cost. Liu et al. have suggested several guidlines for optimizing this process.

$$\hat{t} = \dot{\gamma}_c \sum_{i=1} NP\dot{\gamma}_i \tag{2.38}$$

Chapter 3

Control of rheological properties in a continuous styrene polymerization process

Polystyrene is an extremely important commodity polymer. Atactic polystyrene is usually manufactured using free-radical mechanisms. Styrene homopolymers are manufactured industrially by suspension, mass (bulk) and solution polymerization processes. In solution polymerization, the viscosity of the reaction mixture is much lower than that in the mass process. As a result, temperature control is less difficult. The concentration of the solvent, usually ethyl benzene, in the feed to the reactor is about 5 to 25%. After polymerization, the unreacted monomer and solvent are separated from the polymer and recycled. At an industrial scale, these processes commonly employ one of three reactor types. Recirculated coil and ebullient reactors are single staged and are operated isothermally. Continuous recirculated stratified agitated tower reactors are multistaged and offer nearly plug flow. A temperature profile of 100 to 170^0C is usually maintained across the stages (Choi et al. [23]).

High impact polystyrene (HIPS) processes usually utilize at least two reactors in series in order to handle the highly viscous polymerizing mass. Moreover, quite often a variety of complex initiator systems (e.g., multiple monofunctional initiators and multifunctional initiators) are used. This provides the reactor operators with additional degrees of freedom and so polymers of various grades and desired properties can be produced more effectively. It has often been reported (e.g. Kim et al. [46], Kim and Choi [47]) that when a mixture of monofunctional initiators having significantly different thermal decomposition characteristics are used, it is possible to reduce the reaction time, increase the monomer conversion and polymer molecular weight simultaneously.

In this study, the free-radical solution homo-polymerization of styrene in a system of two jacketed, continuous stirred tank reactors (CSTRs) in series, is chosen as the process. Stabillizing regulatory controllers for the base control of reactor feeds, levels and jacket cooling water temperatures have been provided. A binary initiator system consisting of tert-butyl perbenzoate (Initiator

A - "slow") and benzoyl peroxide (Initiator B - "fast") is utilized. The thermal decomposition rate of the former is much lower than that of the latter at a given temperature. For example, the half-life of tert-butyl perbenzoate at 100^0C is 12.9 h. and that of benzoyl peroxide is 1 h. Additionally, a chain transfer agent (CTA), di-n-butyl persulphide is also injected into the reactors.

In order to study the benefits of incorporating on-line rheological measurements into the cascaded CSTRs' control system, a rigorous first-principles model for the polymerization process is developed first. This model generates the discrete MWD of the product stream as its output which is plugged into a rheological model. Such an arrangement is expected to represent the real world output of an on-line rheometer installed in the product stream and thus providing the molten polymer's viscosity-shear rate data. This is depicted schematically in Figure (3.1).

The sensitivity of the product's quality variables to various operating conditions is studied via a steady state analysis. Based upon this analysis, polymerization process control strategies are devised. The comparative effectiveness of several strategies, in their ability to control the end-use properties during setpoint changes or while rejecting disturbances, is examined. Issues involved in the design of the control system to achieve this target are demonstrated via dynamic simulations.

3.1 Kinetic model

Crowley and Choi [27] proposed "the method of finite molecular weight moments" - a new method for calculating the weight chain length distribution (WCLD) of polymers. The WCLD is the preferred form of representing the MWD, over the number chain length distribution (NCLD), because

1. As noted in Chapter 2, most rheological, mechanical and other end-use properties depend more strongly on the WCLD than on the NCLD. Hence it would be the appropriate form for measurement, estimation and control purposes.

2. Experimentally, polymer molecular weight is measured most conviniently by gel permeation chromatography (GPC). GPC detectors (e.g., UV or IR detectors) are mostly mass-sensitive and so the resulting chromatograms (detector signal vs. retention time) also represent the

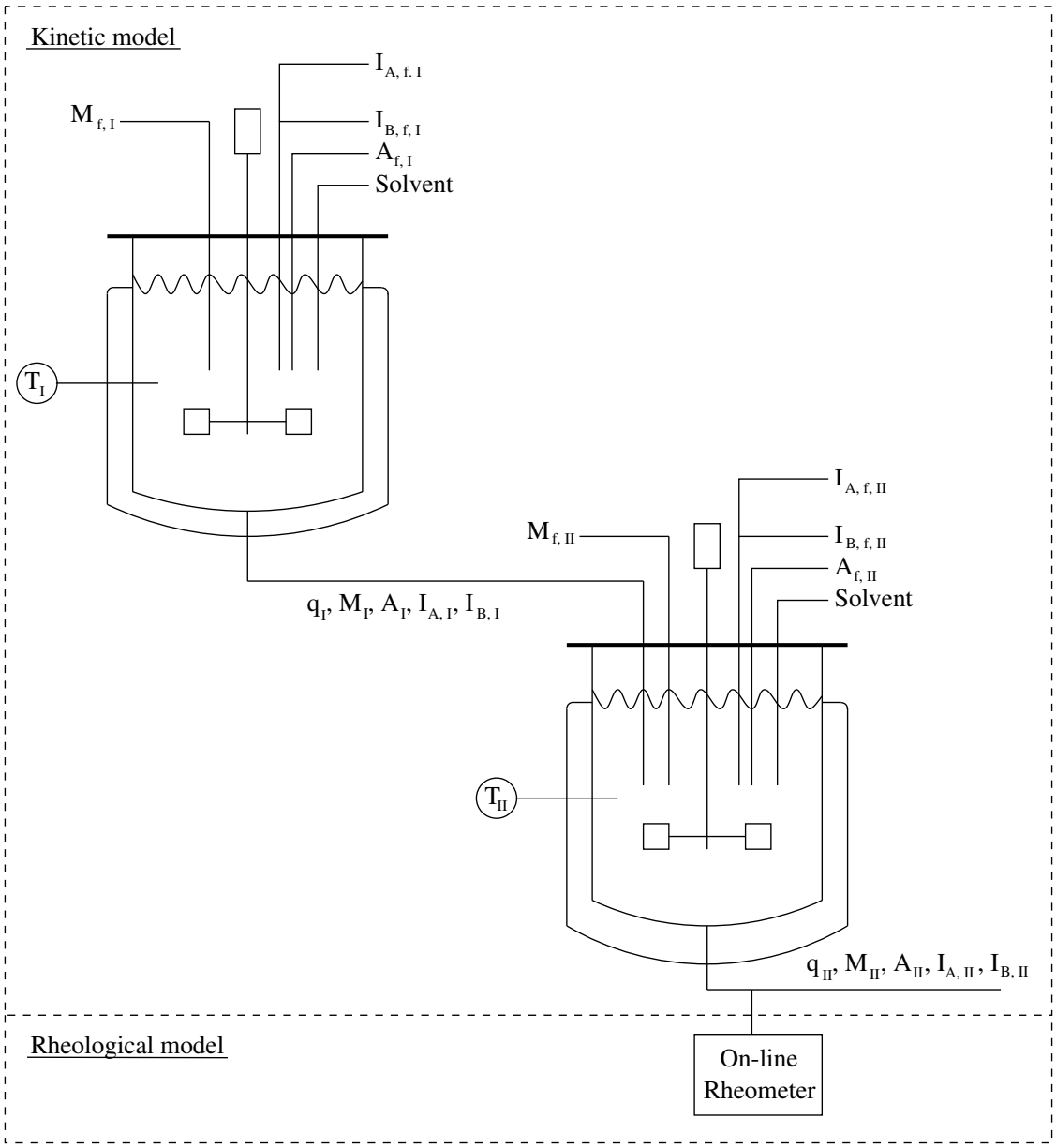

Figure 3.1: Process flow diagram and model structure for the solution polymerization of styrene.

polymer's WCLD. As a result, model validation using experimental data is greatly simplified in this case.

In this approach, the weight fraction of polymers is calculated over a number of finite chain length intervals covering the theoretically infinite chain length domain. It is possible to numerically integrate the kinetic rate expression for dead polymers for chain length values of 2 to ∞. However this method is superior in that the equations expressing the weight fraction of polymers in any given chain length interval are explicit and direct.

In order to derive component population balance equations, this method [28, 29] utilizes the classical model for free-radical polymerization. The symbols used in the subsequent model development are defined either in the text or in the relevant tables. A kinetic scheme for the free-radical solution polymerization of styrene is given in Table (3.1). In styrene polymerizations, termination is usually by combination (coupling) alone i.e. disproportionation termination reactions may be neglected (i.e. $k_{td} \approx 0$). Moreover, it may be safely assumed that the chain transfer reaction to solvent is also insignificant (i.e. $k_{fs} \approx 0$). The kinetic parameters are listed in Table (3.2). Only a fraction of the initiator molecules which decompose into free radicals also successfully initiate the growth of a polymer chain. Here, the initiator efficiency factors f_A and f_B are introduced to account for this fact. Densities of various species are given in Table (3.3) while other parameters and physical property values are given in Table (3.4). These values are used as reported in Crowley [28] and Kim and Choi [47].

In the kinetic scheme, I_A and I_B are the initiators A and B respectively; R is the primary radical; M is styrene, i.e. the monomer; A is the chain transfer agent (CTA); $P_{i,A}$ and $P_{i,B}$ are the live polymer chains with i repeating units generated using catalyst C_A^* and C_B^* respectively while $D_{i,A}$ and $D_{i,B}$ are the dead polymer chains with i repeating units generated using catalyst C_A^* and C_B^* respectively.

For the kinetic scheme described, the rate expressions for reactants, "live" (active) radical species and "dead" polymer products are derived using the following assumptions:

1. All the reactions are irreversible and elementary.

Table 3.1: Kinetic scheme for free-radical solution polymerization of styrene

Initiation by initiators:	$I_A \xrightarrow{k_{dA}} 2R$
	$I_B \xrightarrow{k_{dB}} 2R$
	$R + M \xrightarrow{k_i} P_1$
Thermal initiation:	$3M \xrightarrow{k_{dm}} 2P_1$
Propagation:	$P_i + M \xrightarrow{k_p} P_{i+1}$
Chain transfer to monomer:	$P_i + M \xrightarrow{k_{fm}} D_i + P_1 \quad (i \geq 1)$
Chain transfer to chain transfer agent:	$P_i + A \xrightarrow{k_{fa}} D_i + P_1 \quad (i \geq 1)$
Chain transfer to solvent:	$P_i + S \xrightarrow{k_{fs}} D_i + S\cdot \quad (i \geq 1)$
Combination termination:	$P_i + P_j \xrightarrow{k_{tc}} D_{i+j} \quad (i, j \geq 1)$
Disproportionation termination:	$P_i + P_j \xrightarrow{k_{td}} D_i + D_j \quad (i, j \geq 1)$

2. The primary radicals generated by the decomposition of labile groups in both initiators are indistinguishable in their activities for styrene polymerization.

3. The effects of primary radical termination and induced decomposition of initiators on the kinetics are small.

4. The reaction rate constants are independent of the chain length of the growing polymer molecule - the "long chain hypothesis". Moreover, an Arrhenius-type temperature dependance is also assumed[1].

5. The contents of the reactors are perfectly mixed[2]. As a result, there is no segregation and the temperatures and concentrations are uniform throughout the two vessels.

6. Both the reactors are of constant volumes, i.e. their level control loops are closed under perfect control.

[1] T = Temperature, (K).

[2] In industrial situations, specially designed impellers such as anchors or helical agitators are used to achieve this. Thereby a higher monomer conversion can be obtained at high temperatures.

Table 3.2: Kinetic parameters for solution polymerization of styrene

Initiator A ("slow") efficiency factor	f_A	0.637
Initiator B ("fast") efficiency factor	f_B	0.6
Initiator A decomposition rate const.	k_{dA}	$8.439 \times 10^{13} \exp(-32000/RT)$
Initiator B decomposition rate const.	k_{dB}	$1.200 \times 10^{13} \exp(-28690/RT)$
Thermal initiation rate const.	k_{dm}	$2.190 \times 10^{5} \exp(-27440/RT)$
Chain transfer to monomer rate const. l/(mol.s)	k_{fm}	$2.463 \times 10^{5} \exp(-10280/RT)$
Chain transfer to CTA rate const. l/(mol.s)	k_{fm}	$2.523 \times 10^{4} \exp(-7060/RT)$
Propagation rate const. l/(mol.s)	k_p	$1.051 \times 10^{7} \exp(-7060/RT)$
Combination termination rate const. l/(mol.s)	k_{tc}^*	$1.260 \times 10^{9} \exp(-16800/RT)$

Table 3.3: Densities in styrene polymerization (kg/l)

Monomer (styrene)	ρ_m, ρ_{mf}	$0.924 - 9.18 \times 10^{-4} T$
Initiator	ρ_I, ρ_{If}	1.18
Solvent (ethyl benzene)	ρ_s, ρ_{sf}	1.18
Polymer	ρ_p	$1.085 - 6.05 \times 10^{-4} T$

7. The inner (secondary) loops for the coolant flowing through the jackets are also closed. This is providing perfect and stabillizing jacket temperature control. In other words, the coolant temperature dynamics are extremely fast and so maybe be neglected.

In the following treatment, subscripts I and II are used to denote the first and the second reactors respectively. Obviously, for $r = I$, $r - 1$ denotes feed conditions. The mole balance equation for the primary radicals (R_r, where $r = I, II$) in the rth reactor is:

$$V_r \frac{dR_r}{dt} = V_r(2(f_A k_{dA,r} I_{A,r} + f_B k_{dB,r} I_{B,r} + k_{dm,r} M_r^3)) - k_{i,r} R_r M_r)) + q_{r-1} R_{r-1} - q_r R_r \tag{3.1}$$

Similar equations for the live polymer radicals ($P_{1,r}$) would be

$$V_r \frac{dP_{1,r}}{dt} = V_r(k_{i,r} R_r M_r - k_{p,r} M_r P_{1,r} + k_{fm,r} M_r (P_r - P_{1,r}) - k_{tc,r} P_r P_{1,r}) + q_{r-1} P_{1,r-1} - q_r P_{1,r} \tag{3.2}$$

Table 3.4: System parameters and physical property values in styrene polymerization

Mol. wt. of monomer, g/gmol	M_0	104.15
Initiator	ρ_I, ρ_{If}	1.18
Mol. wt. of solvent, g/gmol	S_0	1.18
Gas constant, kcal/kmol.K	R	1.987
Heat of reaction, kJ/mol	$(-\Delta H_r)$	68.04
Heat capacity of reaction mixture, kJ/ 1K	ρC_P	1.806

and those for the live polymer radicals with i repeating units ($P_{i,r}$, where $i \geq 2$) are

$$V_r \frac{dP_{i,r}}{dt} = V_r(k_{p,r}M_r(P_{i-1,r} - P_{i,r}) - k_{fm,r}M_r P_{i,r} - k_{tc,r}P_r P_{1,r}) \\ +q_{r-1}P_{i,r-1} - q_r P_{i,r} \tag{3.3}$$

The total concentration of live polymers in the rth reactor is defined as

$$\mathcal{P}_r \equiv \sum_{i=1}^{\infty} P_{i,r} \tag{3.4}$$

Using this definition,

$$V_r \frac{d\mathcal{P}_r}{dt} = V_r(k_{i,r}R_r M_r - k_{tc,r}\mathcal{P}_r^2) + q_{r-1}\mathcal{P}_{r-1} - q_r \mathcal{P}_r \tag{3.5}$$

Live polymer radicals are not measurable quantities such as monomer concentrations. Therefore, to simplify the equations and to obtain algebraic expressions for radical species in terms of measurable concentrations, the quasi-steady state approximation (QSSA) is used. As per this assumption, for a very short time interval, the rate of radical generation is almost equal to the rate of radical consumption. As a result, the derivative terms in the above equations reduce to zero, i.e.

$$\frac{dR_r}{dt} = \frac{dP_{1,r}}{dt} = \cdots = \frac{dP_{i,r}}{dt} = \frac{d\mathcal{P}_r}{dt} = 0$$

and so,

$$V_r(2(f_A k_{dA,r} I_{A,r} + f_B k_{dB,r} I_{B,r} + k_{dm,r}M_r^3)) - k_{i,r}R_r M_r)) + q_{r-1}R_{r-1} - q_r R_r \\ = -V_r(k_{i,r}R_r M_r - k_{tc,r}\mathcal{P}_r^2) - q_{r-1}\mathcal{P}_{r-1} + q_r \mathcal{P}_r \tag{3.6}$$

Ray [66] has shown that the loss of live radicals by washout is insignificant and so the flow terms in the corresponding dynamic mole balance equations maybe neglected. Hence, the total concentration of live polymer radicals in the rth reactor is given by:

$$\mathcal{P}_r = \left[\frac{2(f_A k_{dA,r} I_{A,r} + f_B k_{dB,r} I_{B,r} + k_{dm,r} M_r^3)}{k_{tc,r}}\right]^{1/2} \tag{3.7}$$

Next, the probability of propagation in the rth reactor is defined as

$$\alpha_r \equiv \frac{k_{p,r} M_r}{k_{p,r} M_r + k_{tc,r} \mathcal{P}_r + k_{fa,r} A_r + k_{fm,r} M_r} \tag{3.8}$$

Upon doing so the expressions for $P_{1,r}$ and $P_{i,r}$ can be simplified as follows

$$\left.\begin{aligned} P_{1,r} &= (1-\alpha_r)\mathcal{P}_r \\ P_{i,r} &= \alpha_r P_{i-1,r} = \alpha_r^2 P_{i-2,r} = \cdots \\ &= \alpha_r^{i-1} P_{1,r} \\ &= (1-\alpha_r)\alpha_r^{i-1}\mathcal{P}_r \end{aligned}\right\} \tag{3.9}$$

Equation (3.9) is referred to as the Flory or "most probable" chain length distribution. The mole balance equation for the dead polymer of chain length i generated in the rth reactor is:

$$V_r \frac{dD_{i,r}^r}{dt} = V_r \left[k_{fm,r} M_r P_{i,r} + \frac{k_{tc,r}}{2} \sum_{s=1}^{i-1} P_{s,r} P_{i-s,r}\right] - q_{p,r} D_{i,r}^r \tag{3.10}$$

The total concentration of the dead polymer of chain length i in the rth reactor is:

$$D_{i,r} = D_{i,r}^r + \sum_{p=1}^{r-1} D_{i,p}^r \tag{3.11}$$

where, $D_{i,p}^r$ is the concentration of the dead polymer of chain length i measured in the rth reactor but which was generated in the pth reactor. This quantity is evaluated as follows:

$$V_r \frac{dD_{i,p}^r}{dt} = q_{p,r-1} D_{i,p}^{r-1} - q_{p,r} D_{i,p}^r \tag{3.12}$$

Equation (3.9) can now be used to simplify the above equation to obtain the discrete WCLD:

$$\begin{aligned} \frac{dD_{i,r}^r}{dt} &= k_{fm,r} M_r P_{i,r} + \frac{k_{tc,r}}{2}\left[P_{1,r}P_{i-1,r} + P_{2,r}P_{i-2,r} + \cdots + P_{i-1,r}P_{1,r}\right] - \frac{q_r D_{i,r}^r}{V_r} \\ &= k_{fm,r} M_r P_{i,r} + \frac{k_{tc,r}}{2}\left[(i-1)P_{1,r}P_{i-1,r}\right] - \frac{q_r D_{i,r}^r}{V_r} \\ &= k_{fm,I} M_I P_{i,I} + \frac{k_{tc,I}\mathcal{P}_I}{2\alpha_I}(1-\alpha_I)(i-1)P_{i,I} - \frac{q_r D_{i,r}^r}{V_r} \end{aligned} \tag{3.13}$$

In order to take advantage of these features, it is required to develop the corresponding dynamic equations. For the rth reactor these would be

$$\frac{d\lambda_{0,r}}{dt} = \left[\frac{1}{2}k_{tc,r}\mathcal{P}_r + (k_{fm,r}M_r + k_{fa,r}A_r)\alpha_r\right]\mathcal{P}_r - \frac{q_{p,r}\lambda_{0,r}}{V_r} \tag{3.14}$$

$$\frac{d\lambda_{1,r}}{dt} = \left[k_{tc,r}\mathcal{P}_r + (k_{fm,r}M_r + k_{fa,r}A_r)(2\alpha_r - \alpha_r^2)\right]\frac{\mathcal{P}_r}{(1-\alpha_r)} - \frac{q_{p,r}\lambda_{1,r}}{V_r} \tag{3.15}$$

$$\frac{d\lambda_{2,r}}{dt} = \Big[k_{tc,r}\mathcal{P}_r(2-\alpha_r) + (k_{fm,r}M_r + k_{fa,r}A_r)(\alpha_r^3 - 3\alpha_r^2 + 4\alpha_r)\Big]\frac{\mathcal{P}_r}{(1-\alpha_r)^2} - \frac{q_{p,r}\lambda_{2,r}}{V_r} \tag{3.16}$$

In styrene polymerizartion, the chain termination at high monomer conversions (i.e. high polymer concentrations) is often diffusion limited. This is due to the mobility of the individual polymer radicals being impaired by entaglements with neighbouring polymer molecules. Thereby the rate of polymer radical termination is reduced and consequently the radical concentration increases. This results in an autoacceleration of the polymerization rate and is often called the Trommsdorf or "gel" effect. To account for this, the combination termination rate constant at zero monomer conversion (k_{tc}^* of Table (3.2)), is usually modified using an empirical gel-effect parameter (g_t). The correlation for g_t proposed by Hui and Hamielec [44] is applicable for bulk styrene polymerization. So it has to be adjusted for solution polymerization according to Hamer et al. [41].

$$g_t(=\frac{k_{tc}}{k_{tc}^*}) = exp(-2(g_a x_c + g_b x_c^2 + g c x_c^3)) \tag{3.17}$$

where, k_{tc} is the apparent combination termination rate constant

$$\left.\begin{aligned} g_a &= 2.57 - 5.05\times 10^{-3}T \\ q_b &= 9.56 - 1.76\times 10^{-2}T \\ q_c &= -3.03 + 7.85\times 10^{-3}T \end{aligned}\right\} \tag{3.18}$$

and the effective monomer conversion x_c in the presence of the solvent is

$$x_c = X_m(1-\phi_s) \tag{3.19}$$

X_m is the fractional monomer conversion, Moreover, ϕ_m, ϕ_i and ϕ_p represent the volume fractions of the monomer, initiator and polymer, respectively and are given by:

$$\phi_m = \frac{x_m m_t}{\rho_m V} \qquad \phi_p = \frac{1-(x_m + x_i + x_s)m_t}{\rho_p V} \qquad \phi_s = 1 - \phi_m - \phi_p \tag{3.20}$$

where ρ_j represents the density of component j. m_t is the total reaction mass. The total reactor volume, V, is assumed to be an ideal mixture of its components and is given by

$$V = \left(\frac{x_m}{\rho_m} + \frac{x_{p,r}}{\rho_p} + \frac{\hat{x}_{p,r}}{\rho_p} + \frac{x_i}{\rho_i} + \frac{x_s}{\rho_s} + \frac{x_A}{\rho_A} \right) m_t \tag{3.21}$$

Ignoring the generally small contribution of the initiation reaction, the dynamic mole balance equation for the monomer in the rth reactor is given as

$$V_r \frac{dM_r}{dt} = \frac{q_{m,r-1}\rho_{m,r-1}}{M_0} - \left[(k_{p,r} + k_{fm,r})\mathcal{P}_r V_r + q_{p,r} \right] M_r \tag{3.22}$$

Here $q_{m,r-1}$ represents the feed flow rate of styrene monomer, $\rho_{m,r-1}$, the feed monomer density, and M_0, the molecular weight of the monomer. Expressing the reactor mass balance equation above in the more convenient mass units,

$$\frac{dm_{m,r}}{dt} = q_{m,r}\rho_{mf} - (k_{p,I} + k_{fm,I})\mathcal{P}_I m_{m,I} - q_{p,I} M_0 M_I \tag{3.23}$$

Furthermore, since measurements are mass or molar concentrations rather than total mass, it is convenient to transform equation to dimensionless weight fraction units by defining

$$x_m \equiv \frac{m_m}{m_t} \tag{3.24}$$

Differentiating with respect to time yields

$$\begin{aligned} \frac{dx_{m,I}}{dt} &= \frac{1}{m_{t,I}} \frac{dm_{m,I}}{dt} - \frac{m_{m,I}}{m_{t,I}^2} \frac{dm_{t,I}}{dt} \\ &= \frac{q_{m,I}\rho_{mf}}{m_{t,I}} - (k_{p,I} + k_{fm,I})\mathcal{P}_I x_{m,I} - \frac{q_{p,I} x_{m,I}}{V_I} - \frac{x_{m,I}}{m_{t,I}} \frac{dm_{t,I}}{dt} \end{aligned} \tag{3.25}$$

Similarly for the second reactor,

$$\begin{aligned} \frac{dx_{m,II}}{dt} &= \frac{q_{m,II}\rho_{mf}}{m_{t,II}} - (k_{p,II} + k_{fm,II})\mathcal{P}_{II} x_{m,II} \\ &\quad + \frac{1}{V_{II}} \left[q_{p,I} x_{m,I} - q_{p,II} x_{m,II} \right] - \frac{x_{m,II}}{m_{t,II}} \frac{dm_{t,II}}{dt} \end{aligned} \tag{3.26}$$

$$\frac{dx_{IA,r}}{dt} = \frac{q_{I,r} y_{Af} \rho_{If}}{m_{t,r}} - k_{dA,r} x_{IA,r} - \frac{q_{p,r} x_{IA,I}}{V_I} - \frac{x_{IA,I}}{m_{t,I}} \frac{dm_{t,I}}{dt} \tag{3.27}$$

$$\frac{dx_{IB,I}}{dt} = \frac{q_{I,I}(1 - y_{Af})\rho_{If}}{m_{t,I}} - k_{dB,I} x_{IB,I} - \frac{q_{p,I} x_{IB,I}}{V_I} - \frac{x_{IB,I}}{m_{t,I}} \frac{dm_{t,I}}{dt} \tag{3.28}$$

where, y_{Af} is the mass fraction of Initiator A (i.e. tert-butyl perbenzoate) in the mixed initiator feed.

$$\frac{dm_{t,r}}{dt} = q_r\Big(\rho_{mf} + \rho_{If} + \rho_{If}\Big) + \frac{q_{p,I}m_{t,I}}{V_I} - \frac{q_{p,II}m_{t,II}}{V_{II}} \tag{3.29}$$

$$\sum_{i=m}^{n} iP_{i,r} = \left[\frac{m(1-\alpha_r)+\alpha_r}{(1-\alpha_r)}\right]\alpha_r^{m-1}\mathcal{P}_r - \left[\frac{(n+1)(1-\alpha_r)+\alpha_r}{(1-\alpha_r)}\right]\alpha_r^{n}\mathcal{P}_r \tag{3.30}$$

$$\begin{aligned}\sum_{i=m}^{n} i^2P_{i,r} &= \left[\frac{m^2(1-\alpha_r)^2+2\alpha_r m(1-\alpha_r)+\alpha_r^2+\alpha_r}{(1-\alpha_r)^2}\right]\alpha_r^{m-1}\mathcal{P}_r \\ &\quad -\left[\frac{(n+1)^2(1-\alpha_r)^2+2\alpha_r(n+1)(1-\alpha_r)+\alpha_r^2+\alpha_r}{(1-\alpha_r^2)}\right]\alpha_r^{n}\mathcal{P}_r\end{aligned} \tag{3.31}$$

The next step is to define the function $f_r(m,n)$ which represents the weight fraction of the polymer in the product stream leaving the rth reactor with chain lengths within an arbitrary but finite interval m to n i.e.

$$\begin{aligned}f_r(m,n) &\equiv \frac{\text{weight of polymer generated in the } r\text{th reactor with chains lengths from m to n}}{\text{total weight of polymer generated in the } r\text{th reactor}} \\ &= \frac{\sum_{i=m}^{n} iD_{i,r}}{\sum_{i=2}^{\infty} iD_{i,r}} = \frac{\sum_{i=m}^{n} iD_{i,r}}{\lambda_{1,r}}\end{aligned} \tag{3.32}$$

As done before, here too the contribution of live polymers is ignored because their concentrations are very small. Differentiating the above equation,

$$\begin{aligned}\frac{df_r(m,n)}{dt} &= \frac{1}{\lambda_{1,r}}\sum_{i=m}^{n} i\frac{dD_{i,r}}{dt} + \sum_{i=m}^{n} iD_{i,r}\left(-\frac{1}{\lambda_{1,r}^2}\frac{d\lambda_{1,r}}{dt}\right) \\ &= \frac{1}{\lambda_{1,r}}\sum_{i=m}^{n} i\frac{dD_{i,r}}{dt} - \frac{f_r(m,n)}{\lambda_{1,r}}\frac{d\lambda_{1,r}}{dt}\end{aligned} \tag{3.33}$$

$$\begin{aligned}\sum_{i=m}^{n} i\frac{dD_{i,r}}{dt} &= k_{fm,r}M_r\sum_{i=m}^{n} iP_{i,r} + \left[\frac{k_{tc,r}\mathcal{P}_r}{2\alpha_r}(1-\alpha_r)\right]\sum_{i=m}^{n}(i^2P_{i,r} - iP_{i,r}) \\ &\quad -\frac{1}{V_r}\sum_{i=m}^{n} iq_{p,r}D_{i,r})\end{aligned} \tag{3.34}$$

Substituting the appropriate terms using, the dynamic mass fraction equation for the polymer generated in the rth reactor would be

$$\frac{df_r(m,n)}{dt} = \frac{V_r}{\lambda_{1,r}}\left(\frac{k_{tc,r}}{2\alpha_r}P_r^2(1-\alpha_r)\left(\left[\frac{m^2(1-\alpha_r)^2+2\alpha_r m(1-\alpha_r)+\alpha^2+\alpha}{(1-\alpha_r)^2}\right]\alpha_r^{m-1}\right.\right.$$

$$+\left[\frac{(n+1)(1-\alpha_r)+\alpha_r}{(1-\alpha_r)}\right]\alpha_r^n - \left[\frac{m(1-\alpha_r)+\alpha_r}{(1-\alpha_r)}\right]\alpha_r^{m-1}$$
$$-\left[\frac{(n+1)^2(1-\alpha_r)^2+2\alpha_r(n+1)(1-\alpha_r)+\alpha_r^2+\alpha_r}{(1-\alpha_r^2)}\right]\alpha_r^n\Bigg)$$
$$+(k_{fm,r}M_r+k_{td,r}P_r)P_r\Bigg(\left[\frac{m(1-\alpha_r)+\alpha_r}{(1-\alpha_r)}\right]\alpha_r^{m-1}$$
$$-\left[\frac{(n+1)(1-\alpha_r)+\alpha_r}{(1-\alpha_r)}\right]\alpha_r^n\Bigg)\Bigg) - \frac{q_{p,r}}{V_r}f_r(m,n) - \frac{f_r(m,n)}{\lambda_{1,r}}\frac{d\lambda_{1,r}}{dt} \tag{3.35}$$

In order to model the entire shape of the MWD in a computationally efficient manner, the method of finite molecular weight moments is implemented as follows. The minimum chain length, n_{min}, and the number of intervals, n_{int}, are inputs. Although larger values can be used, usually n_{min} is chosen to be 2. An initial value for the maximum chain length, n_{max}, is guessed. The length of each individual interval, l_{int}, is given by:

$$l_{int} = \frac{(n_{max} - n_{min})}{n_{int}} \tag{3.36}$$

Then, for each chain length interval, j, the upper and lower bounds, m and n are:

$$m = n_{min} + (j-1)l_{int} \qquad\qquad n = m + l_{int} \tag{3.37}$$

inserted in the ODE for the mass fraction of polymer. Equation (3.25) to (3.28) and equation(3.35) i.e. $n_{int}+4$ ODEs are solved simultaneously. However, the initial guess for n_{max} might not be appropriate, i.e., the range of molecular weights covered might be too large or too small. Theoretically n_{max} should be close to infinity but an unnecessarily large value would be worthless and could lead to a loss in resolution. In order to ensure that the predicted MWD incorporates the entire significant portion of the distribution, n_{max} is varied and the entire calculation repeated until a certain criteria is satisfied. For example

$$f_{sum} = \sum_{j=1}^{n_{int}} f_{j,II} \geq 0.9999 \tag{3.38}$$

ensures that 99.99% of the MWD range is covered. Such a strict criterion is to ensure that all the high molecular weight fractions are included. This is necessary because the rheological behavior of polymer melts is more sensitive to the higher end of the MWD. It can be seen that in order to

decide a suitable n_{max}, a very large number of ODEs have to be solved simultaneously. In order to reduce this computational burden, which could be particularly acute for very large values of n_{int}, Yoon et al. [84] suggested an improvement in the method and demonstrated it for the thermal polymerization of styrene. Accordingly, for the case of the solution polymerization of styrene, while fixing n_{max} by a trial and error search, instead of the n_{int} ODEs for the mass fractions, a single ODE given by:

$$\begin{aligned}\frac{df_{sum}}{dt} &= \frac{df_{II}(2,n_{max})}{dt} = \frac{V}{\lambda_1}\Bigg(\frac{k_{tc}}{2\alpha}P^2(1-\alpha)\Bigg(\Bigg[\frac{4(1-\alpha)^2+4\alpha(1-\alpha)+\alpha^2+\alpha}{(1-\alpha)^2}\Bigg]\alpha \\ &\quad +\Bigg[\frac{(n_{max}+1)(1-\alpha)+\alpha}{(1-\alpha)}\Bigg]\alpha^{n_{max}} - \frac{(2\alpha-\alpha^2)}{(1-\alpha)} \\ &\quad -\Bigg[\frac{(n_{max}+1)^2(1-\alpha)^2+2\alpha(n_{max}+1)(1-\alpha)+\alpha^2+\alpha}{(1-\alpha^2)}\Bigg]\alpha^{n_{max}}\Bigg) \qquad (3.39) \\ &\quad +(k_{fm}M+k_{td}P)P\Bigg(\frac{(2\alpha-\alpha^2)}{(1-\alpha)} \\ &\quad -\Bigg[\frac{(n_{max}+1)(1-\alpha)+\alpha}{(1-\alpha)}\Bigg]\alpha^{n_{max}}\Bigg)\Bigg) - \frac{q_p}{V}f(2,n_{max}) - \frac{f(2,n_{max})}{\lambda_1}\frac{d\lambda_1}{dt} \qquad (3.40)\end{aligned}$$

may be solved and the condition of Equation (3.38) maybe verified. In this way only 5 ODEs instead of the $n_{int}+4$, have to be solved. And then once n_{max} is fixed, the individual mass fractions may be determined by solving all the ODEs.

3.2 Rheological models

All the empirical correlations for the zero shear viscosity for linear PSs are in the form of Equation (1.4). Bremner and Rudin [15] proposed the following correlations which they claim provides an excellent fit for the melt flow index (MFI), expressed in g/10 min, of a family of PSs having simliar polydispersities:

$$\frac{1}{MFI} = 3.679\times10^{-20}\overline{M}_w^{3.4} \qquad (3.41)$$

From among the several MWD to viscosity (η) versus shear rate ($\dot{\gamma}$) models available, Nichetti and Manas-Zloczowers' method (Section (2.3.3)) is adopted here because of its simplicity and the fact that it is able to predict the second Newtonian region at high shear rates, i.e. the limiting

Table 3.5: Model parameters for polydisperse PS samples at 180^oC.

k	8.43×10^{-13}	p. 962 in Nichetti and Manas-Zloczower [63]
τ_c	33905	p. 962 in Nichetti and Manas-Zloczower [63]
M_c	1100	p. 129 in Graessley [38]
ρ	920	

viscosity η_∞. In order to model the MWD to first normal stress difference (N_1) versus shear stress (τ_w) trends, the following expression, obtained by plugging Equation (2.27) into Equation (1.1), is used:

$$N_1 = 2J_e\tau_w^2 = \Big(\frac{4}{5\rho RT}\Big)\frac{\overline{M}_z\overline{M}_{z+1}}{\overline{M}_w}\tau_w^2 \tag{3.42}$$

As per the discussion in Section (1.6.1), it is obvious that the above approach suffers from inaccurate predictions at high shear stresses. The die swell-ratio is evaluated using the Tanner equation, i.e. Equation (1.2). In order to use the above models for polydisperse PS, the necessary parameters for samples at 180^oC are listed in Table (3.5).

3.3 Steady state parametric sensitivity analysis

It is important to observe the ability of the on-line rheometer to capture the important aspects of the process dynamics. In order to do so one has to study the effect of variations in the operating conditions on the viscoelastic properties of the polymer product. Kim et al. [46] have investigated the dynamics of a similar reactor cascade process and have observed that the system exhibits quite complex nonlinear steady state and transient behavior. The primary sources of nonlinear behavior are the gel-effect and the Arhennius temperature dependence of the rate constants. Bifurcations to various types of periodic solutions such as Hopf bifurcations, isolas, period doubling, period-doubling cascade, and homoclinics were observed. However, in carrying out this steady state parametric sensitivity analysis, it is assumed that operating conditions under consideration correspond to unique and stable steady states only. This is a reasonable assumption because in industrial practice, operating personnel usually prefer to avoid operating conditions

Table 3.6: SOCs in styrene polymerization case study.

Parameter	Reactor I	Reactor II
Reactor volume, V_r (l)	12	12
Total feed/product flow rate, q_r (l/hr)	3	$3 + q_I$
Reactor residence time, θ_r (hr)	4	4
Reactor temperature, T_r (^{o}C)	60	70
Fraction of solvent in feed, $f_{s,r}$	0.2	0.2
Total initiator feed conc., $I_{f,r}$ (mol/l)	0.0025	0.002
Mole fraction of intiator A in feed , $y_{A,r}$	0.75	0.2
Feed chain transfer agent conc., $A_{f,r}$ (mol/l)	1×10^{-3}	5×10^{-2}

associated with multiple steady states since these may give rise to unstable and unpredictable dynamics.

The standard operating conditions (SOCs) for this case study are given in Table (3.6). It should be noted that these SOCs are similar to those reported by Kim and Choi [47]. The aim is to observe the influence of variations in the following parameters on the product's MWD and rheological properties.:

- Reactor volumes (i.e. V_I and V_{II}) and hence the residence times.
- Feed monomer concentrations reflected in the solvent fractions in the feeds (i.e. $f_{s,I}$ and $f_{s,II}$).
- Total initiator feed concentrations (i.e. $I_{f,I}$ and $I_{f,II}$).
- Mole fractions of initiator A in the feeds (i.e. $y_{Af,I}$ and $y_{Af,II}$).
- Reactor temperatures (i.e. T_I and T_{II}).
- Feed chain transfer agent (CTA) concentrations (i.e. $A_{f,I}$ and $A_{f,II}$).

The results are tabulated in Tables (3.7), (3.8) and (3.9) for easier comparison. In these tables, $\overline{M}_{w,I}$ and $\overline{M}_{w,II}$ denote the individual weight average molecular weights while ϕ_I and ϕ_{II} denote the weight fractions of the polymer generated in reactor I and II respectively. $\overline{M}_w$ and $\overline{PD}$ are

the composite weight average molecular weight and polydispersity respectively. $\eta(1)$ and $\eta(100)$ denote the non-Newtonian viscosities in units of Pa.s "measured" at shear rates (i.e. $\dot{\gamma}$) of 1 and 100 $\sec^{-1}$ respectively. MFI, in units of g/10 min. denotes the melt flow index estimated using Equation (3.41). The elastic behavior of different samples are compared at wall stresses found in typical melt indexers i.e. τ_w of about 300 kPa. $N_1(300)$, in units of Pa, denotes the first normal stress difference while $S_R(300)$ is the die swell-ratio at these conditions. The first column in all three tables correspond to values at the standard operating condtions, i.e. Table (3.6). The first row refers to the curve of the corresponding figure as the case may be. Figure (3.2) is a plot displaying product properties at SOCs. Curves corresponding to SOCs are always denoted as "a" in Figure (3.3) to (3.10). When different trends are being compared, the individual curves have been zoomed-in to show greater detail.

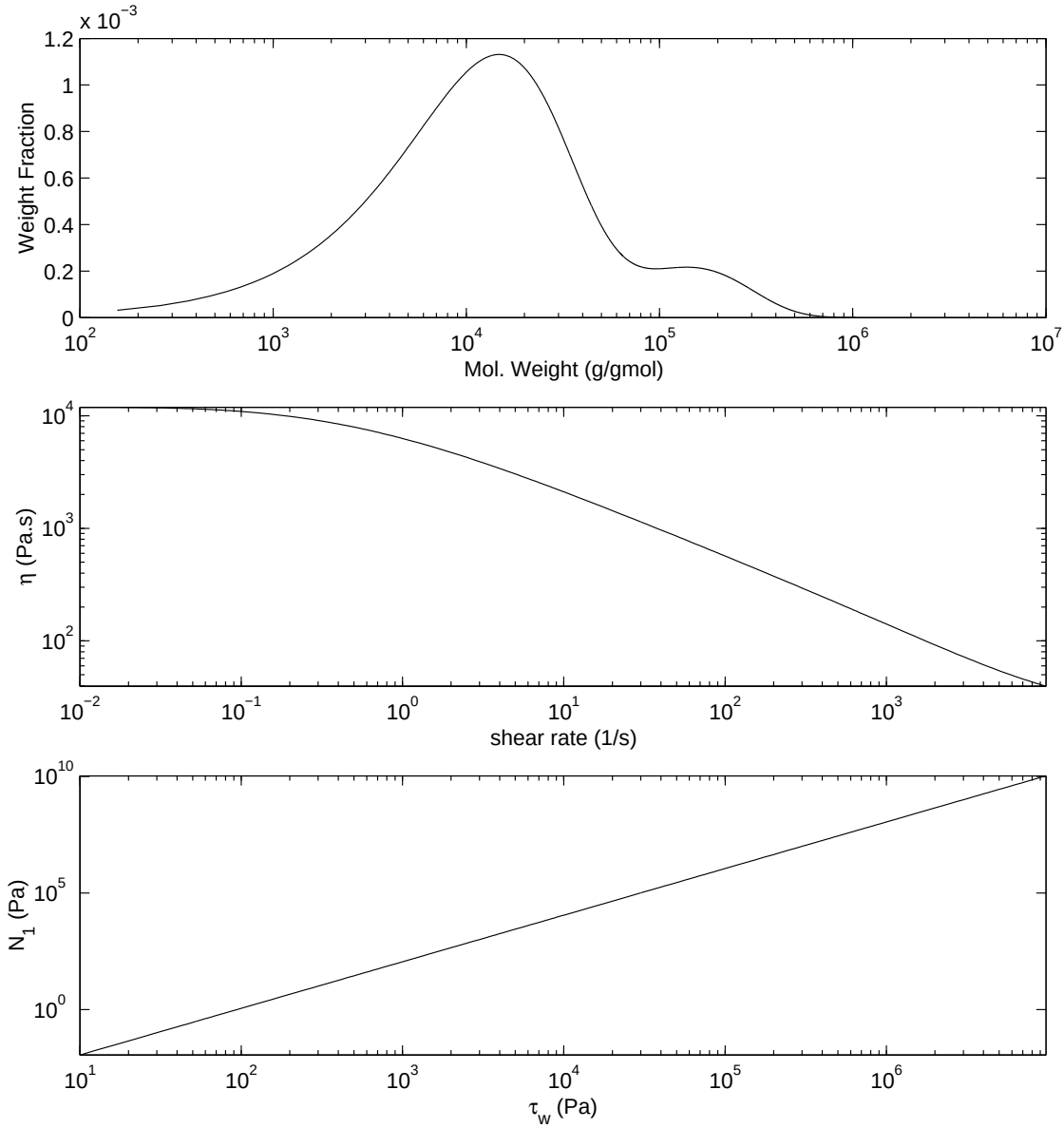

Figure 3.2: Product properties at standard operating conditions (SOCs).

Table 3.7: Sensitivity of product properties to operating conditions.

Parameter ⇒	SOC	V_I (l)		V_{II} (l)		$f_{s,I}$		$f_{s,II}$	
Curve	3.2 & a	3.3 b	3.3 c	-	-	3.4 b	3.4 c	-	-
Property ⇓		9	15	9	15	0.15	0.25	0.15	0.25
$\overline{M}_{w,I} \times 10^{-5}$	2.46	3.14	2.067	2.46	2.46	1.57	3.384	2.46	2.46
ϕ_I	0.6164	0.6316	0.6125	0.6395	0.5902	0.6308	0.5979	0.6308	0.5838
$\overline{M}_{w,II} \times 10^{-4}$	3.41	3.4	3.41	3.4	3.48	3.41	3.408	2.474	4.63
ϕ_{II}	0.3836	0.3684	0.3875	0.3605	0.4098	0.3692	0.4021	0.3692	0.4162
$\overline{M}_w \times 10^{-5}$	2.29	2.97	1.844	2.3	2.27	1.43	3.19	2.34	2.22
$\overline{PD}$	2.0856	2.1137	2.0311	2.0384	2.1345	1.9210	2.2142	2.1317	2.0463
Shape	B	B	B	B	B	B	B	B	U
$\eta(1) \times 10^{-4}$	1.09	2.09	0.629	1.20	0.981	0.343	2.03	1.1	1.02
$\eta(100) \times 10^{-3}$	6.29	9.57	4.32	6.894	5.7	2.81	8.97	6.3	5.97
MFI	16.2	6.684	33.9	15.85	16.71	80.75	5.26	15.16	17.95
$N_1(300)$	447.95	565.2	367.92	445.5	451.2	287.45	611.5	441.8	455.95
$S_R(300)$	1.1310	1.1317	1.1307	1.1310	1.1311	1.1304	1.1319	1.1310	1.1311

Table 3.8: Sensitivity of product properties to operating conditions (contd.).

Parameter ⇒	SOC	$I_{f,I}$ (mol/l)		$I_{f,II}$ (mol/l)		$y_{Af,I}$		$y_{Af,II}$	
Curve	4.2 & a	3.5 b	3.5 c	3.6 b	3.6 c	3.7 b	3.7 c	-	-
Property ⇓		0.002	0.003	0.0015	0.0025	0.5	1.0	0.1	0.7
$\overline{M}_{w,I} \times 10^{-5}$	2.46	2.96	2.13	2.46	2.46	1.50	6.75	2.46	2.46
ϕ_I	0.6164	0.6166	0.6162	0.6152	0.6161	0.6156	0.6255	0.6164	0.6087
$\overline{M}_{w,II} \times 10^{-4}$	3.41	2.43	3.38	3.73	3.15	3.12	3.78	3.28	4.36
ϕ_{II}	0.3836	0.3834	0.3838	0.3848	0.3839	0.3844	0.3745	0.3836	0.3913
$\overline{M}_w \times 10^{-5}$	2.29	2.737	1.97	2.28	2.3	1.367	6.55	2.29	2.25
$\overline{PD}$	2.0856	2.1282	2.0246	2.0619	2.1074	1.9585	2.2485	2.0961	2.0245
Shape	B	B	B	B	B	B	B	B	B
$\eta(1) \times 10^{-4}$	1.09	1.64	7.5	1.1	1.1	0.28	5.97	1.08	1.10
$\eta(100) \times 10^{-3}$	6.29	8.12	4.9	6.4	6.2	2.35	18.4	6.24	6.44
MFI	16.2	18.86	27.27	16.5	15.97	93.8	0.457	16.1	17.16
$N_1(300)$	447.95	527.4	389.4	449.4	446.8	276.7	1193	447.3	452.2
$S_R(300)$	1.1310	1.1314	1.1308	1.1310	1.1310	1.1304	1.1373	1.1310	1.1311

Table 3.9: Sensitivity of product properties to operating conditions (contd.).

Parameter ⇒	SOC	T_I (deg^{0}C)		T_{II} (deg^{0}C)		$A_{f,I}$ (mol/l)		$A_{f,II}$ (mol/l)	
Curve	4.2 & a	3.8 b	3.8 c	-	-	3.9 b	3.9 c	3.10 b	3.10 c
Property ⇓		55	65	65	75	1×10^{-5}	1×10^{-2}	1×10^{-2}	10×10^{-2}
$\overline{M}_{w,I} \times 10^{-5}$	2.46	3.76	1.59	2.46	2.46	2.7	1.233	2.46	2.46
ϕ_I	0.6164	0.6289	0.616	0.6294	0.5991	0.6164	0.6164	0.6164	0.6164
$\overline{M}_{w,II} \times 10^{-4}$	3.41	3.4	3.41	3.78	3.00	3.4	3.4	6.67	2.12
ϕ_{II}	0.3836	0.3711	0.384	0.3706	0.4009	0.3836	0.3836	0.3836	0.3836
$\overline{M}_w \times 10^{-5}$	2.29	3.58	1.442	2.29	2.297	2.59	1.102	2.2	2.346
$\overline{PD}$	2.0856	2.1585	1.9461	2.03606	2.1591	2.1173	1.8541	1.8620	2.2004
Shape	B	B	B	B	B	B	B	B	B
$\eta(1) \times 10^{-4}$	1.09	2.98	3.3	1.175	9.9	1.65	0.927	1.45	0.988
$\eta(100) \times 10^{-3}$	6.29	11.95	2.7	6.76	5.7	8.32	0.876	8.8	9.88
MFI	16.2	3.54	78.28	6.3	16.07	10.7	195.4	18.6	14.97
$N_1(300)$	447.95	672.9	292.6	448.0	447.8	501.1	226.7	452.7	440.8
$S_R(300)$	1.1310	1.1323	1.1304	1.1310	1.1310	1.1313	1.1303	1.1311	1.1310

The overall dependance of the rheological properties on the MWD is consistent with the general observations made in Section (1.6.1) and depicted in Figures (1.2) and (1.3). Specifically,

- The η_0 values increase while the MFIs decrease as the $\overline{M}_w$ increases. At a constant $\overline{M}_w$ these values are almost unaffected by the $\overline{PD}$ (i.e. the breadth of the distribution).
- The onset of non-Newtonian behavior occurs at lower shear rates as the $\overline{M}_w$ increases and as the $\overline{PD}$ increases i.e. the MWD broadens.
- The fluid elasticty, reflected through N_1 and S_R, increases as the $\overline{M}_w$ and the $\overline{PD}$ increase.

Based upon the above arguements, the sensitivity of product properties to operating conditions can be summarized as follows:

1. As seen from Figure (3.3), variations in V_I have a strong influence on the rheological properties eventhough this effect is not very evident from the variations in the MWD. This is primarily because changes in V_I affects the higher end of the MWD. The polymer produced using a higher residence time is less shear-thinning than the one produced with a lower residence time. In contrast, for a similar range of Reactor II volumes observed, V_{II} has a marginal effect on the $\overline{M}_w$ and $\overline{PD}$ because only the lower end of the distribution get affected. As a result, a corresponding effect on the rheological properties is also not seen. In general, an increase in reactor volume increases the reactor residence time (i.e. θ) which changes the relative amounts of chain propagation and non-chain propagation reactions. In industrial practice, limits for the reactor levels are dictated by the vessel and agitator design and so there is very little scope of variation. Reactant flow rates may be adjusted to change the residence times. However, reactor residence times are usually used to set the per pass conversion and/or the production rate. Hence, manipulating the reactor residence time in order to control the polymer product's MWD or it's rheological properties is not an attractive option.
2. Monomer concentration in the feed not only affects the rate of polymerization and hence the production rate but it also alters the MWD significantly. Lower monomer concentrations, i.e.

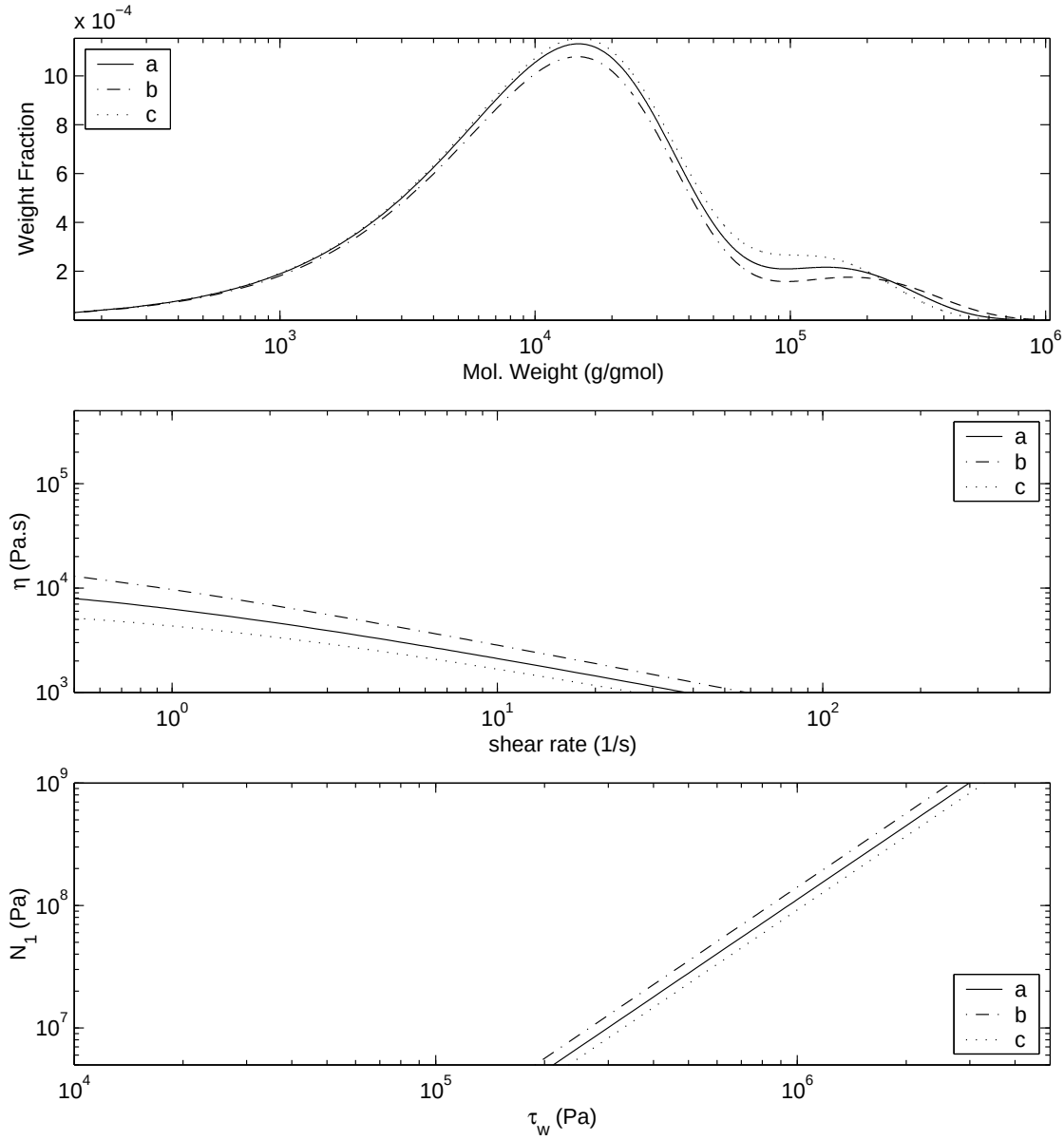

Figure 3.3: Influence of variations in Reactor I volume on product properties a = 12 l, b = 9 l and c = 15 l.

higher solvent fractions (f_s) produce a higher $\overline{M}_w$ polymer because the number of bimolecular termination reactions decrease. Varying the monomer concentraion in Reactor I has a very strong effect on the higher end of the MWD and so the rheological properties are also strongly affected. This is depicted in Figure (3.4). Again it is seen that varying the monomer feed concentration to Reactor II has little effect on the MWD because it primarily alters the lower end of the MWD. The rheological properties are insensitive to this variation. Inspite of the sensitivity to $f_{s,I}$, using the monomer concentration in the reactor as a manipulated variable to control the polymer product's MWD or it's rheological properties is not an attractive option because of its coupled effect on the rate of polymerization.

3. The effect of varying the total initiator feed concentration is similar to that seen for variations in the monomer concentrations, i.e. strong effects when the Reactor I conditions (Figure (3.5)) are varied but very little variation when the conditions in the reactor producing the low $\overline{M}_{w,r}$ portion of the MWD are changed (Figure (3.6). It can be seen that the rheological curves almost coincide. This behavior is representative of all cases wherein the variations are only in the low MW portions of the distribution. Again using the total initiator concentration in the reactors as a manipulated variable to control the polymer product's MWD or it's rheological properties is not a good idea because it has a much stronger effect on the rate of polymerization.

4. The effect of increasing the mole fraction of initiator A ("slow") in the feed to the reactor is that a fewer number of free radicals are available for chain intiation. At the same time the rate of termination also decreases. Consequently the molecular weight decreases. As seen from Figure (3.7), variations in $y_{Af,I}$ has a very strong affect on the MWD and the rheological properties. Undecomposed initiators are carried over onto the second reactor and so there is slight effcet on the polymer generated in the second reactor too. However, this interaction is one way, i.e. increasing the initiator concentration in the second reactor does affect the $\overline{M}_w$ in the first reactor.

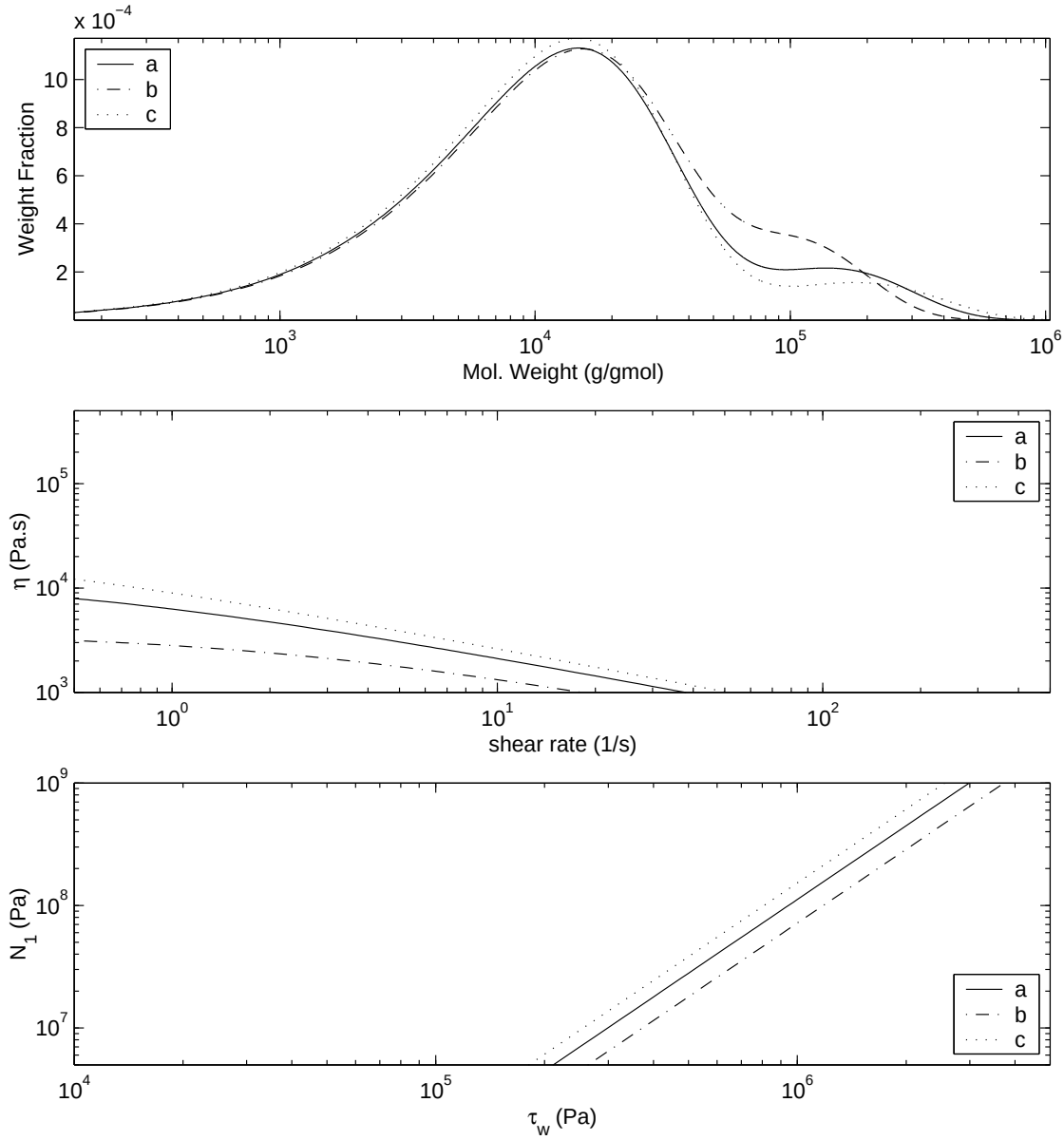

Figure 3.4: Influence of solvent fraction in the feed to Reactor I on product properties a = 0.2, b = 0.15 and c = 0.25.

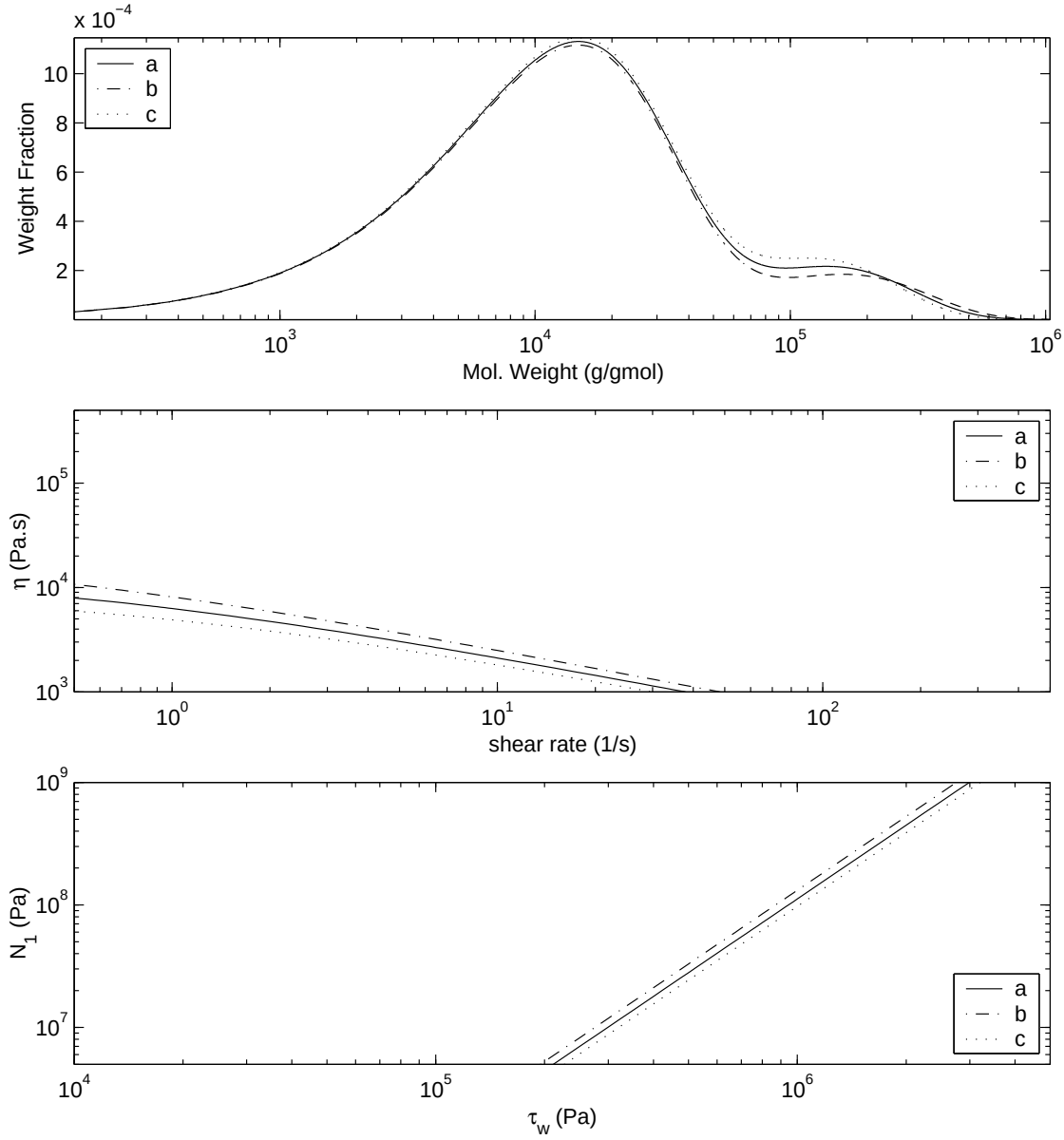

Figure 3.5: Influence of total initiator concentration in feed to Reactor I on product properties a = 0.0025, b = 0.002 and c = 0.003.

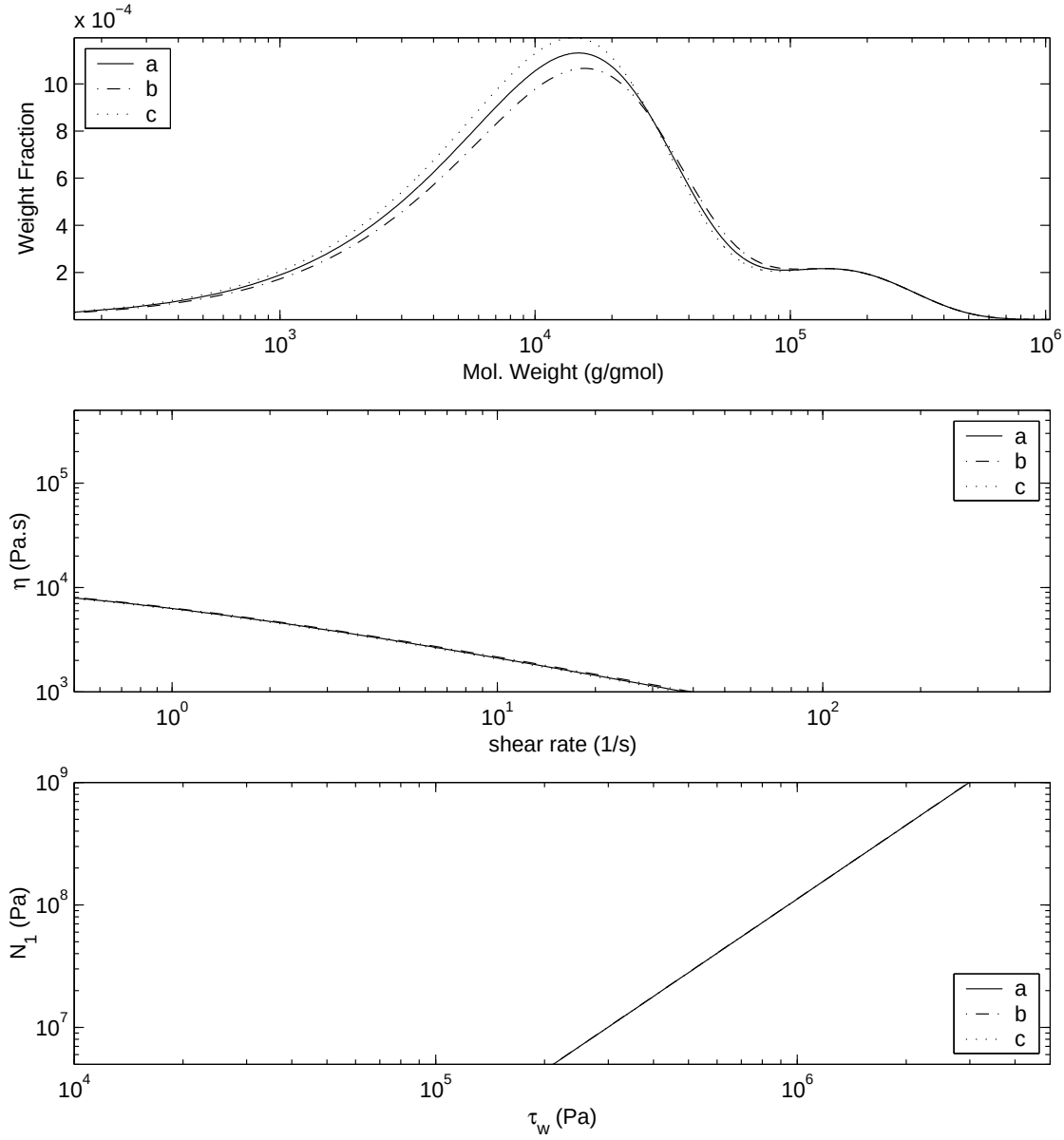

Figure 3.6: Influence of total initiator concentration in feed to Reactor II on product properties a = 0.002, b = 0.0015 and c = 0.0025.

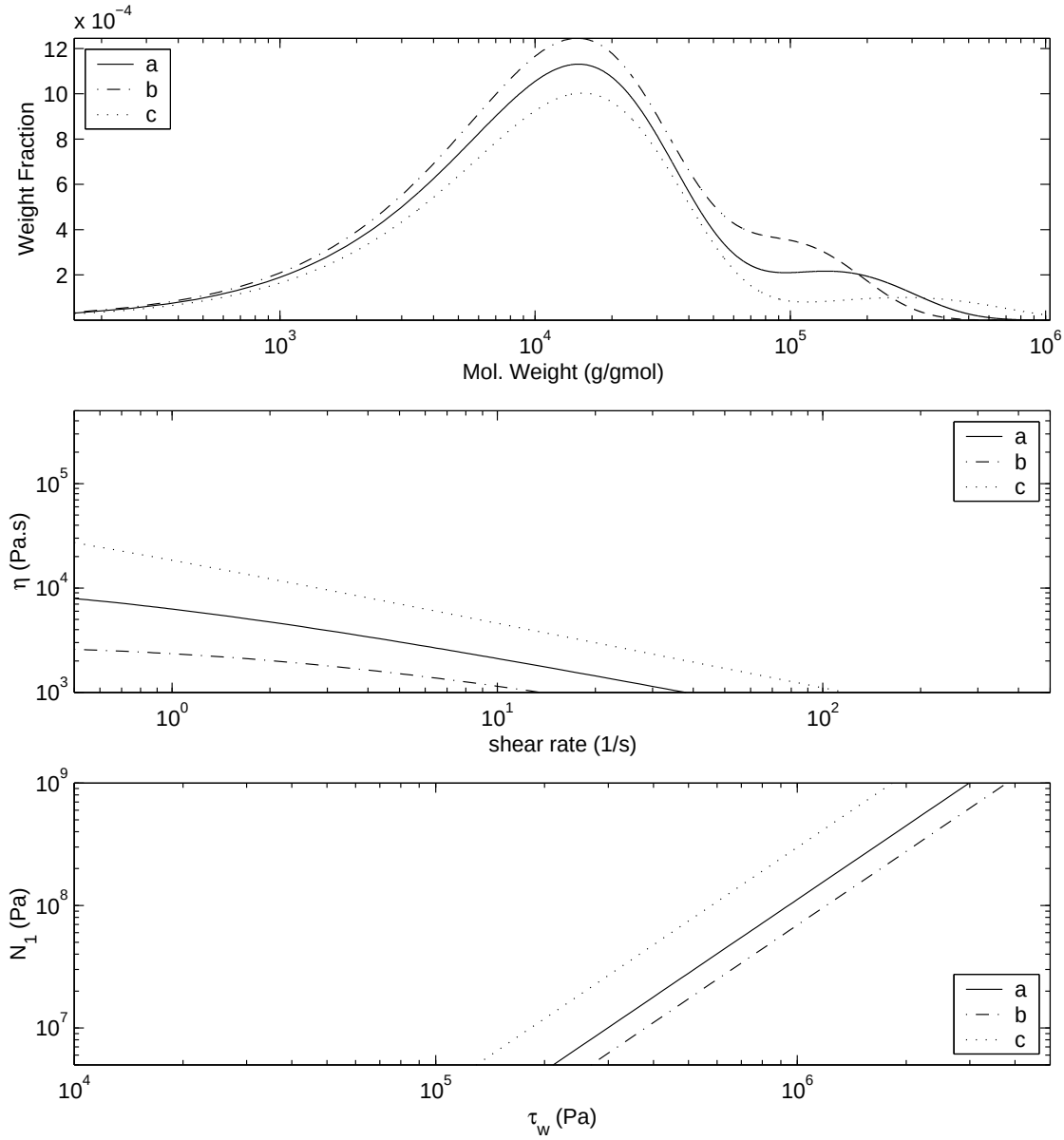

Figure 3.7: Influence of Reactor I initiator mole fraction in feed on product properties a = 0.75, b = 0.5 and c = 1.0.

5. As seen from Figure (3.8) the polymerization temperature has a very strong effect on the MW, MWD and rheological properties. This is also reflected in the rheological properties. As seen in the figure, Reactor I temperature affects the high end of the MWD more than the low end. As a result, there is more than a 25 fold increase in the MFI for a 10^oC rise in Reactor I temperature. Due to a higher $\overline{PD}$, the polymer produced at a lower temperature has a slightly steeper slope in the η versus $\dot{\gamma}$ plot, i.e. it is more shear-thinning. Again, very poor sensitivity to Reactor II conditions is observed. There is very little difference in the η versus $\dot{\gamma}$ plot while the N_1 versus τ_w are almost identical. In other words, the trend is similar to that seen in Figure (3.6). Inspite of this high sensitivity of product properties to Reactor I temperature, it should be pointed out that polymerization temperature also strongly affects the productivity. Moreover, it isn't a good idea to use reactor temperature as a manipulated variable in CSTRs involving exothermic reactions since this could lead to stability problems.

6. Variations in the chain transfer agent (CTA) feed concentrations have a very drastic effect on the product properties. Figure (3.9) and (3.10) show that $\overline{M}_{w,r}$ decreases as the CTA in reactor r increases. The rate of polymer production remains unaffected and so the $\phi_{I,r}$s are the same. The unreacted CTA molecules leaving Reactor I enter Reactor II. However, unlike the case for initiators, the amount of washover of CTA is very small because it's concentration in Reactor I is already very low. Hence, increasing the CTA concentration in Reactor I does not alter the $\overline{M}_w$ of the polymer generated in Reactor II. It should be noted that due to the increase in production of very low $\overline{M}_w$ waxes the maximum CTA concentration is usually not very high. In the case of a two reactor system, this limit also dictates the extent to which the $\overline{PD}$s can be varied. In order to obtain higher $\overline{PD}$s, a different reactor configuration has to be used.

With an aim to tailor the shape of the MWD and hence obtain a product of specifc rheological properties, the above discussion leads to the following conclusions:

- If a SISO control strategy is applied, the shape of the MWD can be altered using a maximum

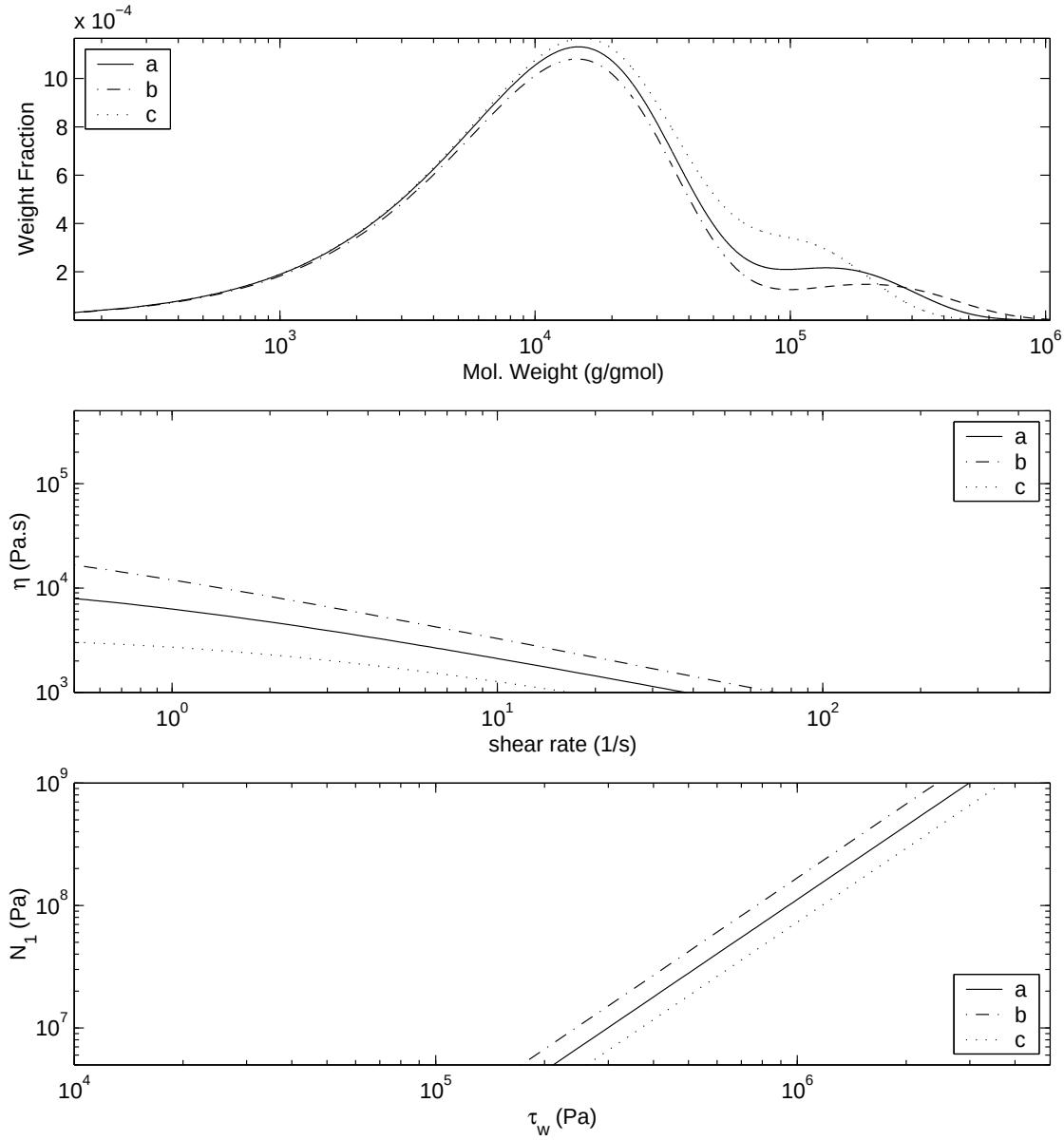

Figure 3.8: Influence of Reactor I temperature on product properties a = 60^oC, b = 55^oC and c = 65^oC.

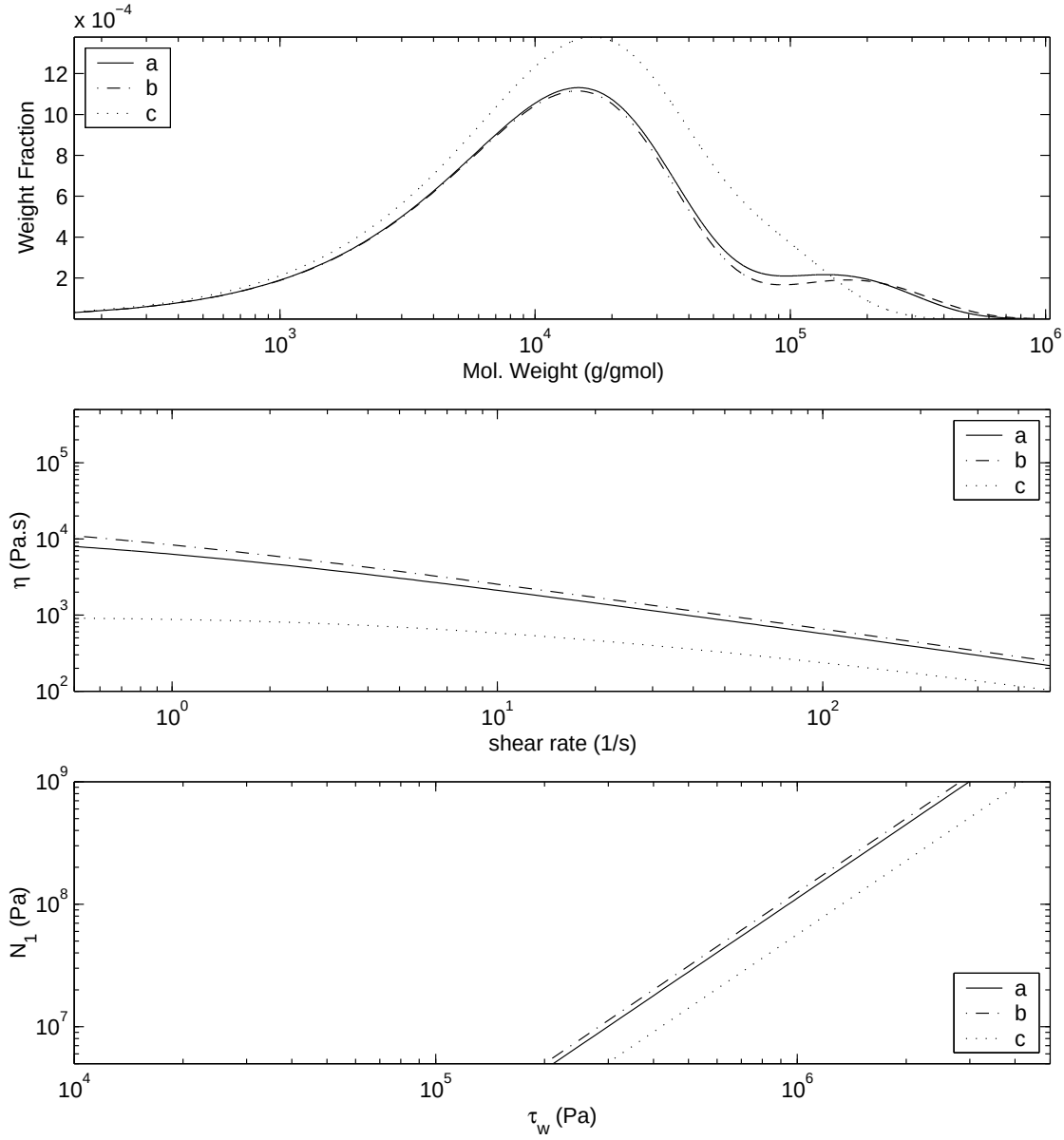

Figure 3.9: Influence of Reactor I feed CTA concentration on product properties a $= 1 \times 10^{-3}$, b $= 1 \times 10^{-5}$ and c $= 1 \times 10^{-2}$, mol/l.

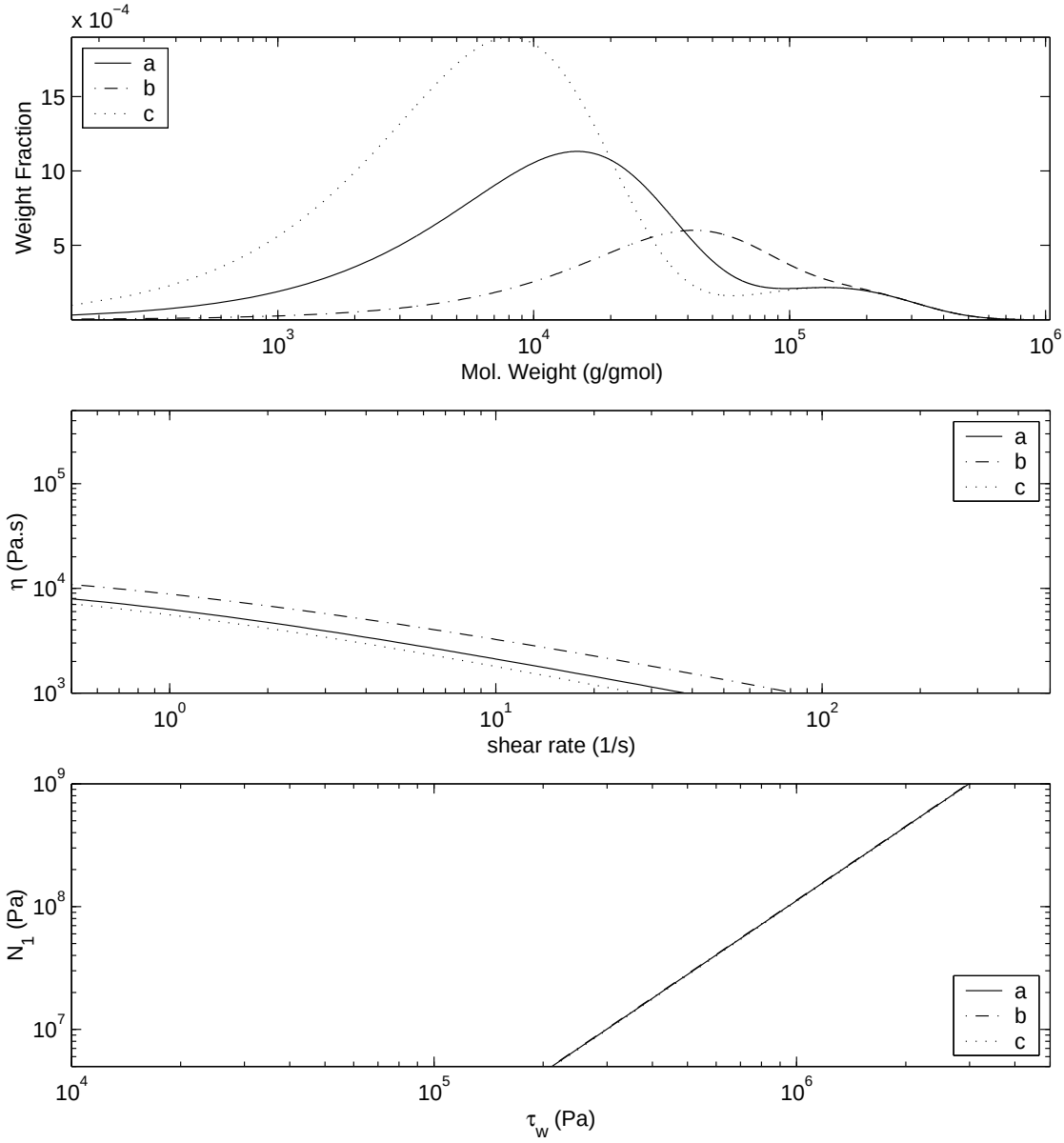

Figure 3.10: Influence of Reactopr II feed CTA concentration on product properties a $= 5 \times 10^{-2}$, b $= 1 \times 10^{-2}$ and c $= 10 \times 10^{-2}$, mol/l.

of two manipulated variables: the CTA concentrations A_I and A_{II} in the two CSTRs. It is not possible to use a third variable without disturbing the production rate.

- Using a multivariable control approach, such as model predictive control (MPC), it would be possible to alter the shape better because more manipulated variables can be altered simultaneously.

- The modality (i.e. the maximum number of peaks in the MWD) for this system is restricted to two.

Relative gain analysis is an effective tool used in process control. In order to carry out RGA, one needs an open-loop process gain matrix, $\mathbf{K}$,

$$\mathbf{y} = \mathbf{K}\mathbf{u} \tag{3.43}$$

Here, $\mathbf{y}$ is the vector of measurements (i.e. outputs y_i) and $\mathbf{u}$ is the vector of controlled variables (i.e. inputs u_j). The element $K_{i,j}$ of the matrix $\mathbf{K}$ relate the ith measurement to the jth manipulated variable. These can be calculated from a process model, or by numerical differentiation of a steady state simulation. The elements, $\lambda_{i,j}$, of the relative gain array (RGA), Λ, are given by the Hadamard product:

$$\lambda_{i,j} = K_{i,j} \times K^{-1}_{j,i} \tag{3.44}$$

For this case study, the RGA for negative perturbations in the manipulated variables is:

$$\begin{array}{ccc} & A_I & A_{II} \\ \eta(1) & 2.0830 & -1.0830 \\ \eta(100) & -1.0830 & 2.0830 \end{array} \tag{3.45}$$

and that for positive perturbations is:

$$\begin{array}{ccc} & A_I & A_{II} \\ \eta(1) & 0.5145 & 0.4855 \\ \eta(100) & 0.4855 & 0.5145 \end{array} \tag{3.46}$$

Since the numbers vary so much between negative and positive perturbations, it can be concluded that the system is highly non-linear. Also, the RGA elements reveal that there are mild interactions and so the loops can be easily de-coupled.

3.4 Notation

CTA	Chain Transfer Agent.
LCA	Long Chain Approximation.
NCLD	Number Chain Length Distribution.
MW	Molecular Weight.
MWD	Molecular Weight Distribution.
QSSA	Quasi Steady State Approximation.
RSSA	Reactor Steady State Approximation.

A	Conc. of chain transfer agent, mol/l.
C_c^*	Conc. of active catalyst of type c.
C_c	Conc. of inactive (deactivated) catalyst of type c.
$D_{i,c}$	Conc. of dead polymer chains with i repeating units generated in reactor r.
$k_{d,r}$	Deactivation rate constant for catalyst of type c.
$k_{p,r}$	Propagation rate constant for catalyst of type c.
$k_{fA,r}$	Chain transfer to CTA rate constant for reactor r.
$k_{fM,c}$	Chain tranfer to monomer rate constant for reactor r.
M	Conc. of monomer, i.e. styrene in reactor r, mol/l.
$\overline{M}_n$	Number average molecular weight.
$\overline{M}_w$	Weight average molecular weight.
$\overline{PD}$	Polydispersity.
$P_{i,r}$	Conc. of live polymer chains with i repeating units in reactor r
$\mathcal{P}_r$	Total conc. of live polymer chains in reactor r.
V_r	Volume of reacor r.

α_r	Probability of propagation for reactor r defined in Equation (3.8)

Chapter 4

Control of rheological properties in a continuous ethylene polymerization process

In terms of annual production, polyethylene (PE) is the largest synthetic commodity polymer. It's versatile physical and chemical properties have resulted in it's world-wide use. There are two major routes to manufacturing polyethylene. The high-pressure, free-radical polymerization process is primarily used to manufacture low density polyethylene (LDPE). The second route is through the use of transition metal catalysts (Ziegler-Natta, chromium oxide and metallocene catalysts) in a low pressure process. Owing to the uniformity of the active catalytic species, single-site catalysts have the unique capability of producing ethylene homo- and copolymers with a controlled narrow MWD (Polydispersity $= \overline{M}_w/\overline{M}_n \approx 2$). Polymer melts with a narrow MWD are usually not shear thinning enough. From a end-user's perspective, this is an undesirable rheological behavior which could create problems during processing. As pointed out earlier, although the rheological properties can be altered to some extent by blending in the last stages of manufacturing, it is preferable that this problem is addressed at the polymerization stage itself. There are two possible strategies to improve the rheological characteristics:

1. The intentional broadening of the MWD by the blending of several polymer samples/streams, each with a polydispersity ≈ 2. This may be achieved by either one of the following two approaches:

   (a) A cascade configuration of two or more reactors with different operating conditions.

   (b) A system of several single-site catalysts having different activities used in combination.

2. The systematic incorporation of long chain branches into the polymer. This is achieved by using a special type of metallocene catalyst: the constrained geometry catalyst (CGC) developed by researchers at Dow (see Batistini [2]; Todo and Kashiwa [76]).

The styrene polymerization case study in Chapter 3 is similar to 1(a) above. In this chapter we adopt the arrangement described in 1(b). The approach described in 2 above is further discussed in Chapter 5. In this study, the solution homo-polymerization of ethylene in a single, continuous stirred tank reactor (CSTR) is chosen as the process. The catalyst system considered is a proprietary high activity, soluble, industrial single-site catalyst used in conjunction with aluminium alkyl cocatalyst. Catalyst deactivition is The chain transfer agent (CTA) used is Hydrogen. Stabillizing base regulatory controllers for the control of reactor feed flows, reactor level, reactor and jacket cooling water temperatures have already been provided. In order to study the benefits of incorporating on-line rheological measurements into the polymerization reactor's control system, a rigorous first-principles kinetic model for the polymerization process is developed first. This model generates the discrete MWD of the product stream as its output which is plugged into a rheological model. Such an arrangement is expected to represent the real world output of an on-line rheometer installed in the product stream and thus providing the molten polymer's viscosity-shear rate data. This is depicted schematically in Figure (4.1). The comparative effectiveness of several strategies, in their ability to control the rheological properties during setpoint changes or while rejecting disturbances, is examined. Issues involved in the design of the control system to achieve this target are demonstrated via simulations.

4.1 Kinetic model

Crowley and Choi [27] proposed "the method of finite molecular weight moments" - a new method for calculating the weight chain length distribution (WCLD) of polymers. The WCLD is the preferred form of representing the MWD, over the number chain length distribution (NCLD), because

1. As noted in Chapter 2, most rheological, mechanical and other end-use properties depend more strongly on the WCLD than on the NCLD. Hence it would be the appropriate form for measurement, estimation and control purposes.

2. Experimentally, polymer molecular weight is measured most conviniently by gel permeation

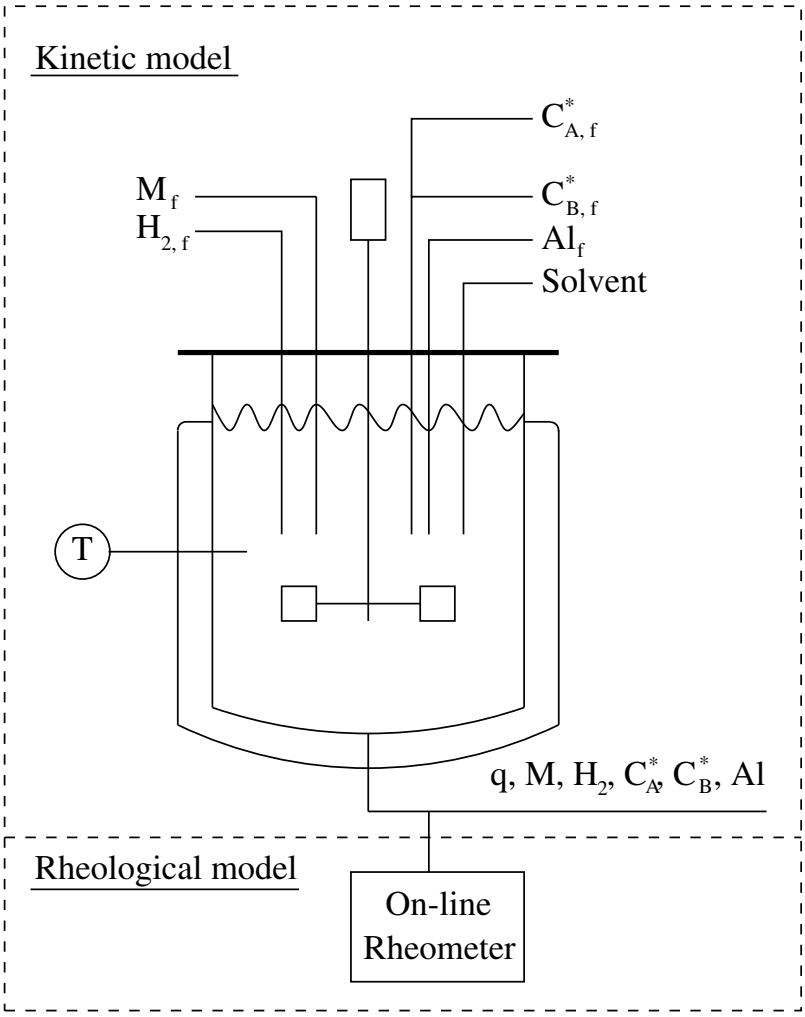

Figure 4.1: Process flow diagram and model structure for the solution polymerization of ethylene.

chromatography (GPC). GPC detectors (e.g., UV or IR detectors) are mostly mass-sensitive and so the resulting chromatograms (detector signal vs. retention time) also represent the polymer's WCLD. As a result, model validation using experimental data is greatly simplified in this case.

In this approach, the weight fraction of polymers is calculated over a number of finite chain length intervals covering the theoretically infinite chain length domain. It is possible to numerically integrate the kinetic rate expression for dead polymers for chain length values of 2 to ∞. However this method is superior in that the equations expressing the weight fraction of polymers in any given chain length interval are explicit and direct.

In order to derive component population balance equations, this method [28, 29] utilizes the classical model for single-site olefin catalyzed polymerization. A kinetic scheme for the solution polymerization of ethylene is given in Table (4.1). In ethylene polymerizations, the dominant form of chain termination is via chain transfer reactions i.e. disproportionation and combination termination reactions are absent. Moreover, it may be safely assumed that the chain transfer reaction to solvent is also insignificant (i.e. $k_{fs} \approx 0$). The kinetic parameters are listed in Table (4.2). These values have been slightly modified owing to the proprietary nature of the catalyst system. However, it can be seen that they are similar to values reported in the open literature (e.g. Kim and Choi [48], Charpentier et al. [21]).

In the kinetic scheme, C_A^* and C_B^* are the active catalyst sites of type A and B respectively; C_A and C_B are the deactivated catalyst sites of type A and B respectively; M is ethylene, i.e. the monomer; H_2 is Hydrogen, which is being used as the chain transfer agent (CTA); $P_{i,A}$ and $P_{i,B}$ are the live polymer chains with i repeating units generated using catalyst C_A^* and C_B^* respectively while $D_{i,A}$ and $D_{i,B}$ are the dead polymer chains with i repeating units generated using catalyst C_A^* and C_B^* respectively.

For the kinetic scheme described, the rate expressions for reactants, "live" (active) species and "dead" polymer products are derived using the following assumptions:

1. Experimental observations suggest complex phenomena such as the dissociative adsorption

Table 4.1: Kinetic scheme for the solution polymerization of ethylene using soluble single-site Catalysts.

Chain initiation:	$C_A^* + M \xrightarrow{k_{i,A}} P_{1,A}$
	$C_B^* + M \xrightarrow{k_{i,B}} P_{1,B}$
Chain propagation:	$P_{i,A} + M \xrightarrow{k_{p,A}} P_{i+1,A} \ \ (i \geq 1)$
	$P_{i,B} + M \xrightarrow{k_{p,B}} P_{i+1,B} \ \ (i \geq 1)$
Chain transfer to monomer:	$P_{i,A} + M \xrightarrow{k_{trM,A}} D_{i,A} + P_{1,A} \ \ (i \geq 1)$
	$P_{i,B} + M \xrightarrow{k_{trM,B}} D_{i,B} + P_{1,B} \ \ (i \geq 1)$
Chain transfer to Aluminium alkyl:	$P_{i,A} + Al \xrightarrow{k_{trAl,A}} D_{i,A} + C_A^* \ \ (i \geq 2)$
	$P_{i,B} + Al \xrightarrow{k_{trAl,B}} D_{i,B} + C_B^* \ \ (i \geq 2)$
Chain transfer to Hydrogen:	$P_{i,A} + H_2 \xrightarrow{k_{trH,A}} D_{i,A} + C_A^* \ \ (i \geq 2)$
	$P_{i,B} + H_2 \xrightarrow{k_{trH,B}} D_{i,B} + C_B^* \ \ (i \geq 2)$
Catalyst deactivation:	$C_A^* \xrightarrow{k_{d,A}} C_A$
	$C_B^* \xrightarrow{k_{d,B}} C_B$
	$P_{i,A} \xrightarrow{k_{d,A}} D_{i,A} + C_A \ \ (i \geq 2)$
	$P_{i,B} \xrightarrow{k_{d,B}} D_{i,B} + C_B \ \ (i \geq 2)$

of Hydrogen, etc. due to which the chain transfer reactions to Hydrogen and Aluminium alkyl are usually not elementary. However, this aspect is ignored here and it is assumed that all the reactions are irreversible and elementary.

2. The long chain approximation (LCA) is used, i.e. reaction rate constants are assumed to be independent of the chain length of the growing polymer molecule. Moreover, an Arrhenius-type temperature dependance is also assumed, i.e. rate constants are of the form $k = k_0 \exp(-\frac{E}{RT})$.

3. The quasi steady state approximation (QSSA) is used. As per this assumption, for a very short time interval, the rate of generation of live polymer or active catalyst sites is almost equal to it's rate of consumption.

4. It is assumed that the catalytic sites are already activated and when the catalyst comes in contact with the monomer, all the catalyst sites are immedeately occupied. Furthermore, the chain initiation rate constant is aasumed to be equal to the chain propagation rate constant, i.e. $k_i = k_p$. Site transformation and branching reactions are neglected.

5. The contents of the reactor are perfectly mixed[1]. As a result, there is no segregation and the temperatures and concentrations are uniform throughout vessel.

6. There are no volume or density changes due to mixing or during reaction. The reactor volume is constant, i.e. the level control loop is closed under perfect control. Hence the total inlet volumetric flow rate is equal to the outlet flow rate.

7. The inner (slave/secondary) loop for the coolant flowing through the jacket and the outer (master/primary) loop for the reactor temperature is closed. This is providing perfect and stabillizing jacket and reactor temperature control. In other words, the coolant and reactor temperature dynamics are extremely fast and so maybe be neglected.

[1] In industrial situations, specially designed impellers such as anchors or helical agitators are used to achieve this. Thereby a higher monomer conversion can be obtained at high temperatures.

Table 4.2: Kinetic parameters for solution polymerization of ethylene

Propagation rate const. l/(mol.s)	$k_{p,c}$	$7.5 \times 10^{11} \exp(-4900/T)$
Catalyst deactivation rate const.	$k_{d,c}$	$2.0 \times 10^{4} \exp(-4000/T)$
Chain transfer to monomer rate const. l/(mol.s)	$k_{trM,c}$	$5.0 \times 10^{21} \exp(-16400/T)$
Chain transfer to Aluminium-alkyl rate const. l/(mol.s)	$k_{trAl,c}$	$4.0 \times 10^{21} \exp(-17000/T)$
Chain transfer to hydrogen (for cat. A) rate const. l/(mol.s)	$k_{trH,A}$	$3.0 \times 10^{10} \exp(-3500/T)$
Chain transfer to hydrogen (for cat. B) rate const. l/(mol.s)	$k_{trH,B}$	$2.2 \times 10^{4} \exp(-2000/T)$

It should be noted that the assumptions made here are only meant to simplify the derivation and the mathematics involved. They do not pose any restrictions on the applicability of the franework nor do they increase the complexity of its implememntation. In the following treatment, the subscript c is used to denote any species associated with catalyst sites of type c. The equations have been derived in a generalized fashion so that they can be applied to systems with an arbitrary number of different catalyst site types. In the present study the number is restricted to two, i.e. $c = A$ or B. First, the total concentration of live polymers generated by a catalyst of type c is defined as

$$\mathcal{P}_c \equiv \sum_{i=1}^{\infty} P_{i,c} \tag{4.1}$$

The sum of the active site, live polymer and dead site concentration is equal to the initial concentration of the catalyst sites in the feed, i.e.

$$C^*_{f,c} = C^*_c + C_c + \sum_{i=1}^{\infty} P_{i,c} = C^*_c + C_c + \mathcal{P}_c \tag{4.2}$$

The dynamic mole balance equations for the monomer, hydrogen and aluminium alkyl are given by

$$V\frac{dM}{dt} = V(-k_{p,c}MC^*_c - k_{p,c}M\sum_{i=1}^{\infty} P_{i,c} - k_{trM}M\sum_{i=1}^{\infty} P_{i,c}) + q(M_f - M) \tag{4.3}$$

$$V\frac{dH_2}{dt} = V(-k_{trH}H_2\sum_{i=2}^{\infty} P_{i,c}) + q(H_{2,f} - H_2) \tag{4.4}$$

$$V\frac{dAl}{dt} = V(-k_{trAl}Al\sum_{i=2}^{\infty} P_{i,c}) + q(Al_f - Al) \tag{4.5}$$

where, V is the reactor volume and q represents the volumetric flow rate of the stream leaving the reactor. As per Assumption (6), this is also the total volumetric flow rate of the feeds to the reactor. The concentration of the feed streams are based on this flow rate. The dynamic mole balance equations for active and inactive (i.e. deactivated) catalyst sites of type c in the reactor are

$$V\frac{dC_c^*}{dt} = V(-k_{i,c}C_c^*M + k_{trH,c}H_2\sum_{i=2}^{\infty}P_{i,c} + k_{trAl,c}Al\sum_{i=2}^{\infty}P_i - k_{d,c}C_c^*) + q(C_{f,c}^* - C_c^*) \quad (4.6)$$

$$V\frac{dC_c}{dt} = V(k_{d,c}C_c^* + k_{d,c}\sum_{i=2}^{\infty}P_{i,c}) - qC_c \quad (4.7)$$

For live polymer chains with one repeating unit, the corresponding equation is

$$V\frac{dP_{1,c}}{dt} = V(k_{p,c}MC^* - k_{p,c}MP_{1,c} + k_{trM,c}M\sum_{i=2}^{\infty}P_{i,c}) - qP_{1,c} \quad (4.8)$$

and that for live polymer chains with i repeating units ($P_{i,c}$, where $i \geq 2$) is

$$V\frac{dP_{i,c}}{dt} = V\Big[k_{p,c}M(P_{i-1,c} - P_{i,c}) - (k_{trM,c}M + k_{trAl,c}Al + k_{trH,c}H_2 + k_{d,c})P_{i,c}\Big] - qP_{i,c} \quad (4.9)$$

Using the definition for the total live polymer concentration, i.e. Equation (4.1) in the above equation,

$$\begin{aligned} V\frac{d\mathcal{P}_c}{dt} &= V\frac{dP_{1,c}}{dt} + V\sum_{i=2}^{\infty}\frac{dP_{i,c}}{dt} \\ &= V(k_{p,c}MC_c^* - (k_{trAl,c}Al + k_{trH,c}H_2 + k_{d,c})(\mathcal{P}_c - P_{1,c}) - q\mathcal{P}_c \end{aligned} \quad (4.10)$$

Live polymer chains are not measurable quantities such as monomer concentrations. Therefore, to simplify the equations and to obtain algebraic expressions for radical species in terms of measurable concentrations, the QSSA is used. As a result, the derivative terms in the above equations reduce to zero, i.e.

$$\frac{dC_c^*}{dt} = \frac{dP_{1,c}}{dt} = \cdots = \frac{dP_{i,c}}{dt} = \frac{d\mathcal{P}_c}{dt} = 0$$

Moreover, Ray [66] has shown that the loss of live polymer by washout is insignificant and so the flow terms in the corresponding dynamic mole balance equations maybe neglected. Hence, from

Equation (4.6) the total concentration of active catalyst sites of type c is given by:

$$C_c^* = \left[\frac{k_{trH,c}H_2 + k_{trAl,c}Al + k_{d,c}}{k_{p,c}M + k_{trM,c}M + k_{trH,c}H_2 + k_{trAl,c}Al + k_{d,c}}\right]\mathcal{P}_c \tag{4.11}$$

Next, the probability of propagation pertaining to catalyst sites of type c is defined as

$$\alpha_c \equiv \frac{k_{p,c}M}{k_{p,c}M + k_{trM,c}M + k_{trAl,c}Al + k_{trH,c}H_2 + k_{d,c}} \tag{4.12}$$

Also, we define the following constants pertaining to the catalyst of type c,

$$\beta_c \equiv \frac{k_{trH,c}H_2 + k_{trAl,c}Al + k_{d,c}}{k_{p,c}M + k_{trM,c}M + k_{trH,c}H_2 + k_{trAl,c}Al + k_{d,c}} \tag{4.13}$$

$$\gamma_c \equiv \frac{k_{p,c}\beta_c + k_{trM,c}}{k_{p,c} + k_{trM,c}} \tag{4.14}$$

$$\mathcal{K}_c \equiv k_{p,c}M\frac{1-\alpha_c}{\alpha_c} \tag{4.15}$$

Upon doing so the expressions for C_c^*, $P_{1,c}$ and $P_{i,c}$ can be simplified as follows

$$\left.\begin{aligned} C_c^* &= \beta\mathcal{P} \\ P_{1,c} &= \gamma_c\mathcal{P}_c \\ P_{i,c} &= \alpha_c P_{i-1,c} = \alpha_c^2 P_{i-2,c} = \cdots = \alpha_c^{i-1}P_{1,c} \\ &= \gamma_c\alpha_c^{i-1}\mathcal{P}_c \end{aligned}\right\} \tag{4.16}$$

Equation (4.16) is referred to as the Flory or "Most Probable" chain length distribution.

$$V\frac{dD_{i,c}}{dt} = V\left[k_{trM,c}M + k_{trAl,c}Al + k_{trH,c}H_2 + k_{d,c}\right]P_{i,c} - qD_{i,c}$$

Equation (4.16) can now be used to simplify the above

$$\frac{dD_{i,c}}{dt} = k_{p,c}MP_{i,c}\frac{1-\alpha_c}{\alpha_c} - \frac{q}{V}D_{i,c} = \mathcal{K}_c\gamma_c\mathcal{P}_c\alpha_c^{i-1} - \frac{q}{V}D_{i,c} \tag{4.17}$$

In order to track the entire discretized MWD, the method of finite molecular weight moments requires calculating only the first moment. However, the first five (leading) moments for the dead polymer chains are trackd here. This is done because $overline M_{z+1}$ needs to evaluated in some of the rheological models and it would be preferable to minimize the errors generated through the discretization process. The dynamic equations for the dead polymer chain moments generated using catalyst of type c are:

$$\frac{d\lambda_{0,c}^d}{dt} = \mathcal{K}_c\gamma_c\mathcal{P}_c\frac{1-\alpha_c}{\alpha_c} - \frac{q\lambda_{0,c}^d}{V} \tag{4.18}$$

$$\frac{d\lambda^d_{1,c}}{dt} = \mathcal{K}_c\gamma_c\mathcal{P}_c\frac{\alpha_c(2-\alpha_c)}{(1-\alpha_c)^2} - \frac{q\lambda^d_{1,c}}{V} \tag{4.19}$$

$$\frac{d\lambda^d_{2,c}}{dt} = \mathcal{K}_c\gamma_c\mathcal{P}_c\frac{\alpha_c(\alpha_c^2-3\alpha_c+4)}{(1-\alpha_c)^3} - \frac{q\lambda^d_{2,c}}{V} \tag{4.20}$$

$$\frac{d\lambda^d_{3,c}}{dt} = \mathcal{K}_c\gamma_c\mathcal{P}_c\frac{\alpha_c(-\alpha_c^3+4\alpha_c^2-5\alpha_c+8)}{(1-\alpha_c)^4} - \frac{q\lambda^d_{3,c}}{V} \tag{4.21}$$

$$\frac{d\lambda^d_{4,c}}{dt} = \mathcal{K}_c\gamma_c\mathcal{P}_c\frac{\alpha_c(16\alpha_c^4-5\alpha_c^3+11\alpha_c^2+\alpha_c)}{(1-\alpha_c)^5} - \frac{q\lambda^d_{4,c}}{V} \tag{4.22}$$

In transition metal catalyzed polymerizations, chain termination occurs when a small molecule displaces the live polymer chain from the active catalyst site. Hence, unlike free-radical polymerizartion, diffusional limitations at high monomer conversions isn't an issue in this situation. The next step is to define the function $f_c(m,n)$ which represents the weight fraction of the polymer generated in the reactor using catalyst of type c and leaving in the product stream with chain lengths within an arbitrary but finite interval m to n i.e.

$$\begin{aligned} f_c(m,n) &\equiv \frac{\text{weight of polymer generated using the } c\text{th catalyst with chain lengths from } m \text{ to } n}{\text{total weight of polymer generated using the } c\text{th catalyst}} \\ &= \frac{\sum_{i=m}^{n} iD_{i,c} + \sum_{i=m}^{n} iP_{i,c}}{\sum_{i=2}^{\infty} iD_{i,r} + \sum_{i=2}^{\infty} iP_{i,c}} = \frac{\sum_{i=m}^{n} iD_{i,c} + \sum_{i=m}^{n} iP_{i,c}}{\lambda^d_{1,c} + \lambda^l_{1,c}} \end{aligned} \tag{4.23}$$

Unlike the case for free-radical polymerization, the contribution of live polymers is not ignored. Differentiating the above equation,

$$\begin{aligned} \frac{df_c(m,n)}{dt} &= \frac{1}{\lambda^d_{1,c}+\lambda^l_{1,c}}\sum_{i=m}^{n}\left(i\frac{dD_{i,c}}{dt} + i\frac{dP_{i,c}}{dt}\right) \\ &\quad + \sum_{i=m}^{n} i(D_{i,c}+P_{i,c})\left(-\frac{1}{(\lambda^d_{1,c}+\lambda^l_{1,c})^2}\left(\frac{d\lambda^d_{1,c}}{dt}+\frac{d\lambda^l_{1,c}}{dt}\right)\right) \\ &= \frac{1}{\lambda^d_{1,c}+\lambda^l_{1,c}}\sum_{i=m}^{n}\left(i\frac{dD_{i,c}}{dt} + i\frac{dP_{i,c}}{dt}\right) - \frac{f_c(m,n)}{(\lambda^d_{1,c}+\lambda^l_{1,c})}\frac{d\lambda^d_{1,c}}{dt} \end{aligned} \tag{4.24}$$

where,

$$\sum_{i=m}^{n}\frac{dD_{i,c}}{dt} = \mathcal{K}_c\gamma_c\mathcal{P}_c\sum_{i=m}^{n}\alpha_c^{i-1} - \frac{q}{V}D_{i,c} \tag{4.25}$$

$$\sum_{i=m}^{n} iP_{i,c} = \frac{\gamma_c\mathcal{P}_c}{(1-\alpha_c)^2}\Big[\alpha_c^{m-1}\{m(1-\alpha_c)+\alpha_c\} - \alpha_c^n\{(n+1)(1-\alpha_c)+\alpha_c\}\Big] \tag{4.26}$$

$$\sum_{i=m}^{n} iP_{i-1,c} = \frac{\gamma_c\mathcal{P}_c}{(1-\alpha_c)^2}\Big[\alpha_c^{m-2}\{m(1-\alpha_c)+\alpha_c\} - \alpha_c^{n-2}\{(n+1)\alpha_c+\alpha_c\}\Big] \tag{4.27}$$

Since the system is assumed to be isothermal, it is not necessary to implement the energy balance. In order to model the entire MWD in a computationally efficient manner, the method of finite molecular weight moments is implemented as follows. Although we are interested in observing the dynamics of a continuous process, the simulation is run in a batch mode. The length of this batch i.e. $t_{initial}$ to t_{final}, is the simulation window which is the time interval over which the system reaches steady state. Since the system under consideration is assumed to be stable, it is reasonable to expect this to happen in finite time. Next we need to fix the chain length interval. The minimum chain length, n_{min}, and the number of intervals, n_{int}, are inputs. Although larger values can be used, usually n_{min} is chosen to be 2. An initial value for the maximum chain length, n_{max}, is guessed. The length of each individual interval, l_{int}, is given by:

$$l_{int} = \frac{(n_{max} - n_{min})}{n_{int}} \tag{4.28}$$

Then, for each chain length interval, j, the upper and lower bounds, m and n are:

$$m = n_{min} + (j-1)l_{int} \qquad\qquad n = m + l_{int} \tag{4.29}$$

inserted in the ODE for the mass fraction of polymer. Equation (4.3) to (4.7) and equation(4.24) i.e. $n_{int} + 5$ ODEs are solved simultaneously. However, the initial guess for n_{max} might not be appropriate, i.e., the range of molecular weights covered might be too large or too small. Theoretically n_{max} should be close to infinity but an unnecessarily large value would be worthless and could lead to a loss in resolution. In order to ensure that the predicted MWD incorporates the entire significant portion of the distribution, n_{max} is varied and the entire calculation repeated until a certain criteria is satisfied. For example

$$f_c^{sum} = \sum_{j=1}^{n_{int}} f_{j,c} \geq 0.9999 \tag{4.30}$$

ensures that 99.99% of the MWD range is covered. Such a strict criterion is to ensure that all the high molecular weight fractions are included. This is necessary because the rheological behavior of polymer melts is more sensitive to the higher end of the MWD. It can be seen that in order to decide a suitable n_{max}, a very large number of ODEs have to be solved simultaneously. In order to

reduce this computational burden, which could be particularly acute for very large values of n_{int}, Yoon et al. [84] suggested an improvement in the method and demonstrated it for the thermal polymerization of styrene. Accordingly, for the case of the solution polymerization of ethylene, while fixing n_{max} by a trial and error search, instead of the n_{int} ODEs for the mass fractions, an ODE for each type of catalyst i.e. f_c^{sum} maybe solved and the condition of Equation (4.30) maybe verified. In this way only 5 ODEs instead of the $n_{int} + 4$, have to be solved. And then once n_{max} is fixed, the individual mass fractions maybe determined by solving all the ODEs.

4.2 Rheological models

All the empirical correlations for the zero shear viscosity for linear PEs are in the form of Equation (1.4). Raju et al. [65] have provided the following relation for the melt viscosity measured at 190^{o}C:

$$\eta_0 = 3.40 \times 10^{-14} \overline{M}_w^{3.60} \tag{4.31}$$

It is applicable to conventional monomodal and bimodal HDPEs, with polydispersities ranging from 1.2 to 34. However it is not applicable to mPEs in most situations (Munoz et al. [62]). Wood-Adams and Dealy have reported the following correlation:

$$\eta_0 = 3.9 \times 10^{-15} \overline{M}_w^{3.65} \tag{4.32}$$

The following correlation has been reported by Munoz et al. [62]:

$$\eta_0 = 4.5 \times 10^{-16} \overline{M}_w^{3.9} \tag{4.33}$$

Huang et al. [43] proposed the following two correlations which they claim provide an excellent fit for the melt flow index (MFI), expressed in g/10 min, of a family of PEs produced with the same catalyst under similar conditions:

$$\frac{1}{MFI} = 8.52 \times 10^{-8} \left(\frac{\overline{M}_w}{1000} \right)^{3.9} \tag{4.34}$$

$$\frac{1}{MFI} = 1.87 \times 10^{-8} \left(\frac{\overline{M}_w}{1000} \right)^{3.7} \tag{4.35}$$

Table 4.3: Model parameters for polydisperse HDPE melt samples at 190^oC.

Parameter	Value	Source
k	8.43×10^{-13}	p. 962 in Nichetti and Manas-Zloczower [63]
τ_c	33905	p. 962 in Nichetti and Manas-Zloczower [63]
M_c	1100	p. 129 in Graessley [38]
ρ	920	

From among the several MWD to viscosity (η) versus shear rate ($\dot{\gamma}$) models available, Nichetti and Manas-Zloczowers' method (Section (2.3.3)) is adopted here because of its simplicity and the fact that it is able to predict the second Newtonian region at high shear rates, i.e. the limiting viscosity η_∞. These authors have also supplied parameters for estimating the zero shear viscosity which are close to the ones given above. In order to model the MWD to first normal stress difference (N_1) versus shear stress (τ_w) trends, the following expression, obtained by plugging Equation (2.27) into Equation (1.1), is used:

$$N_1 = 2J_e\tau_w^2 = \Big(\frac{4}{5\rho RT}\Big)\frac{\overline{M}_z\overline{M}_{z+1}}{\overline{M}_w}\tau_w^2 \tag{4.36}$$

As per the discussion in Section (1.6.1), it is obvious that the above approach suffers from inaccurate predictions at high shear stresses. The die swell-ratio is evaluated using the Tanner equation, i.e. Equation (1.2). In order to use the above models for polydisperse HDPE, the necessary parameters for melt samples at 190^oC are listed in Table (4.3).

4.3 Steady state parametric sensitivity analysis

It is important to observe the ability of the on-line rheometer to capture the important aspects of the process dynamics. In order to do so one has to study the effect of variations in the operating conditions on the viscoelastic properties of the polymer product. In carrying out this steady state parametric sensitivity analysis, it is assumed that operating conditions under consideration correspond to unique and stable steady states only. This is a reasonable assumption because in industrial practice, operating personnel usually prefer to avoid operating conditions

Table 4.4: SOCs in ethylene polymerization case study.

Parameter	Value
Reactor volume, V (l)	15
Total feed flow rate, q (l/min)	3
Reactor residence time, θ (min)	5
Reactor temperature, T (^{o}C)	100
Reactor Pressure, P (psig)	1500
Feed monomer conc., M_f (mol/l)	1
Total catalyst feed conc., $C^*_{A,f} + C^*_{B,f}$ (mol/l)	4.0×10^{-6}
Catalyst feed ratio, $C^*_{B,f}/C^*_{A,f}$	20
Feed aluminium alkyl conc., Al_f (mol/l)	1×10^{-4}
Feed hydrogen conc., $H_{2,f}$ (mol/l)	1×10^{-3}

associated with multiple steady states since these may give rise to unstable and unpredictable dynamics.

The standard operating conditions (SOCs) for this case study are given in Table (4.4). It should be noted that these SOCs are similar to those reported by Charpentier et al. [21]. The aim is to observe the influence of variations in the reactor residence time (θ), reactor temperature (T), feed monomer concentration (M_f), total catalyst feed concentration ($C^*_{A,f} + C^*_{B,f}$), catalyst feed ratio ($C^*_{B,f}/C^*_{A,f}$), feed aluminium alkyl concentration (Al_f) and feed hydrogen concentration ($H_{2,f}$) the on product's MWD and rheological properties. The results are tabulated in Tables (4.5) and (4.6) for easier comparison. In these tables, $\overline{M}_{w,A}$ and $\overline{M}_{w,B}$ denote the individual weight average molecular weights while ϕ_A and ϕ_B denote the weight fractions of the polymer generated using catalyst sites A and B respectively. $\overline{M}_w$ and $\overline{PD}$ are the composite weight average molecular weight and polydispersity respectively. $\eta(1)$ and $\eta(100)$ denote the non-Newtonian viscosities in units of Pa.s "measured" at shear rates (i.e. $\dot{\gamma}$) of 1 and 100 sec^{-1}, respectively. MFI_1 and MFI_2, in units of g/10 min denote the melt flow indices estimated using Equation (4.34) and (4.35) respectively. The elastic behavior of different samples are compared at wall stresses found in typical melt indexers i.e. τ_w of about 300 kPa. $N_1(300)$, in units of Pa, denotes the first normal

stress difference while $S_R(300)$ is the die swell-ratio at these conditions. The first column in both the tables correspond to values at the standard operating condtions i.e. Table (4.4). The first row refers to the curve of the corresponding figure as the case may be. Figure (4.2) is a plot displaying product properties at SOCs. Curves corresponding to SOCs are always denoted as "a" in Figure (4.3) to (4.5). When different trends are being compared, the individual curves have been zoomed-in to show greater detail.

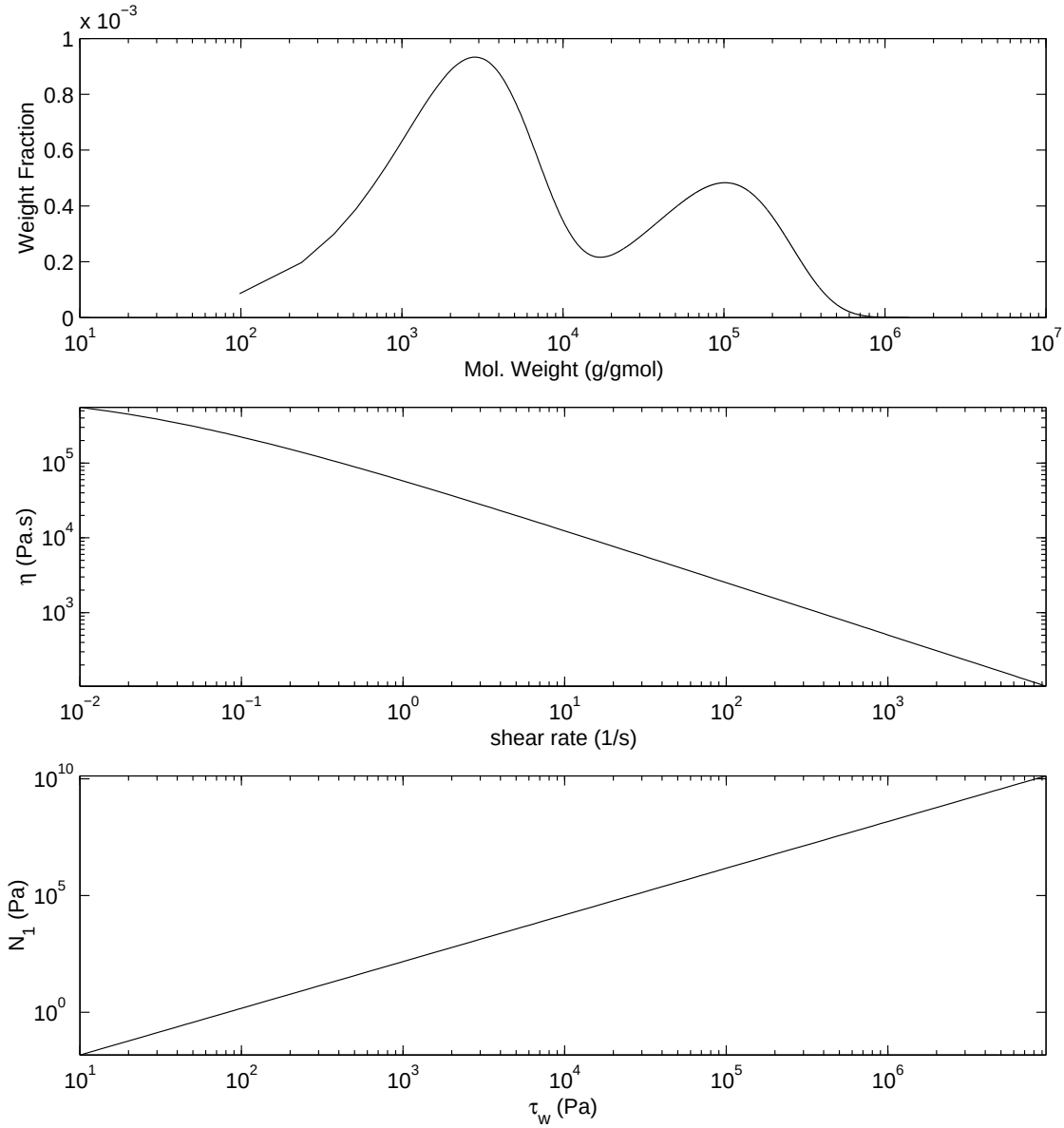

Figure 4.2: Product properties at standard operating conditions (SOCs).

Table 4.5: Sensitivity of product properties to operating conditions.

Parameter ⇒	SOC	θ (min)		T (^{o}C)		M_f (mol/l)	
Curve	4.2 & a	-	-	4.3 b	4.3 c	-	-
Property ⇓		4	6	95	105	0.8	1.2
$\overline{M}_{w,A}$	5.47×10^3	5.66×10^3	5.34×10^3	5.57×10^3	5.36×10^3	4.4×10^3	6.53×10^4
ϕ_A	0.0476	0.0476	0.0476	0.0476	0.0476	0.0476	0.0476
$\overline{M}_{w,B}$	2.03×10^5	2.03×10^5	2.03×10^5	3.09×10^5	1.35×10^5	2.03×10^4	2.03×10^5
ϕ_B	0.9524	0.9524	0.9524	0.9524	0.9524	0.9524	0.9524
$\overline{M}_w$	1.94×10^5	1.94×10^5	1.94×10^5	2.95×10^5	1.29×10^5	1.94×10^5	1.94×10^5
$\overline{PD}$	5.126	5.015	5.206	6.75	4.06	5.91	4.60
Shape	B	B	B	B	B	B	B
$\eta(1)$	5.77×10^4	5.77×10^4	5.77×10^4	9.3×10^4	3.4×10^4	5.75×10^4	5.8×10^4
$\eta(100)$	2.51×10^3	2.52×10^3	2.51×10^3	3.81×10^3	1.66×10^3	2.5×10^3	2.5×10^3
MFI_1	14.2	14.2	14.2	3.43	56.43	14.2	14.1
MFI_2	0.64	0.64	0.64	0.14	2.9	0.64	0.64
$N_1(300)$	1.33×10^7	1.33×10^7	1.33×10^7	2.02×10^7	8.83×10^6	1.33×10^7	1.33×10^7
$S_R(300)$	2.633	2.633	2.633	3.007	2.317	2.633	2.633

Table 4.6: Sensitivity of product properties to operating conditions (contd.).

Parameter ⇒	SOC	$C^*_{A,f} + C^*_{B,f}$ (mol/l)		$C^*_{B,f}/C^*_{A,f}$		Al_f (mol/l)		$H_{2,f}$ (mol/l)	
Curve	4.2 & a	-	-	4.4 b	4.4 c	-	-	4.5 b	4.5 c
Property ⇓		3.2×10^{-6}	4.8×10^{-6}	5	50	0.8×10^{-4}	1.2×10^{-4}	0	2.0×10^{-3}
$\overline{M}_{w,A}$	5.47×10^3	6.08×10^3	5.04×10^3	1.1×10^4	4.12×10^3	5.47×10^3	5.47×10^3	2.04×10^5	2.8×10^3
ϕ_A	0.0476	0.0476	0.0476	0.1667	0.0196	0.0476	0.0476	0.0476	0.0476
$\overline{M}_{w,B}$	2.03×10^5	2.03×10^5	2.03×10^5	2.03×10^5	2.03×10^5	2.03×10^5	2.03×10^5	2.03×10^5	2.03×10^5
ϕ_B	0.9524	0.9524	0.9524	0.8333	0.9804	0.9524	0.9524	0.9524	0.9524
$\overline{M}_w$	1.94×10^5	1.94×10^5	1.94×10^5	1.715×10^5	1.995×10^5	1.94×10^5	1.94×10^5	2.04×10^5	1.94×10^5
$\overline{PD}$	5.126	4.8	5.4	6.54	3.77	5.126	5.126	2.0	8.21
Shape	B	B	B	B	B	B	B	U	B
$\eta(1)$	5.77×10^4	5.77×10^4	5.76×10^4	3.93×10^4	6.32×10^4	5.77×10^4	5.77×10^4	6.75×10^4	5.73×10^4
$\eta(100)$	2.51×10^3	2.52×10^3	2.51×10^3	1.87×10^3	2.73×10^3	2.51×10^3	2.51×10^3	2.9×10^3	2.50×10^3
MFI_1	14.2	14.2	14.2	21.57	12.91	14.2	14.2	12.0	14.3
MFI_2	0.64	0.64	0.64	1.01	0.58	0.64	0.64	0.53	0.65
$N_1(300)$	1.33×10^7	1.3×10^7	1.3×10^7	1.46×10^7	1.26×10^7	1.3×10^7	1.3×10^7	1.27×10^7	1.33×10^7
$S_R(300)$	2.633	2.633	2.633	2.72	2.6	2.633	2.633	2.596	2.633

The overall dependance of the rheological properties on the MWD is consistent with the general observations made in Section (1.6.1) and depicted in Figures (1.2) and (1.3). Specifically,

- The η_0 values increase while the MFIs decrease as the $\overline{M}_w$ increases. At a constant $\overline{M}_w$ these values are almost unaffected by the $\overline{PD}$ (i.e. the breadth of the distribution).
- The onset of non-Newtonian behavior occurs at lower shear rates as the $\overline{M}_w$ increases and as the $\overline{PD}$ increases i.e. the MWD broadens.
- The fluid elasticty, reflected through N_1 and S_R, increases as the $\overline{M}_w$ and the $\overline{PD}$ increase.

It should be noted that although the general trend in the predictions are quite consistent, there is significant mismatch in the MFIs predicted using Equation (4.34) and (4.35). As per Huang et al. [43], the fit by Equation (4.34) was slightly better and so may be chosen as the correct value of the MFI. Based upon the above arguements, the sensitivity of product properties to operating conditions can be summarized as follows:

1. For the range of reactor residence times (θs) observed, θ has a marginal effect on the $\overline{M}_w$ and $\overline{PD}$. As a result, a corresponding effect on the rheological properties is also not seen. The minor influence of variations in θ on product properties is due to the differences in catalyst activities as a result of deactivation. In industrial practice, limits for the reactor levels are dictated by the vessel and agitator design and so there is very little scope of variation. Reactant flow rates may be adjusted to change the residence times. However, reactor residence times are usually used to set the per pass conversion and/or the production rate. Hence, manipulating the reactor residence time in order to control the polymer product's MWD or it's rheological properties is not an attractive option.

2. As seen from Figure (4.3) the polymerization temperature has a very strong effect on the $\overline{M}_w$ and the shape of the MWD. This is also reflected in the rheological properties. As seen, temperature affects the high end of the MWD more than the low end. As a result, there is more than a 15 fold increase in the MFI for a 10^oC rise in polymerization temperature. Due to a higher $\overline{PD}$, the polymer produced at a lower temperature has a slightly steeper slope

in the η versus $\dot{\gamma}$ plot, i.e. it is more shear-thinning. The die swell-ratio (S_R) also shows a marked decrease with an increase in the polymerization temperature. Inspite of this high sensitivity of product properties to polymerization temperature, it should be pointed out that temperature also strongly affects the productivity. Moreover, it is not a good idea to use reactor temperature as a manipulated variable in CSTRs involving exothermic reactions since this could lead to stability problems.

3. The monomer concentration in the feed primarily affects the rate of polymerization and hence the production rate. Its influence on product properties is marginal for the range of M_f values observed. Consequently the rheological properties are almost unaffected by variations in M_f. However, it can be argued that lower monomer concentrations produce a lower $\overline{M}_w$ polymer. This is because as the relative amount of hydrogen increases, the relative amount of chain transfer to CTA reactions compared to propagation reactions increase and the average chain length is lower. Moreover, M_f values are dictated by solubility limitations and so using the monomer concentration in the reactor as a manipulated variable to control the polymer product's MWD or it's rheological properties is not an attractive option.

4. Changing the total amount of catalyst does not affect the $\overline{M}_w$ but it alters the $\overline{PD}$ slightly. However, the total amount of catalyst fed to the reactor has a far greater effect on polymer productivity and so it is preferable to avoid using this variable to alter the product properties.

5. The influence of variations in the catalyst feed ratio on the product properties is interesting for two reasons. Firstly this is the only situation when the indivdual weight fractions (i.e. ϕ_A and ϕ_B) of the polymer produced on the two catalyst sites are altered. The individual weight average molecular weights (i.e. $\overline{M}_{w,A}$ and $\overline{M}_{w,B}$) are only marginally affected. As a result, the $\overline{PD}$ changes significantly without changing the $\overline{M}_w$ much. The second interesting observation is the effect of rheological properies. Curves a and c in Figure (4.4) have very close values of η_0 and MFIs but significantly different shear thinning behavior. One can conclude that by varying the catalyst feed ratio, it is possible to alter the shear thinning behavior without

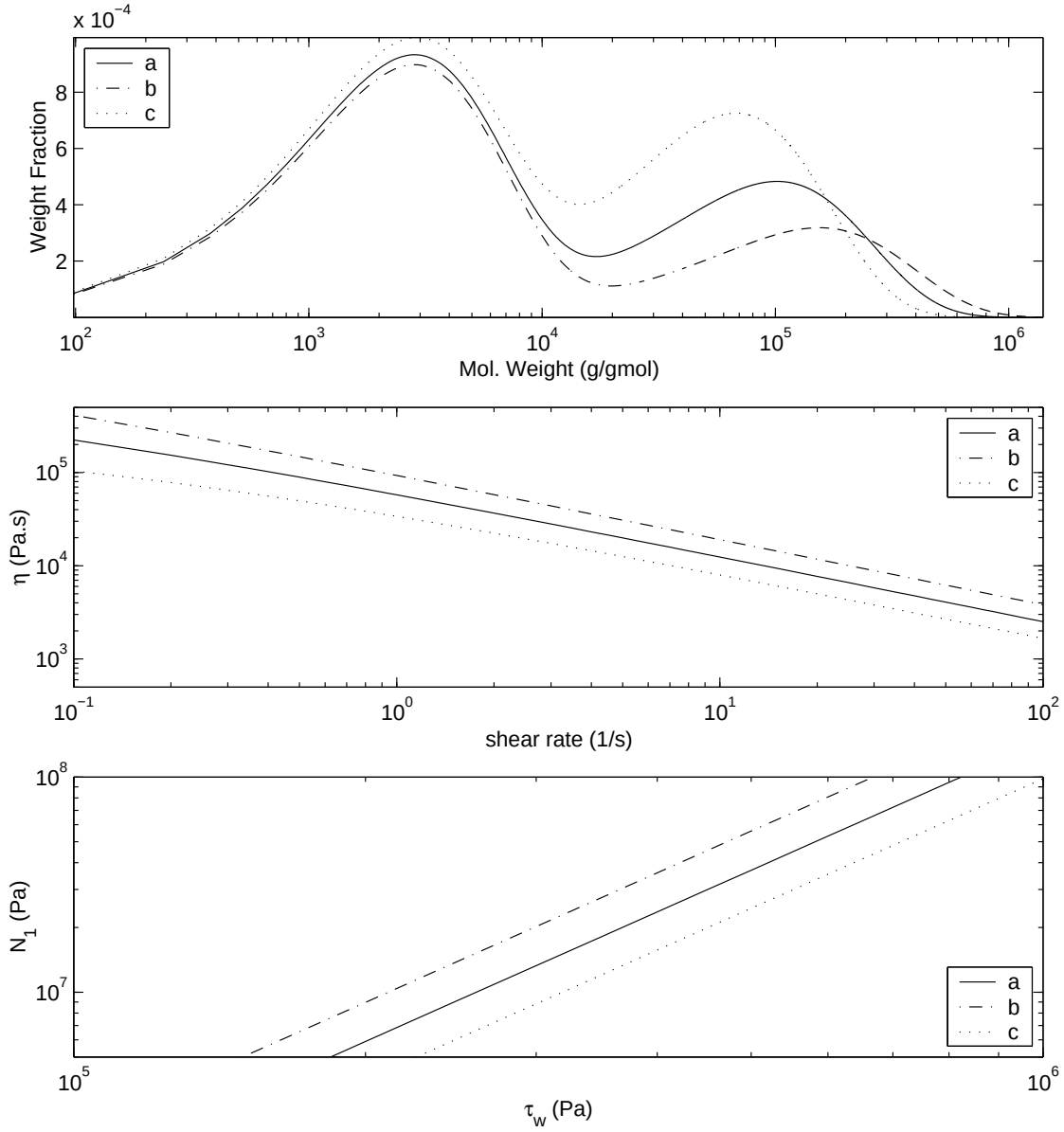

Figure 4.3: Influence of polymerization temperature on product properties a = 100^{o}C, b = 95^{o}C and c = 105^{o}C.

altering the η_0 very much. Unfortunately, owing to the high $\overline{M}_w$, a clear Newtonian region is not seen here. But it can be argued that for lower $\overline{M}_w$ samples, exhibiting distinct Newtonian regions, the onset of shear thinning can be almost independantly controlled using $C^*_{B,f}/C^*_{A,f}$. It should also be noted that the catalyst feed ratio can be varied wihtout disturbing the production rate.

6. From Table (4.6) it is clear that variations in the aluminium alkyl concentration in the reactor has little influence on the MWD and hence the rheological of the product. Although it has not been modeled here, it has been experimentally oberved that catalyst productivity is strongly influenced by Al values. Hence, Al_f isn't a good variable to manipulate for product property control.

7. Variations in the hydrogen feed concentrations has a very drastic effect on the product properties. Figure (4.5) shows that when no hydrogen is fed both the catalyst sites generate nearly identical polymer. This is because apart from their activity towards chain transfer to hydrogen, the two catalysts are identical. Hence the shape of the MWD is unimodal and the overall $\overline{PD}$ is approximately 2 which is customary for Flory's most probable distributions. As the hydrogen concentration in the reactor increases, the $\overline{M}_w$ decreases slightly while $\overline{PD}$ increases significantly. When comparing the properties of the product obtained using hydrogen concentrations of 1×10^{-3} and 2.0×10^{-3} mol/l, it is seen that eventhough the two samples have significantly different $\overline{PD}$s, their MFIs are nearly identical. This clearly exposes the inadequacy of the information provided by the MFI. It can be shown that for larger differences in the $\overline{PD}$s, eventhough the MFIs are similar, their viscosities at very high shear rates are significantly different. As a result, the product's performance in polymer processing equipment involving high shear rates, such as extrusion or injection molding, cannot be accurately predicted using the MFI values alone. It should be noted that due to hydrogen solubility limitations and the increase in production of very low $\overline{M}_w$ waxes the maximum hydrogen concentration is usually not very high. In the case of a two site system, this limit also dictates the extent to which the $\overline{PD}$s can be varied. In order to

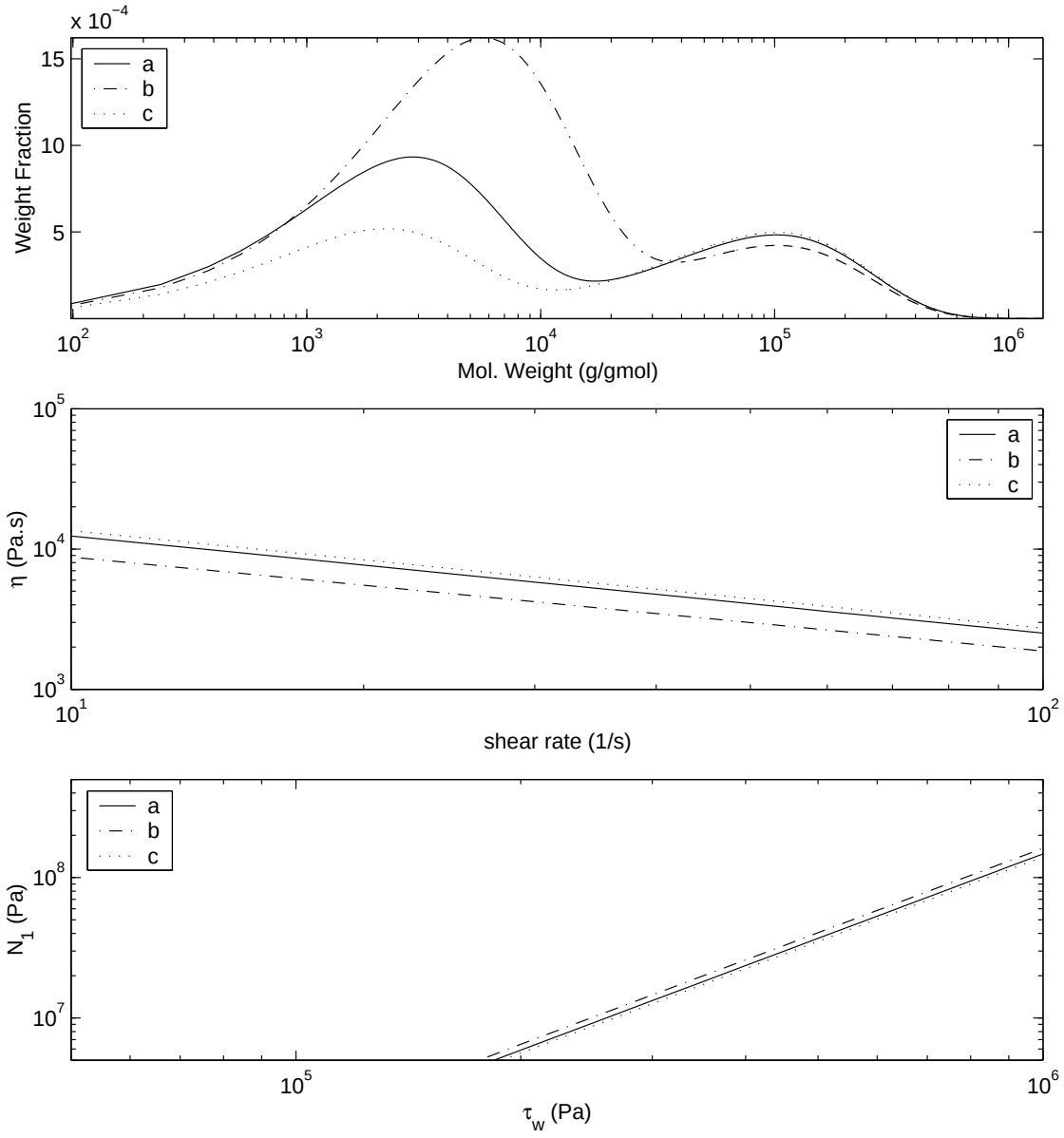

Figure 4.4: Influence of catalyst feed ratio on product properties a = 20, b = 5 and c = 50.

obtain higher $\overline{PD}$s, multiple catalyst sites or a different reactor configuration has to be used.

With an aim to tailor the shape of the MWD and hence obtain a product of specifc rheological properties, the following conclusions can be drawn based on the above discussion:

- If a SISO control strategy is applied, the shape of the MWD can be altered using a maximum of two manipulated variables: the CTA concentration $H_{2,f}$ and the ratio of the two catalysts $C^*_{b,f}/C^*_{A,f}$ in the feed to the reacytor. It is not possible to use a third variable without disturbing the production rate.

- Using a multivariable control approach, such as model predictive control (MPC), it would be possible to alter the shape better because more manipulated variables can be altered simultaneously.

- The modality (i.e. the maximum number of peaks in the MWD) for this system is restricted to two.

For this case study, the relative gain array (RGA) for negative perturbations in the manipulated variables is:

$$\begin{array}{rcc} & C_B/C_A & H_2 \\ \eta(1) & 7.9381 & -6.9381 \\ \eta(100) & -6.9381 & 7.9381 \end{array} \tag{4.37}$$

and that for positive perturbations is:

$$\begin{array}{rcc} & C_B/C_A & H_2 \\ \eta(1) & 0.0004 & 0.9996 \\ \eta(100) & 0.9996 & 0.0004 \end{array} \tag{4.38}$$

Since the numbers vary so much between negative and positive perturbations, it can be concluded that the system is highly non-linear. Also, the RGA elements reveal that there are strong interactions and so the loops cannot be easily de-coupled.

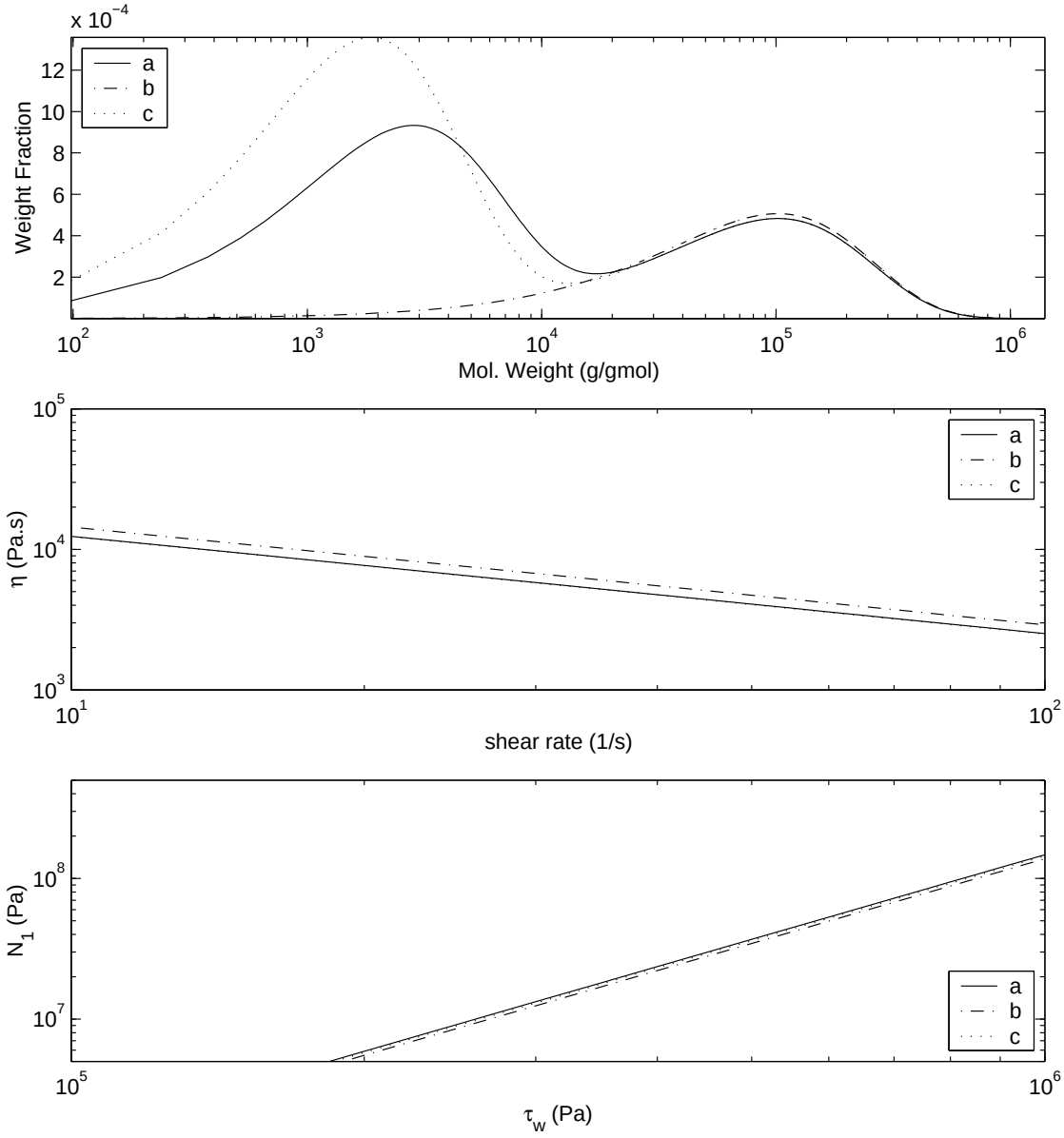

Figure 4.5: Influence of hydrogen feed concentration on product properties a = 1×10^{-3}, b = 0 and c = 2×10^{-3}, mol/l.

4.4 Notation

CTA	Chain Transfer Agent.
LCA	Long Chain Approximation.
NCLD	Number Chain Length Distribution.
MW	Molecular Weight.
MWD	Molecular Weight Distribution.
QSSA	Quasi Steady State Approximation.
RSSA	Reactor Steady State Approximation.

Al	Conc. of Aluminium alkyl.
C_c^*	Conc. of active catalyst of type c.
C_c	Conc. of inactive (deactivated) catalyst of type c.
$D_{i,c}$	Conc. of dead polymer chains with i repeating units generated using catalyst c.
H_2	Conc. of Hydrogen.
$k_{d,c}$	Deactivation rate constant for catalyst of type c.
$k_{p,c}$	Propagation rate constant for catalyst of type c.
$k_{trAl,c}$	Chain transfer to Aluminium-alkyl rate constant for catalyst of type c.
$k_{trH,c}$	Chain transfer to Hydrogen rate constant for catalyst of type c.
$k_{trM,c}$	Chain tranfer to monomer rate constant for catalyst of type c.
$\mathcal{K}_c$	Constant for catalyst of type c defined in Equation (4.15)
M	Conc. of monomer, i.e. ethylene.
$\overline{M}_n$	Number average molecular weight.
$\overline{M}_w$	Weight average molecular weight.
$\overline{PD}$	Polydispersity.
$P_{i,c}$	Conc. of live polymer chains with i repeating units generated using catalyst c
$\mathcal{P}_c$	Total conc. of live polymer chains generated using catalyst c.
V	Reactor volume.

α_c	Probability of propagation for catalyst of type c defined in Equation (4.12)
β_c	Constant for catalyst of type c defined in Equation (4.13)
γ_c	Constant for catalyst of type c defined in Equation (4.14)

Chapter 5

Framework generalization and extensions

The previous two chapters discussed the application of the new framework to linear homopolymers and demonstrated it via styrene and ethylene polymerization case studies. This chapter considers extending the applicabilty to polymer with small amounts of branching. Specifically it discusses applications in reactors for ethylene homopolymerization using constrained geometry metallocene catalysts. This is very important from a commercial point of view.

5.1 Conclusions from case studies

Table (5.1) summarizes the reactor configurations and chemistries of the two representative polymerization processes studied. From the study it was clear that although the two systems are different, there is an underlying similarity in which one is able to manipulate the shape of the MWD. Both systems essentially involve the blending of two polymer streams, each one individually following a known distribution function. Hence, the shape of the MWD was essentially determined by the individual probabilities of propagation i.e. αs and the weight fraction of one of the streams.

In the styrene polymerization case study, the study reveaed that the best manipulated variables for product quality control were the CTA concentrations in the two CSTRs. The two manipulated variables altered the low and high end of the MWD in a decoupled fashion. A possible

Table 5.1: Comparison of case studies

Chapter	3	4
Monomer	Styrene	Ethylene
Reactor configuration	Twin CSTR cascade	Single CSTR
Chain initiation	Free-radical	Transition-metal catalyzed
Chain termination	Combination (coupling)	Chain transfer
Base $\overline{PD}$	1.5	2.0

third manipulated variable was lost because the weight fraction of polymer produced in each reactor could not be altered without upsetting the production rate. In the ethylene polymerization case study, the study revealed that the best manipulated variables for product quality control were the CTA concentration and the ratio of the two catalyst concentrations in the feed. The ratio of the catalyst concentrations in the feed essentially reflects the weight fraction of polymer produced via each catalyst type. There was significant interaction in the way these two manipulated variables altered the shape of the MWD. A possible third manipulated variable was lost because once the probability of propagation associated with one catalyst was fixed, the other α was automatically fixed. Hence, one can conclude from this degree of freedom analysis that for better product property/quality control it is necessary to have more choices of αs and ϕs, i.e. a different reactor configuration is necessary.

5.2 Generalization of proposed framework

The idea of controlling the variable of real interest by computing its value from other less expensive, more reliable measurements is not new. It is the most logical extension to conventional control and has been practised often in the chemical and petroleum industry. Some of the classical applications are

1. Controlling the mass flow rate of a gas computed from pressure, temperature and pressure drop measurements of an orifice meter.

2. Controlling the heat transfer rate computed from flow rate and stream inlet & outlet temperature measurements.

3. Controlling the composition in a distillation column computed from temperature and pressure measurements.

We have tried to apply this idea to polymerization processes based on the fact that in most cases, the variable of real interest (i.e. commercial interest) is closely tied to the polymer product's rheological properties. The proposed framework is depicted in Figure (5.1). As shown in the figure,

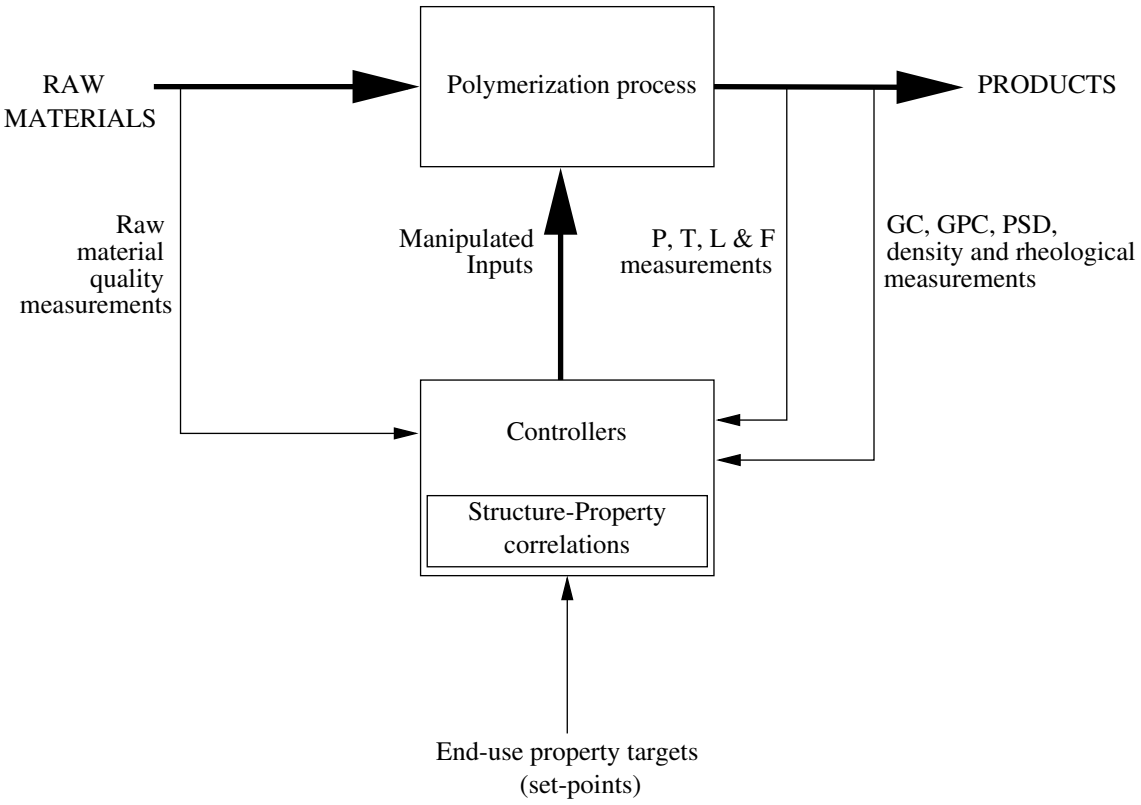

Figure 5.1: Proposed framework for control of end-use properties

the framwork is based on a two-tier hierarchy for the feedback control system. The lower level loops which are based on pressure, temperature, level and flow (PTLF) measurements have a very high reliability and so are used to ensure the stability of the process. These loops have a sampling rate in the order of seconds and so may be referred to as the "fast" loops. The higher level loops are based upon more sophisticated sensors and analysers such as the gas chromatograph (GC), the gel permeation chromatograph (GPC), devices for particle size distribution and density measurements and most importantly, dynamic rheological meaurements. It should be re-emphasized that the rheological measurements aren't merely via a melt-indexer but preferably a full-fledged on-line rheometer capable of meeasuring the viscosity over a reasonably wide range of shear rates. These devices are are aimed at achieveing better quality control. However these measurements are prone to failure and so the entire framework is constructed in a "bottom-up" fashion. in other words, the higher level loops are implemented only after ensuring the sucessful operation of the lower level loops. The higher level loops have turaround rates in the order of minutes or even hours and so may be referred to as the "slow" loops.

The controller is designed based on the performance goals. In case the goal is the control of viscoelastic properties only, then the output of the on-line rheometer can be used directly as the set-point. Of course some sort of signal conditioning might be necessary. However, if the aim is to control some other end-use property which cannot be measured on-line, then a "computed variable"/inferential controller has to be designed. It plays the role of a software sensor for the MWD. A strucure-property correlation would also be necessary to translate the end-use property targets into a desirable MWD whcih would subsequently be used to set targets for the rheological variables that are easier to measure.

Although similar frameworks have been proposed by several other researchers (Congalidis and Richards [25], i.e. Figure (1.1), Soroush [72], and Ogunnaike and Ray [64]), all the elements of the control system were not clearly defined. The implementation was not explained in detail, nor was it demonstrated via any experimentation or simulation.

This framework is unique in that it is the first ocassion when dynamic rheological measurements have been incorporated in the control system in an explicit manner. Moreover, the dual role played by such measurements has been explained clearly.

5.3 Applications in reactors for ethylene homo-polymerization using constrained geometry catalysts (CGCs)

As mentioned earlier, one approach to tackling the undesirable rheological properties of polyethylene generated using single-site catalysts is the introduction of small amounts of long chain branching. The resulting polymer is easier to process. In this section, application of the proposed framework in reactors for ethylene homo-polymerization using constrained geometry catalysts (CGCs) is discussed.

5.3.1 Chain Branching

Chain branching occurs via the in-situ formation of polymer molecules having terminal vinyl unsaturation (macromonomers) by β-hydride elimination reactions and subsequent incorporation in the polymer chains. The branching could be

1. Short (SCB), i.e. 3 to 5 carbon atoms long, or

2. Long (LCB), i.e. comparable in length with the polymer main chain.

The most accurate means of analyzing a polymer sample for it's branching content is the the ^{13}C NMR. However, since it cannot be implemented in an on-line fashion, another means of characterization is necessary. It is often reported (Kim [49]), that SCB mainly controls the density and thermodynamic properties, but has little effect on the melt rheological properties. LCB has little effect on the density and the thermodynamic properties, but it has drastic effects on the melt rheological properties.

Soares et al. [71] have extensively studied the molecular architecture of polyolefins made using Ziegler - Natta catalysts. Their findings may be summarized as follows. When using single-site

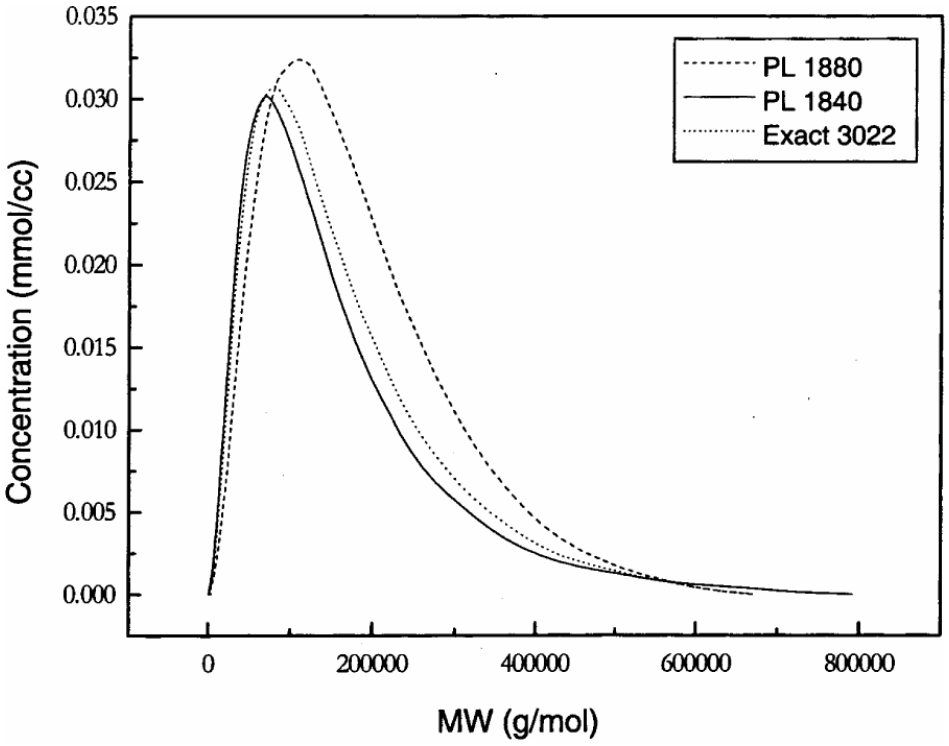

Figure 5.2: MWDs of mPEs.

catalysts, linear polyolefin homopolymer chain lengths follow Flory's most probable distribution. When multiple-site catalysts are used, linear polyolefin homopolymer chain lengths follow a cummulative of several distributions. Each site type produces polymer chains that follow Flory's most probable distribution. Hence, for the whole polymer, the MWD is the weighted sum of individual distributions. We have already observed this through the kinetic model developed in Chapter 4. Although mathematical models for the MWDs, CCDs and LCBDs for polyolefin copolymers made using single and multiple site catalysts have also been presented, such a detailed description of the polymer populations is not considered in the present study.

5.3.2 General observations

The presence of LCB significantly alters the flow behavior of mPEs. For identical molecular weight distributions, the following general observations can be made regarding the presence of LCB:

1. It increases the zero-shear and low-shear viscosity. Moreover, the dependance of η_0 on molec-

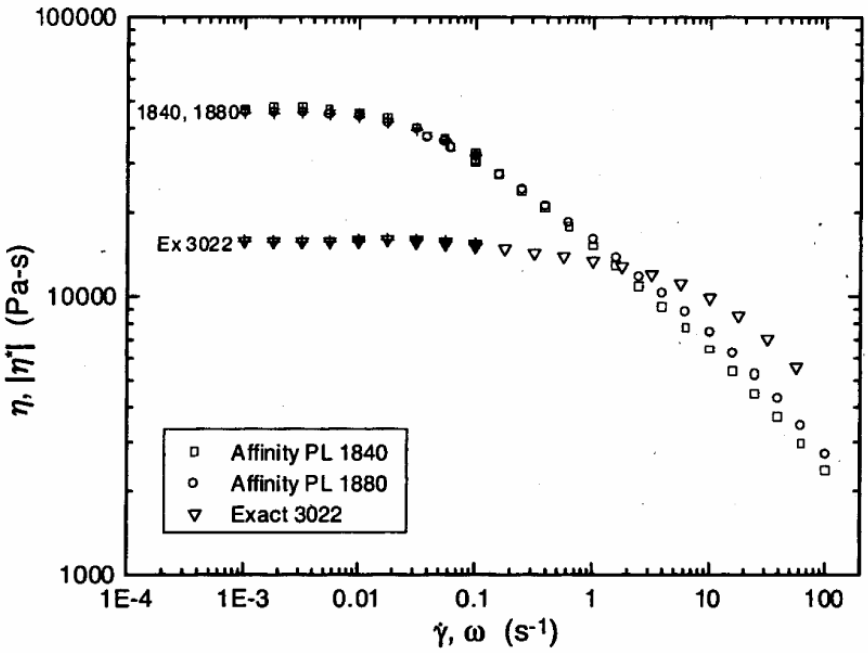

Figure 5.3: Shear flow curves for mPEs at 150 deg^{0}C.

Table 5.2: Reported values of polyethylene E_0s (in kJ/mol) based on η_0s

branching ⇒	HDPE	LLDPE	LDPE
source ⇓	Linear	SCB only	SCB and LCB
Malmberg et al. [55]	26	33	55
Rohn [67]	25	30	55

ular weight is also slightly stronger (Munoz-Escalona et al. [62]).

2. It increases the shear thinning.

3. It delays melt fracture.

4. It increases extrudate swell.

5.3.3 Rheological models

At the present time, there are very few models available in the open literature specifically meant for predicting the rheology of polyethylene with low levels of LCB. The only ones that are available are those related to zero shear conditions.

Rohn [67] has reported the only correlation available in the open literature which directly quantifies the effect of LCB on the zero shear viscosity (η_0). This relation was obtained by studying fifteen LDPE samples of different degrees of long-chain branching.

$$\eta_0 = K\overline{M}_w^{3.36} e^{-6500\lambda} \tag{5.1}$$

An indirect approach to quantifying the presence of LCB is through it's effect on the activation energy of flow. Table (5.2) is a list of reported values of flow activation energy based on the newtonian viscosity.

1. In linear chains, E_0 does not depend on molecular weight.

2. In branched chains, the increase of E_0 above the value of linear polyethylenes is directly proprtional to the branch length.

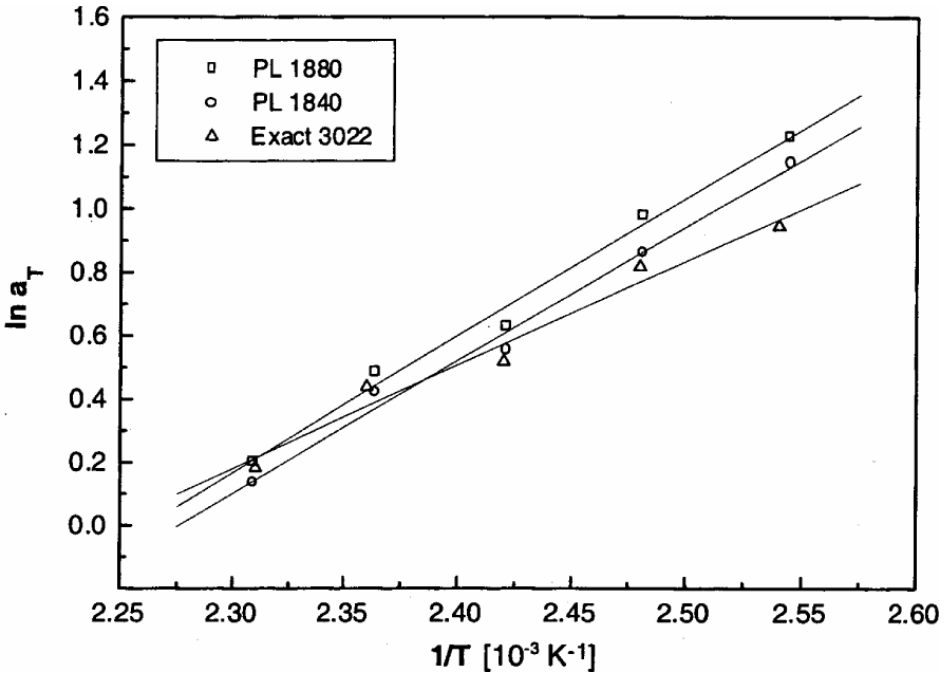

Figure 5.4: Evaluation of flow activation energies for mPEs.

3. In blends of linear and branched polymer, E_0 is proportional to the volume fraction of the branched polymer.

As reported by Hughes [45], the following correlation is applicable for the effect of very low degree of long chain branching on the activation energy of flow

$$\lambda = \frac{(E_0 - 6.24)}{7.93 \times 10^5} \tag{5.2}$$

This equation has been successfully utilized as a tool to determine the number of long chain branches per 1000 C atoms in polyethylene polymerized in the presence of a metallocene complex.

5.3.4 Recipes for synthesizing ethylene homopolymers with target rheological properties

Beigzadeh et al. [3, 4] have proposed a method for designing recipes for synthesizing polyolefins with tailor-made molecular weight, polydispersity index, long chain branching frequencies, and chemical composition using combined metallocene catalyst systems in a CSTR operating at

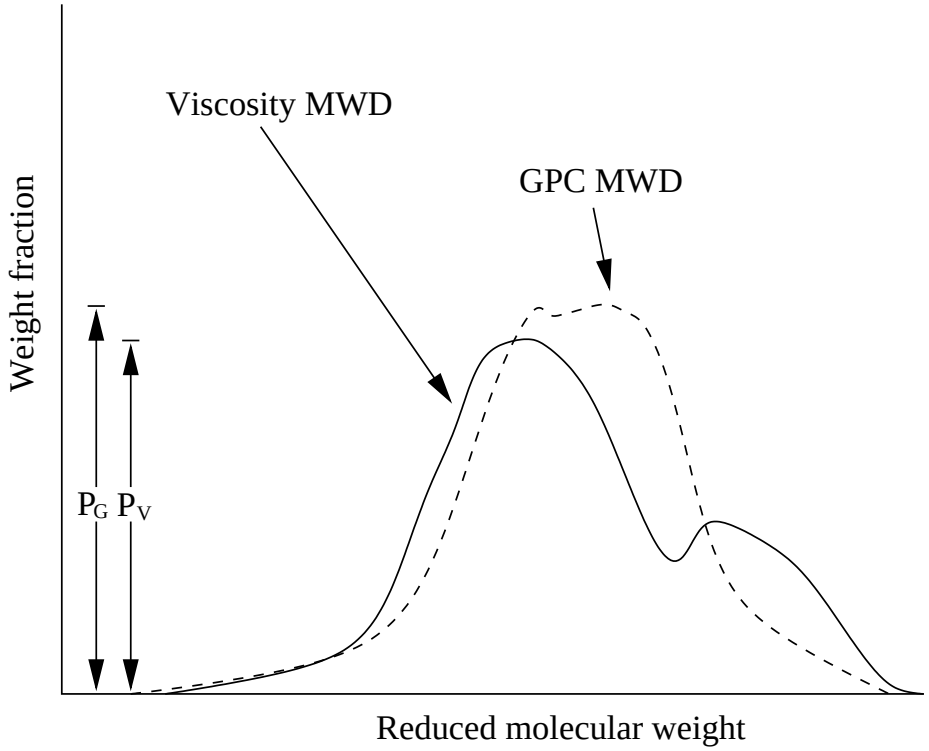

Figure 5.5: Using viscosity data to infer the level of LCB.

it's steady state. By extending this method it is possible to decide the recipe or SOC necessary to manufacture mPEs with target end-use properties.

5.3.5 Use of rheological measurements for process control

The use of rheological measurements for the control of reactors used for mPEs necessiates an appropriate method for viscodity-shear rate data to polymer structure conversion. All the methods discussed in Chapter 2 are strictly applicable to linear (straight chain) polymers only. The presence of LCB in mPEs significantly alters the rheological behavior of the polymer melt. As a result the MWD predicted using the methods discussed thus far would be in gross error. Wood-Adams and Dealy [81, 82] observed that for a branched material the MWD predicted using a modified version of Shaw-Tuminello method deviated significantly from the true MWD obtained using a GPC. The extent of this deviation was found to be dependant on the degree of LCB.

$$\lambda = \begin{cases} 0 & \text{for} \frac{P_G}{P_V} < 1 \\ 11.25 \log\left(\frac{P_G}{P_V}\right) & \text{for} \frac{P_G}{P_V} \geq 1 \end{cases} \tag{5.3}$$

One serious drawback of the Wood-Adams and Dealy method is that it requires both rheological and GPC measuremnts. As a consequence, it is still plagued with problems related to time delays and solvability which are inherent to all GPCs. This makes the method unattractive for on-line implementation. A new method to predict the MWD and number of LCBs in mPEs from rheological data alone is proposed. Upon successful validation, it could be used for on-line estimation and control.

5.3.6 Extension of Liu et al.'s method to mPEs with small amounts of LCB

Liu et al. suggested assuming the shape to be a superposition of several log-normal distributions. However, it is well established that mPEs follow Flory's most probable distribution under ideal conditions. In order to incorporate heat and mass transfer effects, effects of improper mixing in the reactor and other non-idealities, The equation describing the MWD would have to be suitably modified. Moreover, correlations of the form of Equation 1.4 do not take into account the long chain branches. So they are applicable strictly to linear polymers and lead to gross errors in the prediction of eta_0 in the presence of even small amounts of LCB. Instead, Equation 5.1 would be more appropriate for use to determine $\overline{M}_w$.

5.3.7 Overall strategy

A combination of the ideas discussed in the previous sections provides the basis of the proposed methodology. Hughes correlation provides a means of obtaining the degree of long chain bramching. Rohn's correlation provides an estimate of the average molecular weight in PEs with LCB. Bersted's model is useful in estimating the shear dependant viscosity of PEs with LCB. Liu et al.'s method predicts

With this in mind, the overall strategy can be viewed as a series of steps performed iteratively:

1. Obtain viscosity versus shear rate data for the polymer sample at two different temperatures.

2. Use Hughes's correlation to calculate the LCBD (i.e. λ).

3. Use Rohn's correlation to calculate the average molecular weight (i.e. $\overline{M}_w$).

4. Make an initial guess for the parameters in the MWD function.

5. Use the Bersted model to predict the viscosity versus shear rate at the two specified temperatures.

6. Change the parameter values used for the MWD function in order to minimize the difference between the experimental data and the predicted values. A numerical package performing constrained nonlinear least squares fitting may be used in order to carry out this minimization.

Chapter 6

Conclusions

Polymer reaction engineering is a multi-discplinary field involving the design, modeling, optimization and control of polymerization reactors. It is built upon the fundamental principles of chemical engineering like thermodynamics, reaction kinetics, heat & mass transfer and process control. On the other hand, polymer rheology involves the study of the deformation and flow of polymeric materials. This work has attempted to tie these two areas of polymer science in order to build a novel framework for producing polymers with "tailored" molecular structures and specific end-use properties.

This chapter summarizes the main achievements of this study. Practical benefits from an industrial perpective are also pointed out. Finally a few recommendations for future research are put forward.

6.1 Summary of contributions

A review of current practices in polymerization process control and rheological models available in the open literature was conducted. Through this study it was established that:

1. The tight control of end-use properties is the most appropriate performance goal for the reactor control system. Amongst the several end-use properties, the dynamic viscosity of the polymer melt is a possible choice that could be adopted as the controlled variable.

2. Out of the many alternative methods available for polymer characterization, rheological measurements, particularly dynamic viscoelasticity measurements, is the most promising option.

Two continuous polymerization processes with on-line rheological measurements was studied. Product quality control was demonstrated via steady state simulations at industrially relevant

operating conditions. Comprehensive, first-priciples dynamic models were developed for:

1. Modeling equations for the free-radical solution polymerization of styrene using a binary intiator system in a cascade of an arbitrary number of CSTRs in series were developed. A two CSTR system was implemented.

2. Modeling equations for the solution polymerization of ethylene using a mixture of an arbitrary number of soluble single-site transition metal catalysts in a single CSTR were deveoped. A two single site catalyst system was implemented.

3. Rheological models to simulate the behavior of an on-line rheometer were coupled with the above mentioned kinetic models. Using these models, it is possible to predict the dynamic viscosity (i.e. η versus $\dot{\gamma}$), melt flow index (i.e. MFI), first normal stress difference (i.e. N_1 versus τ_w) and extruate/die-swell of the molten product.

Using the above models a thorough study of the influence of various reactor operating parameters on the polymer product's rheological properties was conducted.

6.2 Practical benefits

The practical benefits of the proposed framework in industrial-scale polymer mnaufacturing processes are:

1. Its implementation is simple because of the following reasons:

   (a) Since it is based upon the PID algorithm, it is easily understood by process engineers, control engineers and maintenance personnel.

   (b) This framework can be easily included in distributed control systems (DCSs) and can take full advantage of the functionality built into the available PID algorithms such as set-point tracking, automatic mode switching, etc.

   (c) Since it is built upon establishing the stable functioning of the regulatory (PTLF) loops first, it's actions cannot destabilize the process. This is true even if the on-line rheometer fails or is pulled off-line (i.e. shut off).

2. The ability to predict the influence of polymerization conditions on end-use properties would enable the setting up of more target-oriented operating procedures.

3. *A priori* constraints on the operating conditions would provide invaluable information to prevent the shut-down of post-polymerization polymer processing equipment such as extruders.

4. The use of rheological measurements as a software sensor would help estimate and thereby control the entire MWD or any other end-use property which might might be difficult to measure or track.

6.3 Recommendations for future work

1. The proposed framework may be tested for systems involving the blending of more than two streams with Flory MWDs. In other words, a similar study involving more than two reactors in series or more than two catalysts in a single CSTR would involve more "handles" i.e. manipulated variables and hence a better control of the shape of the MWD may be tried out. The maximum number of modes in the MWD in this study was restricted to two (i.e. bimodal distributions) however the complexity involved in multimodal MWDs needs to be studied.

2. The proposed framework may be tested for more complex, particularly heterogeneous, polymerization systems. For example the applicability of the proposed framework to free-radical emulsion and transition metal catalyzed gas phase olefin polymerization systems need to be investigated.

3. An on-line rheometer can be used as a software sensor to obtain the full MWD. This information may then be plugged into an appropriate structure-property correlation in order to predict any other end-use property. The control of non-measurable properies such as using a "computed variable control" approach needs to be investigated.

4. All the results presented in this study are via computer based simulations. Experimental verification needs to be done.

6.4 Final remarks

The area of product property/quality control is the active focus of research in polymer reaction engineering. Improved methodologies and approaches to the problem need to be developed in the future. The incentives are great, so are the challenges. As far as achieving the ultimate goal is concerned, the contributions of this thesis have barely scratched the surface. Hopefully, this is a promising step in that direction. Paraphrasing from Brooks:" The garden spider (*Araneus diadematus*) produces webs from very fine silk. The silk is composed of a variety of polyamides (proteins), and the fiber properties are changed to fulfill many functions. Five types of silk have been identified, each with a controlled composition. From the precursor materials, spiders produce their silk with much-envied ease at atmospheric temperature. In spite of high humidity, they manage to displace reaction equilibrium very rapidly, achieving high conversion to polymer before vaporization of volatiles occurs. In the web, the drag lines are very strong ... spider silk is stronger than many man-made polymers. Some specialized man-made fibers are as strong as spider silk, but the extension at break is much lower. Although it might be claimed that spiders have been "developing their processes" for a few million years, we must ask if our processes will eventually match those of the spider."

Appendix A

Terminology

In order to use a consistent set of symbols and notations, the official nomenclature of the Society of Rheology as given by Dealy [30] is adopted here. At the same time, some fundamental concepts in polymer rheology are also summarized.

Consider a simple flow geometry consisting of two parallel plates forming a narrow gap whose distance h is very small compared to the width w of the plates (i.e. wh). In such a situation, the velocity field is given by

$$v_z = \dot{\gamma} y, v_x = v_y = 0 \tag{A.1}$$

The stress existing at any point in a material may always be resolved into components acting on the faces of a differential element in three arbitrary directions. The stress components acting on the faces of the element are of two types:

1. Normal stresses (forces acting normal to the surface per unit surface area, and

2. Shear stresses (forces acting parallel to the surface per unit surface area).

In general there are three normal stresses and six shear stresses. These nine quantities, necessary to specify completely the state of stresss at a point, are the components of the stress tensor τ. They are conviniently written in matrix form:

$$\tau = \begin{vmatrix} \tau_{11} & \tau_{12} & \tau_{13} \\ \tau_{21} & \tau_{22} & \tau_{23} \\ \tau_{31} & \tau_{32} & \tau_{33} \end{vmatrix} \tag{A.2}$$

The components of the stress tensor may be expressed in terms of three independent material functions, the shear-dependent (i.e. Non-Newtonian viscosity) $\eta(\dot{\gamma})$, the first normal stress function v$\Psi_1(\dot{\gamma})$ and the second normal stress function $\Psi_2(\dot{\gamma})$. $\Psi_1(\dot{\gamma})$ and $\Psi_2(\dot{\gamma})$ describe the fluid elasticity.

A.0.1 Complex viscosity function ($\eta^*(\omega)$)

It is defined as

$$\eta^*(\omega) = \frac{G^*(\omega)}{\omega} = \left(\left(\frac{G'(\omega)}{\omega} \right)^2 + \left(\frac{G''(\omega)}{\omega} \right)^2 \right)^{1/2} \tag{A.3}$$

A.0.2 Compliance(J_e)

It is often referred to as a measure of the stored elastic energy and is defined as

$$J_e^o = \frac{\int_0^\infty sG(s)ds}{[\int_0^\infty G(s)ds]^2} \tag{A.4}$$

$$J_e^o = \frac{\int_{-\infty}^\infty H(\lambda)\lambda^2 dln\lambda}{[\int_{-\infty}^\infty H(\lambda)\lambda dln\lambda]^2} \tag{A.5}$$

It may also be evaluated using

$$J_e = \frac{\tau_{11} - \tau_{22}}{\tau_w^2} \tag{A.6}$$

A.0.3 Dynamic viscosity function($\eta'(\omega)$)

It is defined as

$$\eta'(\omega) = \frac{G'(\omega)}{\omega} \tag{A.7}$$

A.0.4 First Normal Stress function

It[1] is defined as

$$\tau_{11} - \tau_{22} = \Psi_1(\dot{\gamma})\dot{\gamma}^2 \tag{A.8}$$

For a Newtonian fluid, the first normal stress function is zero.

[1]The stress difference $\tau_{11} - \tau_{33}$ is redundant because $\tau_{11} + \tau_{22} + \tau_{33} = 0$

A.0.5 Intrinsic Viscosity ($[\eta]$)

It is the most important characteristic quantity in a very dilute solution under low deformation rate. It is also referred to as the "limiting viscosity number" and is defined as

$$[\eta] = \lim_{c \to 0} \frac{\eta_{1,2} - \eta_1}{\eta_{1c}} \tag{A.9}$$

A.0.6 Loss Modulus ($G''(\omega)$)

$$G''(\omega) = \int_{-\infty}^{\infty} H(\lambda) \frac{(\omega\lambda)}{1 + (\omega\lambda)^2} dln\lambda \tag{A.10}$$

A.0.7 Molecular Weight Distribution function ($\varphi(M)$)

Let $\varphi(M)dM$ represent the normalized number distribution of molecular weights. Then $\varphi(M)$, being the number fraction of chains of molecular weight in the range M and M + dM, is called the Molecular Weight Distribution function.

A.0.8 Number average molecular weight ($\overline{M}_n$)

It is defined as

$$\overline{M}_n = \int_0^{\infty} M\varphi(M)dM \tag{A.11}$$

A.0.9 Plateau Modulus (G_N^0)

$$G_N^0 = \int_{-\infty}^{\infty} H(\lambda) dln\lambda = \lim_{\omega \to \infty} G'(\omega) \tag{A.12}$$

A.0.10 Relaxation Spectrum (H(λ))

The continuous distribution function of relaxation time λ is called the relaxation spectrum $H(\lambda)$ so that $H(\lambda)d\lambda$ represent the total viscosity of all the Maxwell elements between λ and $\lambda + d\lambda$. Hence,

$$\eta_0 = \int_0^\infty H(\lambda) d\lambda \tag{A.13}$$

All other linear viscoelastic properties can be evaluated from the relaxation spectrum.

A.0.11 Relaxation Time

The ratio of the viscosity to the elastic modulus.

A.0.12 Second Normal Stress function

It is defined as

$$\tau_{22} - \tau_{33} = \Psi_2(\dot{\gamma})\dot{\gamma}^2 \tag{A.14}$$

For a Newtonian fluid, the second normal stress function is zero.

A.0.13 Shear dependant (Non-newtonian) viscosity

A.0.14 Storage Modulus $G'(\omega)$

$$G'(\omega) = \int_{-\infty}^{\infty} H(\lambda) \frac{(\omega\lambda)^2}{1 + (\omega\lambda)^2} dln\lambda \tag{A.15}$$

A.0.15 Weight average molecular weight ($\overline{M}_w$)

It is defined as

$$\overline{M}_n = \frac{\int_0^\infty M^2 \varphi(M) dM}{\int_0^\infty M \varphi(M) dM} \tag{A.16}$$

A.0.16 Zero-shear Viscosity (η_0)

$$\eta_0 = \int_{-\infty}^{\infty} H(\lambda) \lambda dln\lambda = \lim_{\omega \to 0} \frac{G''(\omega)}{\omega} \tag{A.17}$$

Appendix B

Molecular Weight Distributions (MWDs)

B.1 Theoretical distibution functions

Apart from the "Most Probable distribution", the two-parameter Flory distribution (see Tobita and Hamielec [75]) is commonly encountered in the literature. It is given by:

$$w(r) \approx (\tau+\beta)\left[\tau+\frac{\beta}{2}(\tau+\beta)(r-1)\right] r \exp\bigl(-(\tau+\beta)r\bigr) \tag{B.1}$$

In order to discretize this distribution, we utilize the following general result from the Mathematical Handbook, p. 85: If n is a positive integer,

$$\int x^n \exp\{ax\}dx = \frac{\exp\{ax\}}{a}\left[x^n - \frac{nx^{n-1}}{a} + \frac{n(n-1)x^{n-2}}{a^2} - \cdots \frac{(-1)^n n!}{a^n}\right] \tag{B.2}$$

Hence,

$$\int w(r)dr = -\frac{1}{2}\left[2r\tau - \tau\beta r + r^2\beta\tau - r\beta^2 + r^2\beta^2 - \beta + 2r\beta + 2\right]\exp -r(\tau+\beta) \tag{B.3}$$

B.2 MWD Moments and Averages

The kth moments of live and dead polymers are defined as (general case)

$$\lambda_k^l \equiv \sum_{i=1}^{\infty} i^k P_i \qquad\qquad \lambda_k^d \equiv \sum_{i=2}^{\infty} i^k D_i \tag{B.4}$$

Using this definition, the zero'th, first and second molecular weight moments of live polymers in the rth reactor would be

$$\lambda_{0,r}^l \equiv \sum_{i=1}^{\infty} P_{i,r} \qquad \lambda_{1,r}^l \equiv \sum_{i=1}^{\infty} iP_{i,r} \qquad \lambda_{2,r}^l \equiv \sum_{i=1}^{\infty} i^2 P_{i,r} \tag{B.5}$$

In a similar way, the leading moments of dead polymers in the rth reactor would be

$$\lambda_{0,r}^d \equiv \sum_{i=2}^{\infty} D_{i,r} \qquad \lambda_{1,r}^d \equiv \sum_{i=2}^{\infty} iD_{i,r} \qquad \lambda_{2,r}^d \equiv \sum_{i=2}^{\infty} i^2 D_{i,r} \tag{B.6}$$

Upon examining the above equations, it is worth taking note that the zero'th moment (λ_0^d) is simply the total number of polymer molecules per unit volume and the first moment (λ_1^d) is the total weight of polymer per unit volume. As per Ray [66], it is possible to reconstruct the entire MWD from an infinite set of moments. The leading moments for the dead polymers are important because they are useful in making reasonable approximations of the entire distribution. As a result, a few key polymer properties of interest can be predicted. For example, in general, the number and weight average molecular weights can be obtained as follows.

$$\overline{M}_n = M_0 \overline{X}_n = M_0 \frac{\lambda_1^l + \lambda_1^d}{\lambda_0^l + \lambda_0^d} \approx M_0 \frac{\lambda_1^d}{\lambda_0^d} \tag{B.7}$$

$$\overline{M}_w = M_0 \overline{X}_w = M_0 \frac{\lambda_2^l + \lambda_2^d}{\lambda_1^l + \lambda_1^d} \approx M_0 \frac{\lambda_2^d}{\lambda_1^d} \tag{B.8}$$

From this the Polydispersity Index, which is indicative of the breadth of the molecular weight distribution, can be obtained using

$$\overline{PD} \equiv \frac{\overline{M}_w}{\overline{M}_n} = \frac{\overline{X}_w}{\overline{X}_n} \approx \frac{\lambda_2^d \lambda_0^d}{(\lambda_1^d)^2} \tag{B.9}$$

Furthermore, as this method demonstrates, just the first moment is good enough to obtain the discrete WCLD.

B.3 Blending of multiple polydisperse streams

One of the main advantages of dealing with moments is that when several streams are blended, the moments of the resulting stream is simply the sum of the individual moments.

Hence,

$$\overline{X}_n = \frac{\sum_{s=1}^{N_s} \lambda_{1,s}}{\sum_{s=1} N_s \lambda_{0,s}} \overline{X}_w = \frac{\sum_{s=1}^{N_s} \lambda_{2,s}}{\sum_{s=1} N_s \lambda_{1,s}} \tag{B.10}$$

BIBLIOGRAPHY

[1] Baird, D. G. and D. I. Collias, "Polymer Processing Principles and Design", John Wiley and Sons, Inc. (1998).

[2] Batistini, A., "New Polyolefin plastomers and elastomers made with INSITE technology: Structure -property relationship and benefits in flexible thermoplastic applications", *Macromol. Symp.*, Vol. 100, 137 to 142, (1995).

[3] Beigzadeh, D., Soares, J. B. P. and A. E. Hamielec, "Study of long-chain branching in ethylene polymerization", *Polymer React. Eng.*, Vol. 5, No. 3 pp. 141 to 180, (1997).

[4] Beigzadeh, D., Soares, J. B. P. and A. E. Hamielec, "Recipes for Synthesizing Polyolefins with Tailor-Made Molecular Weight, Polydispersity Index, Long Chain Branching Frequencies, and Chemical Composition Using Combined Metallocene Catalyst Systems in a CSTR at Steady State", *J. App. Poly. Sci.*, Vol. 71, pp. 1753 to 1770, (1999).

[5] Bersted, B. H., "An Empirical Model relating the Molecular Weight Distribution of High - Density Polyethylene to the Shear Dependence of the Steady Shear Melt Viscosity", *J. App. Poly. Sci.*, Vol. 19, pp. 2167 to 2177, (1975).

[6] Bersted, B. H., "A Model Relating the Elastic Properties of High-Density Polyethylene Melts to the Molecular Weight Distribution", *J. App. Poly. Sci.*, Vol. 20, pp. 2705 to 2714, (1976).

[7] Bersted, B. H. and J. D. Slee, "A Relationship Between Steady-State-Shear Melt viscosity and Molecular Weight Distribution in Polystyrene", *J. App. Poly. Sci.*, Vol. 21, pp. 2631 to 2644, (1977).

[8] Bersted, B. H., "Prediction of Dynamic and Transient Rheological Properties of Polystyrene and High-Density Polyethylene Melts from the Molecular Weight Distributions", *J. App. Poly. Sci.*, Vol. 23, pp. 1279 to 1289, (1979).

[9] Bersted, B. H., "Modification of a Model Relating Rheological Behavior of Polymer Melts to the Molecular Weight Distribution", *J. App. Poly. Sci.*, Vol. 23, pp. 1867 to 1869, (1979).

[10] Bersted, B. H., "Effect of Molecular Weight Distribution on Elongation Viscosity of Undiluted Polymer Fluids", *J. App. Poly. Sci.*, Vol. 24, pp. 671 to 682, (1979).

[11] Bersted, B. H., J. D. Slee and C. A. Richter, "Prediction of Rheological Behavior of Branched Polyethylene from Molecular Structure", *J. App. Poly. Sci.*, Vol. 26, pp. 1001 to 1014, (1981).

[12] Bersted, B. H., "On the Effects of Very Low Levels of Long Chain Branching on Rheological Behavior in Polyethylene", *J. App. Poly. Sci.*, Vol. 30, pp. 3751 to 3765, (1985).

[13] Bin Wadud, S.E. and D. G. Baird, "Rheology of Metallocene-catalyzed Polyethylenes - Effects of Branching", *Macromol. Symp.*, Vol. 100, 137 to 142, (1995).

[14] Bin Wadud, S.E. and D. G. Baird, "Shear and extensional rheology of sparsely branched metallocene-catalyzed polyethylenes", *J. Rheology*, Vol. 44, 1151 to 1167, (2000).

[15] Bremner, T. and A. Rudin, "Melt Flow Index Values and Molecular Weight Distributions of Commercial Thermoplastics", *J. App. Poly. Sci.*, Vol. 41, pp. 1617 to 1627, (1990).

[16] Brooks, B. W., "Why are Polymerization Reactors Special ?", *Ind. Eng. Chem. Res.*, Vol. 36, No. 4, 1158 to 1162, (1997).

[17] Bueche, F., "Influence of Rate of Shear on the Apparent Viscosity of A - Dilute Polymer Solutions, and B - Bulk Polymers", *J. of Chem. Phys.*, Vol. 22, No. 9, 1570 to 1576, (1954).

[18] Carella, J. M., J. T. Gotro and W. W. Graessley, "Thermorheological Effects of Long-Chain Branching in Entangled Polymer melts", *Macromolecules*, Vol. 19, No. 3, 659 to 667, (1986).

[19] Carella, J. M., "Comments on the Paper "Comparison of the Rheological properties of Metallocene-Catalyzed and Conventional High-Density Polyethylenes".", *Macromolecules*, Vol. 29, pp. 8280 to 8281, (1996).

[20] Chai, C. K., "Melt Rheology and Processability of Conventional and Metallocene Polyethylenes", *Macromol. Symp.*, Vol. 100, 137 to 142, (1995).

[21] Charpentier, P. A., S. Zhu, A. E. Hamielec, and M. A. Brook, "Continuous Solution Polymerization of Ethylene Using Metallocene Catalyst System, Zirconium Dichloride/Methylaluminoxane/Trimethylaluminium", *Ind. Eng. Chem. Res.*, Vol. 36, 5074 to 5082, (1997).

[22] Choi, K. Y., "Control of Molecular Weight Distribution of Polyethylene in Continuous Stirred Tank Reactors with High Activity Soluble Ziegler-type catalysts", *J. App. Poly. Sci.*, Vol. 30, 2707 to 2710, (1985).

[23] Choi, K. Y., B. G. Kwag, S. Y. Park and C. H. Cheong, "Technical Processes for Industrial Production", in "*Handbook of Radical Vinyl Polymerization*, M. K. Mishra and Y. Yagci, Marcel Dekker, New York, (1998).

[24] Clarke-Pringle, T. and J. F. MacGregor, "Product Quality Control in Reduced Dimensional Spaces", *Ind. Eng. Chem. Res.*, Vol. 37, 3992 to 4002, (1998).

[25] Congalidis, J. P. and J. R. Richards, "Process control of polymerization reactors: An Industrial perspective", *Polymer Reaction Eng.*, Vol. 6, 71 to 111, (1998).

[26] Crowley, T. J., "Theoretical and Experimental Study of Molecular Weight Distribution Modeling and Control in Polymerization Reactors", *Ph.D. Thesis (Univ. of Maryland)*, (1997).

[27] Crowley, T. J. and K. Y. Choi, "Calculation of Molecular Weight Distribution from Molecular Weight Moments in Free Radical Polymerization", *Ind. Eng. Chem. Res.*, Vol. 36, No. 5, pp. 1419 to 1423, (1997).

[28] Crowley, T. J. and K. Y. Choi, "Discrete Optimal Control of Molecular Weight Distribution in a Batch Free Radical Polymerization Process", *Ind. Eng. Chem. Res.*, Vol. 36, No. 9, pp. 3676 to 3684, (1997).

[29] Crowley, T. J. and K. Y. Choi, "Experimental Studies on Optimal Molecular Weight Distribution Control in a Batch Free Radical Polymerization Process", submitted to *Ind. Eng. Chem. Res.*, (1998).

[30] Dealy, J. M., "Rheology as a tool for quality control", *Macromol. Symp.*, Vol. 100, 137 to 142, (1995).

[31] Dealy, J. M., "Official nomenclature for material functions describing the response of a viscoelastic fluid in various shearing and extensional conformations", *J. Rheology*, Vol. 39, No. 1, 253 to 265, (1995).

[32] De Laney, D. E. and J. F. Reilly, "A New Approach to Polymer Rheology for Process and Quality Control", *Plastics Engineering*, Vol. LIV, No. 6, 45 to 47, (1998).

[33] Des Cloizeaux, J., "Double reptation vs simple reptation in polymer melts", *Europhys. Lett.*, Vol. 5, 437 to 442, (1988).

[34] Doi, M. and S. F. Edwards, "The Theory of Polymer dynamics", Clarendon Press, Oxford, (1986).

[35] Ferry, J. D., "Viscoelastic Properties of Polymers", 3/e, John Wiley & Sons, Inc. , New York, (1980).

[36] Fried, J. R., "Polymer Science and Technology", Prentice-Hall, Englewood Cliffs, (1995).

[37] Gordon, G. V. and M. T. Shaw, "Computer Programs for Rheologists", Hanser/Gardner Publ., New York, (1994).

[38] Graessley, W. W., "Viscoelasticity and Flow in Polymer Melts and Concentrated Solutions", in James E. Mark et al. "Physical Properties of Polymers", 2/e, American Chemical Society, Wash. DC, (1993).

[39] Gupta, R. K., "Polymer and Composite Rheology", Marcel Dekker, Inc. , New York, (2000).

[40] Han, C. D., "Rheology in Polymer Processing", Academic Press, Inc. , New York, (1976).

[41] Hamer, J. W., T. A. Akramov and W. H. Ray, "The dynamic behavior of continuous polymerization reactors - II Nonisothermal solution homopolymerization and copolymerization in a CSTR", *Chemical Engineering Science*, Vol. 36, Issue 12, 1897 to 1914, (1981).

[42] Harold, M. P. and B. A. Ogunnaike, "Process engineering in the evolving chemical industry", *AIChE Journal*, Vol. 46, Issue 11, 2123 to 2127, (2004).

[43] Huang, J. C. K., Y. Lacombe, D. T. Lynch and S. E. Wanke, "Effects of Hydrogen and 1-Butene Concentrations on the Molecular Properties of Polyethylene Produced by Catalytic Gas-Phase Polymerization", *Ind. Eng. Chem. Res.*, Vol. 36, 1136 to 1143, (1997).

[44] Hui, A. and A. E. Hamielec, "Thermal polymerization of styrene at high conversions and temperatures. An experimental study", *J. Appl. Polym. Sci.*, Vol. 16, Issue 3, 749 to 769, (1972).

[45] Hughes, J. K., "Analysis of long chain branching in High density Polyethylene", *SPE Antec Tech. Papers*, Vol. 29, 306 to 303, (1983).

[46] Kim, K. J., K. Y. Choi and J. C. Alexander, "Dynamics of a Cascade of Two Continuous Stirred Tank Polymerization Reactors With a Binary Initiator Mixture", *Polymer Eng. Sci.*, Vol. 31, No. 5, 333 to 351, (1991).

[47] Kim, K. J. and K. Y. Choi, "On-line estimation and control of a continuous stirred tank polymerization reactor", *J. Proc. Cont.*, Vol. 1, March, 96 to 110, (1991).

[48] Kim, K. J. and K. Y. Choi, "Continuous Olefin Copolymerization with Soluble Ziegler-Natta Catalysts", *AIChE J.*, Vol. 37, No. 8, August, 1255 to 1260, (1991).

[49] Kim, Y. S., C. I. Chung, S. Y. Lai and K. S. Hyun, "Processability of Polyethylene homopolymers and copolymers with respect to their molecular structure", *Korean J. of Chem. Eng.*, Vol. 13, No. 3, 294 to 303, (1996).

[50] Kim, Y. S., C. I. Chung, S. Y. Lai and K. S. Hyun, "Melt Rheological and Thermodynamic Properties of Polyethylene Homopolymers and Poly(ethylene/α olefin) Copolymers with Respect to Molecular Composition and Structure", *J. App. Poly. Sci.*, Vol. 59, No. 3, 125 to 137, (1996).

[51] Liu, Y., "Determination of the MWD from the viscosity data of Polymer melts", Ph.D. thesis, University of Connecticut, (1996).

[52] Liu, Y. Shaw M. T. and W. H. Tuminello, "Optimized Data Collection for Determination of the MWD from the Viscosity Data of Polymer Melts", *Poly. Eng. Sci.*, Vol. 38, No. 1, 169 to 176, (1998).

[53] Liu, Y. and M. T. Shaw, "Investigation of the non-linear mixing rule for its adequacy in viscosity to molecular weight distribution transforms", *J. Rheology*, Vol. 42, No. 2, 267 to 279, (1998).

[54] Liu, Y., M. T. Shaw and W. H. Tuminello, "Obtaining molecular-weight distribution information from the viscosity data of linear polymer melts", *J. Rheology*, Vol. 42, No. 3, 453 to 476, (1998).

[55] Malmberg, A., Kokko, E., Lofgren, B. and J. V. Seppala, "Long Chain Branched Polyethene Polymerized by Metallocene Catalysts $Et[Ind]_2ZrCl_2/MAO$ and $Et[IndH_4]_2ZrCl_2/MAO$", *Macromolecules* , Vol. 31, No. 24, 8448 to 8454 (1998).

[56] Maranas, C. D., "Optimal Computer-Aidid Molecular Design: A Polymer Design Case Study", *Ind. Eng. Chem. Res.*, Vol. 35, No. 10, 3403 to 3414, (1996).

[57] Mavridis H. and R. N. Shroff, "Temperature dependence of Polyolefin Melt Rheology", *Poly. Eng. Sci.*, Vol. 32, No. 23, 1778 to 1791, (1992).

[58] Mavridis H. and R. N. Shroff, "Appraisal of a Molecular Weight Distribution-to-Rheology Conversion Scheme for Linear Polyethylenes ", *J. App. Poly. Sci.*, Vol. 49, 299 to 318, (1993).

[59] Mead, D. W., "Numerical Interconversion of linear viscoelastic material functions", *J. Rheology*, Vol. 38, No. 6, 1769 to 1795, (1994).

[60] Mead, D. W., "Determination of molecular weight distributions of linear flexible polymers from linear viscoelastic material functions", *J. Rheology*, Vol. 38, No. 6, 1797 to 1827, (1994).

[61] Middleman, S., "Effect of Molecular Weight distribution on Viscosity of Polymeric Fluids", *J. App. Poly. Sci.*, Vol. 11, 417 to 424, (1967).

[62] Munoz-Escalona, A., P. Lafuente, J. F. Vega and A. Santamaria, "Rheology of Metallocene-Catalyzed Monomodal and Bimodal Polyethylenes", *Poly. Eng. Sci.*, Vol. 39, 2292 to 2302, (1999).

[63] Nichetti, D. and I. Manas - Zloczower, "Viscosity model for polydisperse polymer melts", *J. Rheol.*, Vol. 42, No. 4, pp. 951 to 969, (1998).

[64] Ogunnaike, B. A. and W. H. Ray, "Process Dynamics, Modeling, and Control", Oxford Univ. Press, New York (1994).

[65] Raju, V. R., G. G. Smith, G. Marin, J. R. Knox and W. W. Graessley, "Properties of Amorphous and Crystallizable Hydrocarbon Polymers. 1. Melt Rheology of Fractions of Linear Polyethylene", *J. App. Poly. Sci.*, Vol. 17, 1183 to 1195, (1979).

[66] Ray, W. H., " The Quasi-Steady-State Approximation in Continuous Stirred Tank Reactors", *Canadian. J. Chem. Eng.* , Vol. 47, 503 to 508, (1969).

[67] Rohn, Charles E., "Analytical Polymer Rheology", Hanser/Gardner Publ., Cincinnati (1995).

[68] Seo, Y and K. U. Kim, "A new model for rapid evaluation of the degree of long-chain branching in polymers", *POLYMER* , Vol. 35, No. 19, 4163 to 4167, (1994)

[69] Shroff, R, Prasad,A. and C. Lee, "Effects of Molecular Structure on Rheological and Crystallization Properties of Polyethylenes", *J. Poly. Sci., Part B: Polymer Physics* , Vol. 34, 2317 - 2333, (1996)

[70] Shroff, R. and H. Mavridis, "Long - Chain - Branching Index for Essentially Linear Polyethylenes", *Macromolecules*, Vol. 32, 8454 to 8464, (1999).

[71] Soares, J. B. P., J. D. Kim and G. L. Rempel, "Analysis and Control of the Molecular Weight and Chemical Composition Distributions of Polyolefins Made with Metallocene and Ziegler-Natta Catalysts", *Ind. Eng. Chem. Res.*, Vol. 36, 1144 to 1150, (1997).

[72] Soroush, M., "State and parameter estimations and their applications in process control", *Computers and Chemical Engineering*, Vol. 23, 229 to 245, (1998).

[73] Spiegel, Murray R., "Mathematical Handbook", Schaum's outline series, McGraw-Hill Publ., New York (1968).

[74] Thimm, W., C. Friedrich, M. Marth, and J. Honerkamp, "An analytical relation between relaxation time spectrum and molecular weight distribution", *J. Rheol.*, Vol. 43, 1663 to 1672, (1999).

[75] Tobita, H. and A. E. Hamielec, "Polymerization processes", in *Ullmann's Encyclopedia of Industrial Chemistry* , Vol. A21, p. 326, Fifth edition, Barbara Elvers et al. (eds.), VCH Publ. Incl., New York, (1992).

[76] Todo, A. and N. Kashiwa, "Structure and Properties of new Olefin Polymers", *Macromol. Symp.*, Vol. 101, 301 to 308, (1996).

[77] Vaidyanathan, R. and M El-Halwagi, "Computer-Aided Synthesis of Polymers and Blends with Target Properties", *Ind. Eng. Chem. Res.*, Vol. 35, No. 2, 627 to 634, (1996).

[78] Vega, J. F., A. Munoz-Escalona, A. Santamaria, M. E. Munoz and P. Lafuente, "Comparison of the Rheological properties of Metallocene-Catalyzed and Conventional High-Density Polyethylenes", *Macromolecules*, Vol. 29, 960 to 965, (1996).

[79] Vega, J. F., A. Santamaria, A. Munoz-Escalona and P. Lafuente, "Comparison of the Rheological properties of Metallocene-Catalyzed and Conventional High-Density Polyethylenes", *Macromolecules*, Vol. 31, 3639 to 3647, (1998).

[80] Yan, D., W. J. Wang and S. Zhu, "Effect of long chain branching on rheological properties of metallocene polyethylene", *POLYMER* , Vol. 40, 1737 to 1744, (1999).

[81] Wood-Adams, P. M. and J. M. Dealy, "Using Rheological Data To Determine the Branching Level in Metallocene Polyethylenes", *Macromolecules*, Vol. 33, No. 20, 7481 to 7488, (2000).

[82] Wood-Adams, P. M., J. M. Dealy, A. W. deGroot and O. D. Redwine,"Effect of Molecular Structure on the Linear Viscoelastic Behavior of Polyethylene ", *Macromolecules*, Vol. 33, No. 20, 7489 to 7499, (2000).

[83] Yiannoulakis, H., A. Yiagopoulos, P. Pladis and C. Kiparissides, "Comprehensive Dynamic Model for the Calculation of the Molecular Weight and Long Chain Branching Distributions in Metallocene-Catalyzed Ethylene Polymerization reactors", *Macromolecules*, (2000).

[84] Yoon, W. J., Ryu, J. H., Cheong, C. and K. Y. Choi, "Calculation of molecular weight distribution in a batch thermal polymerization of styrene", *Macromol. Theory Simul.*, Vol. 7, pp. 327 to 332, (1998).